

Modulation of Nerve Growth Factor Receptor Expression in the Urothelium and its Relevance to Ketamine Induced Cystitis

Elizabeth Anne Kidger MBChB MRCS

**Submitted in accordance with the requirements for the
award of MD**

**The University of Hull and the University of York
Hull York Medical School**

September 2014

Abstract

Ketamine-induced cystitis (KIC) is a form of bladder pain syndrome (BPS) that usually arises following recreational abuse. Urothelial expression of the p75 low-affinity nerve growth factor receptor (NGFR) has been implicated in the aetiopathology of BPS. The aim of this project was to examine the expression of NGFR in urothelium and KIC and to identify modulators of NGFR expression. From the literature, candidate modulators identified were: ketamine, the transcriptional regulator Early growth response (Egr-1), glucocorticoids, cytokines, brain derived neurotrophic factor (BDNF) and ibuprofen, a non-steroidal anti-inflammatory drug.

Immunoperoxidase labelling and semi-quantitative analysis was performed on normal and KIC surgical specimens for NGFR and Egr-1. Cell and organ culture systems were developed from which NGFR transcript and protein expression were assessed following exposure to the candidate modulators.

NGFR was expressed by basal cells in all normal urothelial samples and extended suprabasally in KIC samples. A case study revealed widespread urothelial destruction and a non-patent urachal remnant with normal NGFR basal expression, in comparison to NGFR suprabasal extension in Von Brunn's nests, which were patent with the luminal surface of the bladder. Using an in vitro approach NGFR transcript was most highly expressed by proliferating normal human urothelial cell cultures and was immunolocalised basally in differentiated cell sheets and organ cultures. Glucocorticoids, cytokines, BDNF and Egr-1 did not modulate NGFR expression. Cell death inducing concentrations of ibuprofen, ketamine or G418 up-regulated NGFR transcript and protein in cell and organ cultures.

This study supports a urinary-mediated urothelial damage process in KIC and implicates NGFR upregulation in the pathogenesis. Ketamine and other toxins are able to directly up-regulate expression of NGFR in the urothelium and this study has laid the foundation for future exploration of the role of NGFR in the urothelial damage response.

Table of Contents

Abstract	2
Table of Contents	3
Figure list	8
Table list	10
Acknowledgements	11
1 Introduction	12
1.1 Urothelium	12
1.2 Role of the urothelium in disease	14
1.3 The urothelium and lower urinary tract dysfunction (LUTD)	14
1.3.1 Bladder pain syndrome/Interstitial cystitis (BPS/IC)	14
1.3.2 Overactive bladder syndrome (OABS)	15
1.3.3 Urodynamic stress incontinence (USI)	16
1.4 Ketamine-induced cystitis (KIC)	16
1.4.1 Ketamine	17
1.4.2 Histopathology of KIC	18
1.5 Nerve growth factor receptor (NGFR)	19
1.5.1 Role of NGFR and NGF in the bladder	20
1.6 Hypothesis, aims and objectives	24
2 Materials and Methods	25
2.1 Cell recovery and culture	25
2.1.1 Isolation of human urothelium and normal human urothelial (NHU) cell culture	25
2.1.2 Induction of urothelial differentiation	26

2.1.3	Alamar Blue Growth Assay	27
2.2	Organ Culture	27
2.2.1	Preparation of ureteric sample for organ culture	27
2.2.2	Organ culture constructs	28
2.3	Tissue processing	28
2.3.1	Paraffin wax-embedded tissue sections	28
2.3.2	Paraffin wax-embedded differentiated cell sheets	29
2.3.3	Haematoxylin and Eosin (H&E) Staining	29
2.4	Immunolabelling	30
2.4.1	Immunohistochemistry	30
2.4.2	Enhancement of IHC detection	31
2.5	Microscopy and image analysis	32
2.6	RNA extraction and c-DNA synthesis	35
2.6.1	RNA extraction	35
2.6.2	cDNA Synthesis	35
2.7	Polymerase Chain Reaction (PCR)	36
2.7.1	Primer design	36
2.7.2	Reverse transcribed PCR (RT-PCR)	36
2.7.3	Quantitative PCR (Q-PCR)	37
2.8	Ethics approval	38
3	NGFR and Egr-1 in KIC ‘in situ’	39
3.1	Introduction	39
3.2	Aim	40
3.3	Experimental approach	40
3.3.1	NGFR and Egr-1 Scoring	41
3.4	Results	42

3.4.1	NGFR and Egr-1 expression in normal urothelium	42
3.4.2	NGFR and Egr-1 expression in KIC in situ	46
3.5	Results Summary	53
4	NGFR in KIC – Case study	54
4.1	Introduction	54
4.2	Aim	55
4.3	Experimental approach	55
4.4	Results	56
4.4.1	Haematoxylin and Eosin staining	60
4.4.2	NGFR Labelling	63
4.4.3	Urachus	66
4.4.4	Labelling of the Urachus	69
4.4.5	Nerve distribution	74
4.5	Results Summary	77
5	In-vitro expression of NGFR by urothelium	78
5.1	Introduction	78
5.2	Aim	79
5.3	Experimental approach	79
5.3.1	Transcript expression	79
5.3.2	Differentiated cell sheets	79
5.3.3	Organ culture	80
5.4	Results	81
5.4.1	Transcript expression of NGFR	81
5.4.2	Barrier forming differentiated cell sheets	83
5.4.3	Formation of artificial basement membrane	86

5.4.4	Organ culture	90
5.5	Results Summary	93
6	Modulators of NGFR	94
6.1	Introduction	94
6.2	Aim	94
6.3	Overall Experimental Approach	96
6.4	Results	98
6.4.1	Ketamine	98
6.4.2	Glucocorticoids (dexamethasone)	101
6.4.3	Cytokines	107
6.4.4	BDNF	109
6.4.5	NSAID (Ibuprofen)	111
6.4.6	Results	111
6.4.7	Ketamine and ibuprofen	114
6.5	Results Summary	136
7	Discussion	137
7.1	In situ expression of NGFR	137
7.2	NGFR in vitro expression	140
7.3	Modulation of NGFR expression	141
7.4	Limitations	143
7.5	Conclusions	144
8	References	145
9	Appendices	155
9.1	Abbreviations	155
9.2	List of Surgical samples	157

9.3	List of antibodies	159
9.4	List of primers	160
9.5	List of suppliers	161

Figures

Figure 1-1	Haematoxylin and eosin cross-section of the human urinary bladder	13
Figure 2-1	Example of image analysis using TissueGnostic software	34
Figure 3-1	NGFR expression in normal bladder and normal ureter sections	44
Figure 3-2	Egr-1 expression in normal bladder and normal ureter sections	45
Figure 3-3	NGFR expression in KIC samples	47
Figure 3-4	Scoring of NGFR expression in normal human urothelium and KIC in situ	48
Figure 3-5	Egr-1 expression in KIC samples	50
Figure 3-6	Scoring of Egr-1 expression in normal human urothelium and KIC in situ.	51
Figure 3-7	Linear regression analysis of NGFR and Egr-1 samples	52
Figure 4-1	CT KUB in end stage KIC	58
Figure 4-2	Macroscopic images of resected bladder of patient with KIC	59
Figure 4-3	H&E staining of the case study KIC bladder	62
Figure 4-4	NGFR labelling on KIC bladder.....	65
Figure 4-5	H+E staining of the urachus	67
Figure 4-6	Cystogram from patient with KIC.....	68
Figure 4-7	NGFR Labelling on Urachal remnant and in Von Brunn's Nests	70
Figure 4-8	CK13 Labelling on Urachal remnant and in Von Brunn's Nests.....	71
Figure 4-9	CK20 Labelling on Urachal remnant and in Von Brunn's Nests	72
Figure 4-10	UPK3A Labelling on Urachal remnant and Von Brunn's Nests.....	73
Figure 4-11	Representative peripheral nerve fascicle distribution	75
Figure 4-12	Co-localisation of NGFR, NFP and S100.....	76
Figure 5-1	NGFR transcript expression in PO, proliferating and differentiated normal human urothelial cells.	82
Figure 5-2	NGFR expression on barrier forming differentiated cell sheets.....	85

Figure 5-3	Transepithelial electrical resistance (TER) for differentiated cell sheets with artificial extracellular membrane.....	86
Figure 5-4	NGFR expression in barrier forming differentiated cell sheets with artificial basement membrane	89
Figure 5-5	NGFR expression in urothelial organ culture	92
Figure 6-1	Immunohistochemical expression of NGFR in differentiated cell sheets treated with ketamine	100
Figure 6-2	AlamarBlue® Assay for proliferating NHU cells treated with dexamethasone.....	102
Figure 6-3	Transcript expression of NGFR in differentiated NHU cells treated with ketamine and log concentrations of dexamethasone	103
Figure 6-4	TER for differentiated cell sheets treated with dexamethasone and dexamethasone with ketamine.	104
Figure 6-5	Immunohistochemical expression of NGFR in differentiated cell sheets treated with dexamethasone and ketamine	106
Figure 6-6	Transcript expression of NGFR in NHU cells treated with proinflammatory cytokines	108
Figure 6-7	Transcript expression of NGFR in proliferating NHU cells treated with log concentrations of BDNF	110
Figure 6-8	Proliferating NHU cell populations in culture with ibuprofen treatment	112
Figure 6-9	Transcript expression of NGFR in proliferating NHU cells treated with ibuprofen	113
Figure 6-10	Transcript expression of NGFR in proliferating cells treated with ketamine	115
Figure 6-11	Proliferating NHU cell populations in culture with ketamine, ibuprofen, Staurosporine and G418 treatment	118
Figure 6-12	Quantitative RT-PCR – Expression of NGFR in proliferating cells treated with ibuprofen, ketamine, G418 and Staurosporine	119
Figure 6-13	Organ Culture with immunohistochemical labelling of NGFR at 3 day time point	123
Figure 6-14	Organ Culture with immunohistochemical NGFR labelling at 7 day time point	124

Figure 6-15	Organ Culture with immunohistochemical labelling of NGFR at 14 day time point	125
Figure 6-16	Organ Culture with immunohistochemical labelling for Ki67	129
Figure 6-17	Organ Culture with immunohistochemical labelling for CK13.....	131
Figure 6-18	Organ Culture with immunohistochemical labelling for CK5.....	133
Figure 6-19	Organ culture with immunohistochemical labelling for P53	135

Tables

Table 6-1	Literature review of candidate modulators of NGFR	95
Table 6-2	Table to summarise experimental approach for chapter 6	97
Table 6-3	Organ culture treatments and time points	115
Table 6-4	Summary of the expression of the markers for the organ culture at all-time points	127
Table 9-1	Table of Surgical specimens in all chapters.....	157
Table 9-2	Table of surgical KIC specimens used in chapter 3	158
Table 9-3	Table of Primary antibodies	159
Table 9-4	List of primers	160

Acknowledgements

I would especially like to thank Mr Simon Fulford for giving me this opportunity and for his continued support throughout the last two years.

I thank Professor Jenny Southgate and Dr Simon Baker for their excellent supervision and guidance at all stages of the project.

Further thanks to all members of my trainee advisory panel including Dr Roger Sturmeay and Miss Mary Garthwaite.

Finally, I thank all the members of the Jack Birch Unit of Molecular Carcinogenesis, Department of Biology, University of York for all their help and always keeping me smiling.

Author's Declaration

I confirm that this work is original and that if any passage(s) or diagram(s) have been copied from academic papers, books, the internet or any other sources these are clearly identified by use of quotation marks and the reference(s) is fully cited. I certify that, other than where indicated, this is my own work and does not breach the regulations of HYMS, the University of Hull or the University of York regarding plagiarism or academic conduct in examinations. I have read the HYMS Code of Practice on Academic Misconduct, and state that this piece of work is my own and does not contain any unacknowledged work from any other sources. I confirm that any patient information obtained to produce this piece of work has been appropriately anonymised.

1 Introduction

1.1 Urothelium

The urothelium is the epithelial lining of the urinary tract which is highly specialised and structurally unique. The urothelial lining extends from the renal pelvises through the ureters and bladder to the proximal urethra. The bladder is a storage reservoir which assists in maintaining continence by its ability to hold increasing volumes of urine at low pressure. The urothelium is able to adapt its surface area to these often rapid and large changes in volume.

The principal function of the urothelium is to act as a physical urine-blood barrier which protects underlying tissue from direct contact with urine and its constituent waste products, which are potentially carcinogenic (Cohen, 1998). The urothelium also prevents the loss of fluid from isotonic blood into the hypertonic urine. The permeability function of the urothelium is also maintained during the changes in surface area of the bladder. In addition to its permeability function the urothelium has a more dynamic role in bladder sensation, protein secretion and bacterial protection (reviewed by (Deng et al., 2001, Birder and Andersson, 2013).

The urothelium is a transitional epithelium as its organisation resembles a transition between simple columnar and stratified squamous epithelium. It rests on a basement membrane with an underlying lamina propria which contains vessels and nerves. The muscle surrounding the lamina propria is a smooth muscle known as the detrusor muscle. Finally, there is an outer serosal layer surrounding the entire structure (figure 1.1) (reviewed by (Young, 2013). The urothelium consists of 3-6 cell layers: a single basal layer, a multiple intermediate cell layer and finally a single superficial cell layer consisting of terminally differentiated urothelial cells often referred to as 'umbrella' cells as each cell covers several of the underlying intermediate cells (reviewed by (Khandelwal et al., 2009). The superficial cells maintain the barrier function by the expression of selective claudins and urothelium-

specific uroplakins. Claudins are known to regulate paracellular function through their contribution to intercellular tight junctions (Varley et al., 2006). Uroplakins are transmembrane proteins that form plaques of asymmetric unit membrane (AUM) which are unique to urothelium and contribute to transcellular barrier function (Yu et al., 1994, Deng et al., 2002, Hu et al., 2005)

Phenotypically the urothelium can be classified using the cytokeratins (CK) which are cytoskeleton protein that display differentiation stage-related expression. CK 7, CK 8, CK18 and CK 19 are found in all layers of the urothelium. CK 5 and CK 17 are expressed by the basal urothelial layer only. CK 13 is seen in all but the superficial layer and CK 20 is only associated with superficial cells (Southgate et al., 2002). Ki67 is a marker of proliferation. The urothelium is mitotically quiescent (Ki67-) but cells will re-enter the cell cycle and express Ki67 in response to damage (Varley et al., 2005). Understanding of the mechanisms of urothelial function may provide insights into the role of the urothelium in benign bladder disorders.

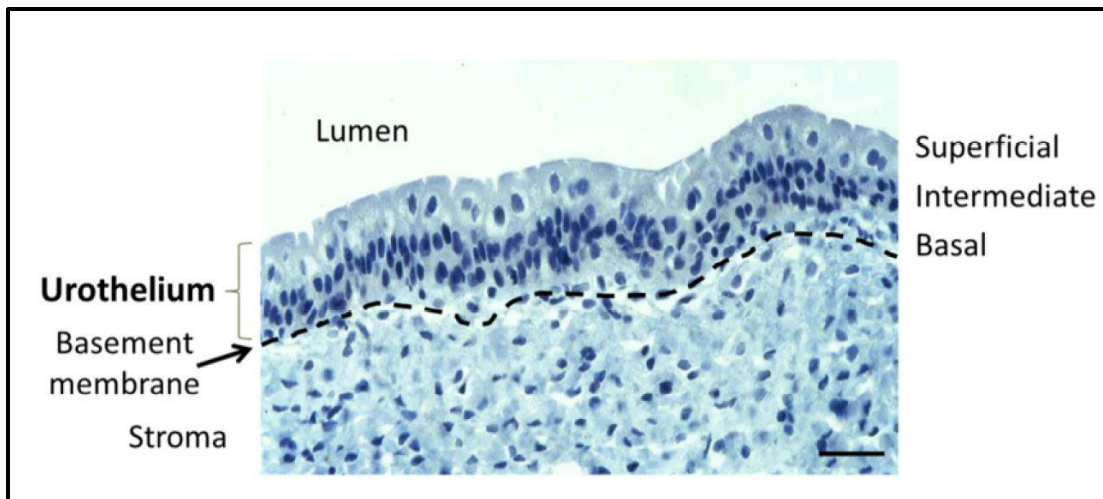


Figure 1-1 Haematoxylin and eosin cross-section of the human urinary bladder

Section shows the normal human urothelium with superficial, intermediate and basal cell layers with underlying stroma. Image provided by Prof. J. Southgate. Scale = 30 μ m

1.2 Role of the urothelium in disease

A number of diseases are known to affect the urothelium and can be subcategorised into benign and malignant conditions. It is outside the remit of this thesis to discuss the aetiology and pathogenesis of urothelial cancer and other malignant urothelial conditions. Benign disorders include a spectrum of conditions described collectively as bladder or lower urinary tract dysfunction (LUTD).

1.3 The urothelium and lower urinary tract dysfunction (LUTD)

LUTD is a term that encompasses the symptoms which accompany benign functional disorders including Bladder Pain Syndrome (BPS)/interstitial cystitis (IC), Overactive bladder syndrome (OABS) and urodynamic stress incontinence (USI). Lower urinary tract (LUTS) symptoms are classified into 3 groups: storage (frequency, urgency and nocturia), voiding symptoms (hesitancy and poor flow) and post micturition (feeling of incomplete emptying and post micturition dribbling). Genital and lower urinary tract pain may also be categorised within LUTS (Abrams et al., 2002). In certain conditions such as BPS and OABS the aetiopathology is thought to involve the urothelium and in other conditions the aetiopathology is thought to be exclusive of the urothelium (USI). The terminology surrounding LUTD was standardised by a sub-committee of the International Continence Society in 2002 (Abrams et al., 2002).

1.3.1 Bladder pain syndrome/Interstitial cystitis (BPS/IC)

BPS has been described for over 100 years with varying nomenclatures and definitions (Skene, 1887, Hunner, 1915). In 2008 the European Society for the study of Bladder Pain Syndrome/Interstitial Cystitis (ESSIC) published comprehensive guidance on the definition concluding that: Bladder Pain Syndrome (BPS) is a chronic (>6 months) pelvic pain, pressure, or discomfort *perceived to be* related to the urinary bladder accompanied by at least one other urinary symptom such as persistent urge to void or frequency (van de Merwe et al., 2008). It is a debilitating condition with additional quality of life implications. The prevalence is estimated around 300 per

100,000 women and a male prevalence of 10 to 20% of the female estimate (Hanno et al., 2009). There are many unanswered questions around the precise aetiology and pathophysiology of BPS/IC as summarised by an International Consultation on Bladder Pain Syndrome (Hanno et al., 2009). Aetiological factors implicated include mast cell activation, glycosaminoglycan GAG layer defects, inhibition of urothelial bladder cell proliferation, autoimmune mechanisms, infection and toxic agents. Although no specific aetiological factor is identified it is thought that triggers lead to an intrinsic epithelial dysfunction with loss of barrier function and a state of bladder sensory dysfunction. Hanno and colleagues made no significant conclusive evidence on the pathophysiology of disease but the consultation did conclude that the syndrome is likely to be a spectrum of conditions rather than a single pathological process (Hanno et al., 2009).

1.3.2 Overactive bladder syndrome (OABS)

Overactive bladder (OAB) refers to common and bothersome storage LUTS including frequency, urgency and nocturia. OABS is defined by the International Continence Society (ICS) as urgency with or without urge urinary incontinence, usually with frequency and nocturia in the absence of local or metabolic factors to explain these findings (Abrams et al., 2002). OABS is a highly prevalent disorder that affects the lives of millions of people globally creating a significant economic burden (Wein and Rovner, 2002). The symptoms of OABS are usually attributed to detrusor overactivity which is a urodynamic observation characterised by involuntary detrusor contractions during the filling phase which can be further qualified into idiopathic detrusor overactivity (no defined cause) or neuropathic detrusor overactivity (known relevant neurological condition) (Abrams, 2003). OABS may generally be classified according to the following aetiologies: neurogenic (e.g. spinal cord injury), myogenic (e.g. obstruction), inflammatory (e.g. BPS) or idiopathic (reviewed (Chu and Dmochowski, 2006, Steers, 2002). All patients regardless of the aetiological cause present with similar symptoms suggesting a similar pathobiology. This has been attributed to alterations in the neurological regulation of the micturition cycle,

altered responsiveness in the detrusor smooth muscle, and urothelial sensation (see section 1.1) which may underlie the development and maintenance of the condition (Steers, 2002).

1.3.3 Urodynamic stress incontinence (USI)

USI is defined as the involuntary leakage of urine during increased abdominal pressure, in the absence of detrusor contraction (Abrams et al., 2002). USI occurs when bladder pressure exceeds urethral pressure due to a sudden increase in intra-abdominal force. The principal mechanisms include anatomical change (typically loss of bladder neck support/bladder neck hypermobility) or due to neuromuscular compromise to the sphincter itself. However the collective view is that most patients have elements of both disorders (Norton and Brubaker, 2006). There is no evidence to suggest that urothelium is involved in the aetiopathology of the condition.

Clinically, the lack of aetiological and pathological consensus for benign bladder disorders, particularly in relation to BPS/IC, means that management is often challenging with limited therapeutic options available.

1.4 Ketamine-induced cystitis (KIC)

Ketamine-induced cystitis (KIC) was first reported in 2007 (Shahani et al., 2007). One year later, Chu et al looked at a series of 59 patients and retrospectively analysed the clinical presentations, video urodynamic studies, cystoscopic findings, histological features of bladder biopsies and radiological findings of these patients. The authors concluded 'a syndrome of cystitis and contracted bladder can be associated with street-ketamine abuse' but the report failed to establish the precise cause and incidence (Chu et al., 2008a). The clinical syndrome includes bladder pain, urinary frequency and reduced bladder capacity. This can progress to incontinence and renal damage and may be associated with hepatic dysfunction. (Shahani et al., 2007, Chu et al., 2008a). Chu et al went on to propose several hypotheses for the possible

mechanisms of damage including direct toxic damage to the urinary tract by ketamine and/or its metabolites, microvascular damage by ketamine and/or its metabolites, autoimmunity triggered by either circulating or urinary ketamine and unrecognised bacteriuria. A review of the literature in 2010 highlighted the above clinical syndrome and examined the possibility of an adulterant effect but concluded that this was highly unlikely due to several reasons: the use of adulterants would be expected to be variable, ketamine appears to be the common factor; low cost of ketamine means that the use of regular adulterants is less likely; a causal link in an animal model has been reported; there are case reports in paediatric and adult populations using therapeutic doses of ketamine; and there is both a dose and time relationship. The review concluded that there was a direct interaction between ketamine and the urothelium and that ketamine +/- its metabolites were the likely cause of the LUTS associated with KIC but acknowledged the lack of direct evidence to support this theory (Wood et al., 2011).

1.4.1 Ketamine

Ketamine, first synthesised by Stevens in 1962, is a glutamatergic N-methyl-d-aspartate (NMDA) antagonist. The NMDA receptor is an ion channel-coupled receptor with excitatory properties which has been linked to the mechanisms of general anaesthesia and analgesia. Ketamine is a non-competitive antagonist of the NMDA Ca^{2+} pore binding at an allosteric site; it also interacts at certain concentrations with the phencyclidine (PCP) binding site when the NMDA receptor is open (Hirota and Lambert, 1996). Ketamine is rapidly metabolised to an active metabolite norketamine via a cytochrome P450 enzyme in the liver. Both ketamine and norketamine are excreted via the renal system in the urine (Moore et al., 2001)

The first reported use of ketamine in the clinical setting was three years after its initial synthesis in 1965 (Domino et al., 1965). Clinically ketamine has been used for induction and maintenance of anaesthesia; more recent use is in chronic pain

management (Hocking and Cousins, 2003) and in the emergency setting (for safe sedation) (Herring et al., 2012, Lester et al., 2010, Svenson and Abernathy, 2007). Ketamine is also used as a recreational drug. The first reported use of ketamine for recreational practice was in the 1960s (Siegel, 1978) but use was rare in Europe until the 1990s where its usage was noted on the 'Rave scene' (Dalgarno P. J., 1996). The use of ketamine recreationally has been on the increase since this period (UNODC, 2010). This dissociative sensation known as the 'K hole' is described as pleasurable to some. Ketamine is also readily available and inexpensive anecdotally 'cheaper than a night on alcohol' (Tori, 1996).

1.4.2 Histopathology of KIC

In 2009, Oxley et al, looked at series of KIC bladder biopsies and remarked that KIC could lead to reactive urothelial changes that mimicked carcinoma in situ (Oxley et al., 2009). Seventeen KIC urothelial biopsies were examined and described extensive urothelial damage with urothelial ulceration as the commonest finding. Immunohistochemical analysis was performed on 10 of the KIC biopsies and found that 9/10 had high p53 immunoreactivity and 7/10 had moderate to high levels of Ki67 reactivity which are seen in the majority of cases of carcinoma in situ (McKenney et al., 2001, Kunju et al., 2005). However, all were negative for cytokeratin 20 which is atypical of carcinoma in situ and would support a diagnosis of reactive atypia (Oxley et al., 2009), although the original CK20 report classified a negative CK20 finding in the urothelium as non-informative with respect to CIS (Harnden et al., 1995, Harnden et al., 1996, Harnden et al., 1999b). Other case reports including histological examination have found chronic inflammatory changes with infiltrations of lymphocytes and variable number of eosinophils (Chen et al., 2011, Lai et al., 2012). In 2013, Baker et al reported an expansion of nerve growth factor receptor (NGFR), from the usual basal-restricted pattern seen in the urothelium (Wezel et al., 2014), into the intermediate and where present the superficial urothelial layer of patients with KIC (Baker et al., 2013). NGFR has been implicated in other disease processes

within the bladder and may be of relevance into pathogenesis of KIC and wider benign bladder disorders.

1.5 Nerve growth factor receptor (NGFR)

The low affinity p75 nerve growth factor receptor (NGFR; p75^{NTR}; CD271) is a member of the tumour necrosis factor receptor superfamily. It was initially shown to be involved in the regulation of cell survival and death (Ross et al., 1984). It is a 75kDa protein and was first cloned and detected in 1984 (Ross et al., 1984). NGFR expression is widespread within the central and peripheral nervous systems (Ruit et al., 1990, Verge et al., 1989). Outside of the nervous system NGFR is expressed in a variety of tissues including the urinary tract, colon, breast and respiratory tract (Mukai et al., 2000, Reis-Filho et al., 2006, Vizzard, 2000). The ligands of NGFR are the neurotrophins: NGF (nerve growth factor), BDNF (brain derived neurotrophic factor), NT-3 and NT-4 (Mukai et al., 2000) which are expressed in both pro- and mature forms. In the nervous system the neurotrophins comprise a large family of highly conserved trophic factors crucial for neuronal survival and protection. NGFR binds all members of the neurotrophin family with equal affinity (Sofroniew et al., 2001, Mukai et al., 2000). NGFR is a 427 amino acid transmembrane receptor containing an extracellular domain, a single transmembrane domain and a cytoplasmic/intracellular domain. The intracellular domain is highly conserved between species (Metsis, 2001).

The signal transduction pathways of NGFR are extremely variable because they are strongly dependent on cell type, cell differentiation status, neurotrophin binding, availability of intracellular adaptor molecules, presence of interacting transmembrane co-receptors and post-translational modification expression which lead to the plethora of cellular responses associated with NGFR activated (Lu et al., 2005, Barker, 2004, Schecterson and Bothwell, 2010). The tyrosine kinase (Trk) receptors of neurotrophins (Trk A for NGF, Trk B for BDNF and NT-4/5, Trk C for NT-3) are one of the well-recognised groups of co-receptors of NGFR. Particularly

studied is the relationship between the co-receptors NGFR and Trk A; when expressed together this complex has a higher affinity for binding NGF than the two receptors do when expressed separately (reviewed by (Schechter and Bothwell, 2010). Other co-receptors include sortilin (SORT1), Nogo receptor (NogoR) and Lingo-1 (Lu et al., 2005, Barker, 2004). Interactions with co-receptors are dependent on NGFR cellular location, cellular differentiation and its post translation modifications (Lu et al., 2005). Furthermore, the pro-neurotrophins are reported to have a relatively greater affinity for NGFR whereas mature neurotrophins have a relatively greater affinity for the Trks. The capacity for the pro-neurotrophins to selectively activate NGFR is dependent on NGFR's association with sortilin (Teng et al., 2005). Broadly it is considered that the NGFR/Trk combination is pro-survival and the activation of NGFR whether in association with sortilin or in its own right leads to apoptosis (Chao et al., 1998, Chao, 2003, Teng et al., 2005, Teng et al., 2010).

1.5.1 Role of NGFR and NGF in the bladder

The roles of NGFR and the neurotrophins in the bladder have been a subject of interest for over a decade. As previously stated, NGFR is expressed in the basal layer of the urothelium (Baker et al., 2013, Wezel et al., 2014). NGF is undisputably the most studied of the neurotrophins. NGF has been reported to be produced in vitro by human urothelial cells in response to oestrogen stimulation and it appears, like in other cell systems, that it is an important modulator of proliferation (Teng et al., 2002). In pathological processes, initial studies in animal models suggested that NGF played a key role in the development of inflammatory pain and hyperalgesia in the urinary bladder. NGFR was also found to be up-regulated in inflamed tissue in a rat model of cystitis, in which the authors concluded that NGFR and NGF binding may participate in the induced hyperalgesia (Steers et al., 1991, Dmitrieva and McMahon, 1996, Dmitrieva et al., 1997, Wakabayashi et al., 1996). In humans, urinary NGF levels are reported as increased in the urinary bladders of women with idiopathic sensory urgency and IC (Lowe et al., 1997). Furthermore, Vaidyanathan et al investigated the expression of NGFR in neuropathic bladder samples and reported

that in half of the series (n=26) there was an extension in NGFR expression to the superficial cells of the urothelium (Vaidyanathan et al., 1998a). Since these initial findings, extensive research has been directed into the role of NGFR and the neurotrophins (predominantly NGF) in the bladder principally towards understanding the function of NGFR and NGF in inflammatory pathologies of the bladder.

The vast majority of the experimental research conducted has continued in rat models by eliciting a chemically-induced cystitis with cyclophosphamide (CYP). Initial studies using the CYP-induced cystitis model in rats demonstrated an increase in urinary bladder neurotrophins mRNA (NGF, BDNF, NT-3, NT4/5) in acute (4 days) and chronic (4 weeks) time periods. However total urinary NGF protein decreased despite the abundance of NGF transcript (Vizzard, 2000). Follow up to this work focused initially on the Trk receptors and reinforced the findings above and additionally found that CYP-induced cystitis led to an increase in Trk A and Trk B expression in the post-ganglion cells and dorsal root ganglia. The authors hypothesised that the decrease in total urinary neurotrophins was due to their transportation away to the dorsal root ganglia rapidly after their translation from mRNA (Qiao and Vizzard, 2002, Murray et al., 2004). In 2008 Vizzard et al examined the expression of NGFR in the urinary bladder of the rat and its regulation in cyclophosphamide (CYP)-induced cystitis (Klinger and Vizzard, 2008). The study reported that NGFR was expressed throughout the urinary bladder: present in the nerve fibres of the detrusor smooth muscle and suburothelial nerve plexus, urothelial cells and nerve fibres associated with the suburothelial bladder vasculature. Total urinary bladder NGFR increased after CYP infusion but further distinction was not made between the different areas of the bladder. Blockade of the NGFR receptor increased bladder hyperreflexia (Klinger and Vizzard, 2008). To examine the relationship between NGFR and NGF in the urothelium further a transgenic mouse model of chronic NGF overexpression in the urothelium using the urothelium-specific uroplakin II (UPK2) promoter was created. NGF mRNA and protein were expressed at higher levels in the bladders of NGF-overexpressing (NGF-OE) transgenic mice compared to control wild type (WT) mice. NGF was found to: stimulate neuronal

sprouting and proliferation in the urinary bladder, to produce local inflammatory changes in the urinary bladder, produce hyperreflexia and resulted in increased referred somatic hypersensitivity (Schnegelsberg et al., 2010). Further study to establish NGFR expression in NGF-OE found no change in NGFR transcript expression in the urothelium of NGF-OE but transcript expression was increased in the detrusor muscle suggesting a mesenchymal interaction. The authors concluded that increased NGFR expression in the detrusor muscle may promote an NGF-NGFR signalling mechanism to reduce voiding frequency in NGF-OE mice (Girard et al., 2011).

Clinically, NGF has been reported as increased in the urine of patients with idiopathic urgency and IC (Lowe et al., 1997). Further investigation also revealed increased urinary NGF in patients with OABS, USI and bladder outflow obstruction (Kim, 2005, Kim et al., 2004, Liu and Kuo, 2008, Liu and Kuo, 2009). More recently NGF transcript has been shown to increased in concordance with severity of inflammation in BPS/IC and correlated to clinical symptoms (Homma et al., 2013, Liu et al., 2014). These findings support the theories above that NGF plays an important role in both somatosensory and visceral nociception and is implicated in producing hyperalgesia by acting directly on sensory nerve endings or by indirectly increasing the expression of neuropeptides (Schnegelsberg et al., 2010). This is further supported, firstly, the use of a humanised monoclonal antibody (tanezumab) to specifically inhibit NGF which has shown efficacy in the treatment of pain associated with IC (Evans, 2011) and secondly there is some evidence to suggest that that the decrease in detrusor overactivity following Botulinum toxin A injections could be due to repression of NGF release (Giannantoni, 2006, Liu et al., 2009, Giannantoni et al., 2013).

As discussed earlier in this section NGFR has been reported as up-regulated in the urothelium of patients with neuropathic bladders (Vaidyanathan et al., 1998a), in patients with bladder outflow obstruction (Eryildirim et al., 2006) and in patients with KIC (Baker et al., 2013). However, there is some controversy in relation to expression of NGFR and benign bladder conditions; further to the examination of KIC samples Baker et al reviewed a series of surgical specimens from patients with OABS (n=6), USI (n=4) and BPS/IC (n=11) and did not observe a basal expansion of NGFR in a significant number of the samples (Baker et al., 2013). There is also evidence

emerging that expression of NGFR in the normal urothelium may have an outside role in addition to bladder inflammatory pathologies. Wezel et al, has displayed evidence that NGFR may be involved in regeneration of the urothelium during aging and after injury by displaying evidence that basal (NGFR⁺) cells represent a primed, highly proliferative and clonogenic subpopulation (Wezel et al., 2014). Furthermore, NGFR has been implicated in stem cell biology (reviewed in (Tomellini et al., 2014).

In summary, NGFR is implicated in benign conditions of the bladder but the expression and the role of NGFR is not yet clearly established. In KIC, the up-regulation of NGFR in the urothelium maybe a link into establishing the modulation and function of NGFR in the urothelium and moreover into disease processes in benign bladder conditions.

1.6 Hypothesis, aims and objectives

The overall hypothesis of the study is that NGFR plays a role in the pathogenesis of KIC and other inflammatory pathologies associated with the urinary bladder, including BPS. Therefore the normal basal expression of NGFR in the urothelium will be altered in response to inflammatory mediators.

The aim of this project was to examine the expression of NGFR in the normal urothelium and in KIC and to examine possible modulators of NGFR expression in the urothelium.

The objectives are:

- Describe the expression of NGFR in the normal urothelium and KIC in situ.
- Examine NGFR expression using an in vitro model of normal human urothelium
- Identify modulators of NGFR expression in vitro

2 Materials and Methods

2.1 Cell recovery and culture

All cell and organ culture procedures were performed under aseptic conditions in a class II laminar air flow cell culture safety cabinet with high efficiency particulate air (HEPA) filters (Medical Air Technology).

2.1.1 Isolation of human urothelium and normal human urothelial (NHU) cell culture

Previously described methods for NHU cell culture were employed (Southgate et al., 1994, Southgate et al., 2002) and performed by laboratory technicians. Briefly, normal human urothelial cells were obtained from samples taken from patients with no history of urothelial malignancy. Samples taken aseptically were immediately placed in transport medium consisting of Hank's balanced salt solution (HBSS; GIBCO) containing 10mM HEPES, pH 7.6 (GIBCO) and 20 kallikrein-inhibiting units (KIU)/ml of aprotinin (Trasylol; Bayer Pharmaceuticals) and transported to the Jack Birch Unit at the University of York. Upon receipt, samples were sectioned under aseptic conditions into pieces approximately 1cm² and placed in 'stripper medium' consisting of HBSS (without Ca²⁺ or Mg²⁺) containing 10mM HEPES, pH 7.6, 20 KIU/ml Trasylol, and 0.1% (w/v) EDTA and incubated at 37°C for 4 hours or at 4°C overnight. The urothelial cell sheets were then removed using sterile forceps and placed in collagenase type IV (200U/ml, Sigma Aldrich) for 20min at 37°C before the addition of 3ml of keratinocyte serum-free medium (KSFMc; Gibco) supplemented with recombinant epidermal growth factor (5ng/ml), bovine pituitary extract (50µg/ml) and cholera toxin (30ng/ml) (with supplements media is KSFMc) and then centrifuged for 5 minutes at 250g. After centrifugation, supernatant was aspirated and the pellet flicked and resuspended in KSFMc for culture. Primary cultures were established

using a minimum seeding density of 4×10^4 cells/cm². Cultures were medium changed twice weekly or subcultured at just confluence.

The cells adopt a proliferative, non-differentiated phenotype and are serially propagated as monolayers in serum-free culture medium (KSFMc) in low calcium (0.09mM) on Primaria™-coated 25 or 75cm² tissue culture flasks (BD Biosciences). Urothelial cell cultures were maintained at 37°C in a humidified atmosphere of 5% CO₂ in air. Medium was changed at 48-72 hour intervals. When cells reach approximately 90% confluence, culture medium was aspirated and cells were incubated in 10ml 0.1% (w/v) EDTA in PBS for 5-10 minutes at 37°C. The EDTA was aspirated when the cells appear rounded and separated. 1ml of trypsin in versene (0.25% (w/v) trypsin in PBS containing 0.02% (w/v) EDTA) was applied to the cells and maintained for a further 2-4minutes at 37°C until the cells lift from the surface of the substrate. The trypsin activity was inhibited immediately by the addition of KSFMc containing 1.5mg/ml of soybean trypsin inhibitor (TI) and cells were pelleted by centrifugation at 250g for 4 minutes. The subsequent cell pellet was flicked to resuspend in KSFMc and reseeded at the required density after counting into Primaria™ flasks or culture dishes for use in further experiments.

2.1.2 Induction of urothelial differentiation

Induction of urothelial differentiation used the method established by Cross et al (Cross et al., 2005). The medium on the proliferating NHU cells was supplemented with 5% adult bovine serum (ABS) for 4-5 days before passaging. 24h post-passage the exogenous calcium concentration was increased to 2mM (addition 180µl 1M CaCl₂ to 100ml of medium) this was then maintained for 7-9 days, or as indicated.

For measurements of transepithelial electrical resistance (TER) (indicator of barrier formation) or for histological analysis of differentiated cell sheets, cultures were pretreated as above in KSFMc + 5%ABS for 4-5 days. Cells were then seeded on Snapwell™ (Corning®, Costar®) or ThinCert™ (Greiner bio-one) cell culture membranes in a density of 5×10^5 in 500µL volume and culture medium placed into

the outer well (Snapwell™ – 4ml; Thincert™ 1-3ml). Exogenous calcium was increased to 2mM 24h after seeding. The transepithelial electrical resistance (TER) was measured on alternate days using an EVOM™ epithelial voltohmmeter (World Precision Instrument) under sterile conditions. A functional barrier is considered to be achieved when TER > 500 Ω /cm².

2.1.3 Alamar Blue Growth Assay

AlamarBlue® (Serotec) is an indicator dye incorporating an oxidation reduction indicator which changes colour in response to the chemical reduction of growth medium, resulting from cell metabolic activity. It is designed to quantitatively measure the changes in biomass in cell cultures by assuming metabolic activity of the culture is proportional to cell number. Proliferating NHU cell were seeded to Primaria®-coated 96 well plates at a density of 2×10^4 /mL 200 μ l in each well (5 replicates) and left for 24h to adhere. Treatments were applied in a log concentration at day 0. Growth assays were taken on days 0, 1, 3, 6 and 7. On the day of the assay cells were resuspended in alamarBlue® mixed 1:10 with culture medium. These were then incubated for 4 hours in a humidified incubator at 37°C, 5%CO₂ in air. Optical density of each well was recorded using a Multiskan Ascent 96/384 Plate Reader (Thermo Scientific) at test and reference wavelengths of 570nm and 630nm. Percentage cell reduction was calculated.

2.2 Organ Culture

2.2.1 Preparation of ureteric sample for organ culture

The ureteric sample was removed from the transport medium and placed in a Petri dish (Sterilin) using sterile forceps. Excess fatty tissue was removed from the exterior of the ureter. Sterile scissors were used to section the length of the ureter which was

the opened out to expose the urothelial surface. The ureter was then cut into pieces approximately 0.5cm² pieces and held in transport medium until use.

2.2.2 Organ culture constructs

Organ cultures were maintained on the membrane of a cell culture well insert with 3µm pores (BD Falcon™, catalogue number 734-0034) in a six well plate (Corning® Costar®). 2mL of RPMI:DMEM(1:1) supplemented with 5% fetal bovine serum (FBS) and 2mM L-Glutamine was added to the wells of a six well plate ensuring the area between the base of the well and the membrane of the cell culture insert was just filled (approximately 2ml). Sterile de-ionised water was added to the central area of the 6-well plate to ensure a humidified environment. The medium was changed every 48hours and organ cultures were harvested at varying time points e.g. 3 days, 7 days and 14 days.

2.3 Tissue processing

2.3.1 Paraffin wax-embedded tissue sections

Tissue samples were fixed in 10% (v/v) formalin in phosphate-buffered saline (PBS) for at least 24 hours depending on the size of the sample. Samples were then transferred into 70% (v/v) ethanol until further processing. Tissues were initially placed and appropriately labelled in an embedding cassette and submerged in fresh 70% (v/v) ethanol. The cassettes were then submerged into absolute ethanol (3x10 minute washes), isopropanol (2x10 minute washes) and xylene (4x10 minute washes). Samples were then embedded in paraffin wax. 5µm sections were cut using a Leica RM2135 rotary microtome and collected onto electrostatically charged Super Frost Plus™ microscope slides (BDH).

2.3.2 Paraffin wax-embedded differentiated cell sheets

To conserve differentiated cell sheets for histological analysis, medium was removed and cell sheets rinsed in Dulbecco's phosphate buffered saline (D-PBS) solution. The D-PBS was aspirated and the wells flooded with 2% (w/v) dispase (Sigma D-4693) and incubated at 37°C for 20-30 minutes under frequent observation until the cell sheets start to lift. Cell sheets were then collected and placed in a 'cell safe' histology case and appropriately labelled cassette and submerged in 10% (v/v) formalin in phosphate-buffered saline (PBS) for 24 hours and then transferred into 70% (v/v) ethanol until further processing. Samples were then submerged in fresh 70% (v/v) ethanol (1x5minutes), absolute ethanol (3x5minutes), isopropanol (2x5minutes) and xylene (4x5minutes) and then embedded in paraffin wax and sectioned as described in section 2.2.1.

2.3.3 Haematoxylin and Eosin (H&E) Staining

Tissue sections were de-waxed in xylene and rehydrated through absolute ethanol, 70% (v/v) ethanol to water. Sections were stained in Mayer's haematoxylin for 2 minutes and washed immediately to remove residual stain. The slides were immersed in Scott's tap water before a further wash in tap water. Slides were stained with aqueous 1% (w/v) eosin (Thermo Scientific – RA Lamb) for 30 seconds and washed immediately in running tap water to remove any residual stain. The slides were dehydrated from water through to absolute ethanol, followed by xylene (2x1min) immersion, before mounting with DPX mounting fluid (Cell Path) and cover slips.

2.4 Immunolabelling

2.4.1 Immunohistochemistry

Immunolabelling on paraffin wax-embedded tissue sections was performed using an indirect streptavidin/biotin 'ABC' immunoperoxidase method. Sections (5µm) of the paraffin embedded tissue were dewaxed in xylene and rehydrated through to 70% ethanol and then to water. For native tissue sections, endogenous peroxidase activity was blocked with 3% (v/v) hydrogen peroxide for 10 minutes before washing for 10 minutes in running tap water. Tissue sections were then subjected to antigen retrieval to restore immunoreactivity of antigens lost during tissue processing by one of three methods: (i) Heat induced retrieval by boiling sections for 10 minutes in 10mM (pH6.0) citric acid or 1mM EDTA (pH 8.0) in a microwave oven (ii) Enzymatic treatment with 0.1% (w/v) trypsin solution (Sigma) in 0.1%(w/v) CaCl₂ pH 7.8 for 10 min or (iii) Combined enzymatic and heat-induced retrieval method involving 1 min trypsinisation followed by microwave boiling as indicated above. Slides were then placed in Shandon™ Sequenzas™ (Thermoscientific) and Tris-buffered saline solution (TBS) (pH7.6) was used to check the Sequenza system for leaks. Endogenous avidin binding sites were blocked with avidin/biotin blocking kit (Vector Catalogue number: sp-2001). Non-specific background labelling was eliminated by blocking with 10% serum of the host species of the respective secondary antibody before the addition of the primary antibody and subsequent incubation for 1 hour (ambient temperature) or overnight (4°C). Secondary biotinylated anti-Ig antibodies (30 minutes) and streptavidin/horse radish peroxidase (HRP) ABC complex (Vectastain elite ABC kit; Vector Labs) (30 minutes) were applied subsequently with TBS (pH7.6) washes incorporated between each step. Bound antibody was visualised with 3,3-diaminobenzidine substrate (DAB, Sigma) reaction catalysed by H₂O₂ for 12 minutes before being counterstained with Mayers' haematoxylin (Sigma) and being dehydrated and mounted in DPX mounting fluid (CellPath). Primary and secondary antibodies are listed in appendix. Positive and negative controls were included and

normal human ureter was usually used for both control and TBS diluent replaced the primary antibody in the negative control.

2.4.2 Enhancement of IHC detection

A tyramide-based catalysed signal amplification kit (Dako Catalogue number: k1500) and an ImmPRESS™ Excel staining kit (Vector Laboratories: MP-7602) were used according to manufacturer's instructions to improve sensitivity of antibody labelling detection. See appendix for details on the antibodies which required enhancement for IHC detection.

2.4.2.1 Tyramide-based catalysed signal amplification (CSA)

The CSA system is a sensitive immunohistochemical staining procedure incorporating a signal amplification method based on the peroxidase-catalysed deposition of biotinylated phenolic compound, followed by a secondary reaction with streptavidin peroxidase. Sections are prepared as previously described in section 2.4.1 up to placement in Shandon™ Sequenzas™ (Thermoscientific). Endogenous avidin binding sites were blocked with avidin/biotin blocking kit (Vector Catalogue number: sp-2001). Protein block contained within the CSA kit was then applied to each slide and incubated for 5 minutes to eliminate non-specific background labelling, before the application of the primary antibody and subsequent incubation for 1 hour (ambient temperature) or overnight (4°C). Primary antibody concentrations were made up using antibody diluent (DAKO). The link antibody, streptavidin-biotin complex, amplification reagent and streptavidin-peroxidase were applied respectively for 15 minutes each with TBS (pH7.6) containing 0.1% Tween-20 washes incorporated between each step. Bound antibody was visualised with 3,3-diaminobenzidine substrate (DAB, Sigma) reaction catalysed by H₂O₂ for 5 minutes before counterstain with Mayers' haematoxylin (Sigma) and dehydration and mounting in DPX (CellPath).

2.4.2.2 ImmPRESS™ Excel staining kit

The ImmPRESS™ Excel amplified HRP (peroxidase) polymer staining kit (Manufacturer: Vector Laboratories; Catalogue number: MP-7602) is an enzymatic, non-biotin amplification system. The system uses a ready-to-use amplifier antibody followed by a ready to use ImmPRESS™ excel polymer reagent. The reagents are affinity-purified and cross-adsorbed to ensure high sensitivity and low background. Sections were prepared up to placement in Shandon™ Sequenzas™ (Thermoscientific) as previously described in section 2.4.1. Sections were incubated for 20 minutes with 2.5% normal horse serum to eliminate non-specific background labelling before the addition of the primary antibody and subsequent incubation for 1 hour (ambient temperature) or overnight (4°C). Primary antibody concentrations were made up with TBS (pH7.6). Sections were incubated with Amplifier Antibody (15 minutes), ImmPRESS™ Excel reagent (30 minutes) with TBS (pH7.6) 0.1% Tween-20 washes incorporated between each step. ImmPACT™ DAB EqV was then applied for 5 minutes before being counterstained with Mayers' haematoxylin (Sigma) and dehydration and mounting with DPX (CellPath).

2.5 Microscopy and image analysis

Microscopy was performed using an Olympus BX60 microscope with an Olympus DP50 camera and Image ProPlus software version 4.5.1.29 or with the Zeiss Axioscan. TissueGnostic image analysis software was used to analyse differentiated cell sheets for total number of cells and number of marker/antibody (DAB) positive cells (section 2.4.1) see figure 2.2 for TissueGnostic analysis process.

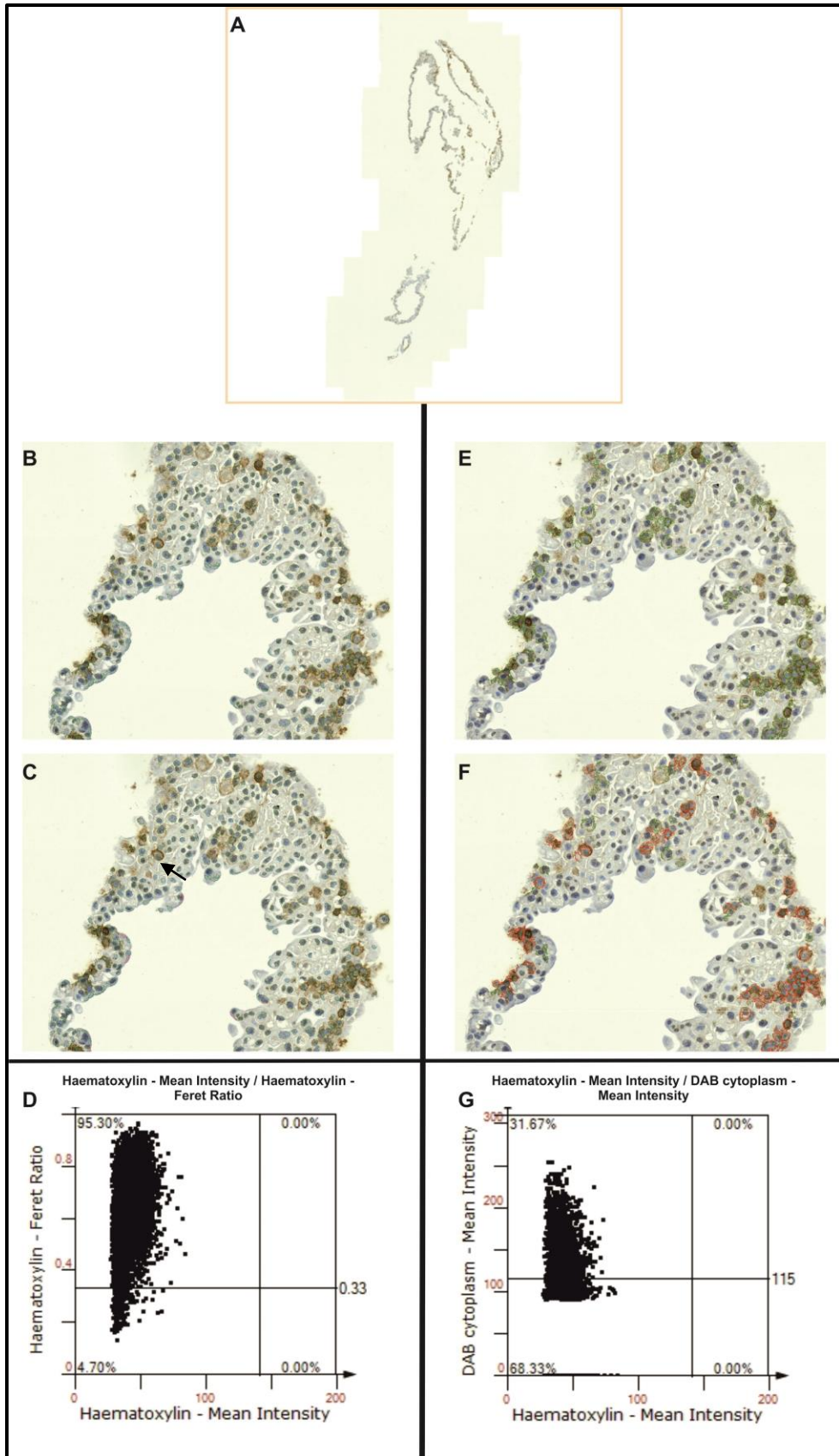


Figure 2-1 Example of image analysis using TissueGnostic software

Sections were scanned using Zeiss Axioscan and up-loaded into TissueGnostic software (**A**). **B**) Haematoxylin intensity settings were established to identify nuclei (number of cells). Nuclei are outlined in green. **C**) A Feret ratio (measure of an object size along a specified diameter) was used to exclude the thin membrane plaques. Plaques are outlined in red (arrowed) and excluded from analysis. **D**) A scattergram representing all haematoxylin mean intensity nuclei (x axis) and haematoxylin Feret ratio (y axis) with cut off at 0.33 defining nuclei and plaques. The cut off was defined after visual examination of the images throughout the series to allow comparable data. **E**) DAB cytoplasm intensity settings were defined (DAB cells outlined in green). **F**) A parameter was set visually to define positive cells against cells with very weak labelling considered to be background staining rather than a true NGFR⁺ cell. Red ringed cells are considered DAB and therefore NGFR⁺, the areas highlighted green are negative. **G**) A scattergram of haematoxylin mean intensity (x axis) and DAB cytoplasm mean intensity (y axis) which shows the cut-off of DAB cytoplasm mean intensity at 115 for DAB positive and negative cells. This cut off was again decided after visual examination of the images throughout the series to allow comparable data. The results were then analysed using Graph Pad Prism version 6 software.

2.6 RNA extraction and c-DNA synthesis

2.6.1 RNA extraction

RNA was isolated from cells using the Trizol™ reagent extraction method. Cells were solubilised in Trizol™ (Invitrogen) using manufacturer's recommended volumes. Cell lysate was collected by scraping using a sterile plastic scraper and collected into a nuclease-free 13ml tube and stored at -80°C until further processing.

Samples were thawed on ice and 0.2ml of neat chloroform/ml of Trizol™ was added. The tubes were vortexed, left at ambient temperature for 2 minutes and centrifuged at 12,000g for 15 minutes at 4°C. The upper clear aqueous phase was then carefully collected and transferred into fresh nuclease free-treated tubes. Isopropanol (0.5ml per ml of Trizol™) was added to the RNA and then centrifuged at 12,000g for 10 minutes at 4°C. The RNA pellet was washed with 75% (v/v) ethanol (1ml per ml Trizol used) and centrifuged at 7,500g for 5 minutes twice. The pellets were dried under a light source and resuspended in 30µl of nuclease-free water. Contaminating DNA was removed from RNA preparations using the DNA-free kit (Ambion) according to the manufacturer's instructions. Quality and quantity of RNA samples was verified spectroscopically using a Nanodrop™ UV/visible spectrophotometer (Shimadzu).

2.6.2 cDNA Synthesis

RNA was reverse-transcribed to cDNA using Superscript first strand synthesis system™ (Invitrogen). cDNA was synthesised from 1µg of RNA and every RNA sample included two reactions: reverse transcriptase positive (RT +ve) and reverse transcriptase negative (RT-ve). The RT -ve samples were included to check for DNA or PCR product contamination. Primers were annealed by combining 1µg RNA, hexamers (50ng/µl) and nuclease-free water and then incubated at 65°C for 10 minutes. A master mix containing 5x first-strand buffer, 0.1M DTT and dNTP mix was then added prior to the addition of the Superscript II Reverse transcriptase (50U/µl)

to the RT +ve samples. Nuclease free-H₂O was added to the RT-ve samples. Samples were then incubated at 25°C for 10 minutes, 42°C for 50 minutes and finally the reverse transcriptase was inactivated by heating at 70°C for 15 minutes. The cDNA was stored at -80°C until further use.

2.7 Polymerase Chain Reaction (PCR)

2.7.1 Primer design

Primer pairs for tested genes were designed using published sequences (NCBI/Ensembl) and checked for specificity using the Ensembl BLAST database, In-Silico-PCR and NCBI Primer Blast. See appendix for primer sequences used.

2.7.2 Reverse transcribed PCR (RT-PCR)

PCR reactions were carried out using a Bio-Rad T100 thermal cycler. For each cDNA sample a 19µl PCR mix was prepared on ice containing 8.5µl ddH₂O, 4µl Go Taq buffer (Promega), 0.4µL dNTPs (10mM)(Invitrogen), 2µLMgCl₂ (25mM) (Promega), 2µl (10mM) forward primer, 2µL (10mM) reverse primer and 0.1µl Go Taq polymerase (Promega). 1µl of cDNA was added to 19µl of master mix. cDNA integrity was checked using GAPDH primer. Genomic, brain or pooled cell lines DNA served as a positive controls and ddH₂O served as a negative/no template control. cDNA was denatured for 5 min at 95°C followed by 24-40 cycles at 95°C for 30 seconds, annealing for 30 seconds at the pre-determined temperature and 72°C for extension at appropriate length of time for primer. A final elongation phase of 72°C for 5 min was followed by incubation at 4°C.

Optimal annealing temperatures for primers were defined using a gradient of increasing annealing temperatures ranging from 60°C to 70°C using genomic cDNA.

DNA separation was routinely carried out using 2% agarose gels. Gels were made up using electrophoresis grade agarose (Invitrogen) in TBE buffer with addition of GelRed at 1:10000 dilution. Size determination of fragment was achieved using GeneRuler 1Kb and 100bp Neb ruler.

2.7.3 Quantitative PCR (Q-PCR)

cDNA was made as previously described in section 2.6.2, and each sample was made up to 100µl with DEPC-H₂O. A primer efficiency test was performed by setting up a standard curve in triplicate using genomic DNA in serial dilutions. A mix was prepared for each cDNA sample combining 10µl FAST SYBR® Green master mix (Invitrogen), 0.6µl Forward primer (10µM), 0.6µl Reverse primer (10µM), and 3.8µl ddH₂O. Each sample of cDNA was run in triplicate and RT-ve controls were included. GAPDH was used as a housekeeping gene to enable quantification against a known target. A 96-well optical reaction plate (Applied Biosystems, code 128) was loaded with 15µl of master mix and then 5µl of cDNA. The plate was then sealed and stored at 4°C until the run. Q-PCR reaction was performed. All Q-PCR reactions were performed in the Technology Facility, Department of Biology, University of York, on an ABI Prism 7000 sequence detection system (Applied Biosystems). The thermal profile used was a 2 minute hold at 50°C, then incubation at 95°C for 10 minutes, followed by 40 cycles of denaturation at 95°C for 15 seconds and 1 minute at 65°C for annealing and extension. Background signals were detected in all wells during early PCR cycles and established a baseline fluorescent level before significant amplification of the product was detected. Threshold values were set in the region of exponential amplification across all of the amplification plots. Results were analysed using ABI Prism® sequence and Excel® 2010 (Microsoft). The average of triplicate readings was used to estimate target and GAPDH expression levels in original samples. Normalised values of the target mRNA were then obtained by dividing the target amount by the GAPDH reference amount.

2.8 Ethics approval

Ethics approval was granted with NRES committee North East – York:

Feasibility study of comparison of ketamine- induced bladder dysfunction and interstitial cystitis (painful bladder syndrome)

Ref: 10/H0903/43

3 NGFR and Egr-1 in KIC ‘in situ’

3.1 Introduction

As discussed in the section 1.5, the low affinity p75 nerve growth factor receptor (NGFR; p75^{NTR}; CD271) is a member of the tumour necrosis factor superfamily. It was initially shown to be involved in the regulation of cell survival and death and has widespread expression within and outside of the nervous system including in the urinary tract (Ross et al., 1984, Ruit et al., 1990, Verge et al., 1989, Mukai et al., 2000, Reis-Filho et al., 2006, Vizzard, 2000). Within the urothelium the expression of NGFR is restricted to the basal urothelial cells (Wezel et al., 2014). In 2013, Baker et al reported urothelial NGFR expansion into the intermediate and where present the superficial urothelial layer of bladders from patients with ketamine induced cystitis (KIC) (Baker et al., 2013). Further studies describing the expression of NGFR in the urothelium and in relation to pathological processes are discussed in section 1.6. Together these studies highlight the apparent importance of NGFR in pathological processes in the bladder particularly in relation to bladder pain syndromes including KIC. However, very little is known about urothelial expression and role of NGFR in the urothelium and moreover its contribution to disease processes.

Early growth response – 1 (Egr-1; NGFI-A; zif268; Krox-24; TIS8) is a zinc finger transcriptional regulator (Sukhatme et al., 1987). Egr-1 is localised to the nucleus and is implicated in multiple functions including cell proliferation, differentiation, apoptosis and neovascularisation (Sukhatme et al., 1987, Sukhatme et al., 1988). Expression has been noted previously in human bladder cancers: Egerod et al found high expression of Egr-1 in human bladder cancer was associated with invasive tumours (Egerod et al., 2009a). Furthermore, expression has been found to be inducible in different cell types and by a variety of stimuli including inflammatory cytokines (Sukhatme et al., 1987, Sukhatme et al., 1988, Autieri et al., 2004). Nikam et al reported that Egr-1 was one of the early response genes expressed by Schwann cells after injury. Examination of the 5’ upstream sequence of the NGFR promoter

revealed a possible binding site for Egr-1 (Nikam et al., 1995). The paper displayed indirect evidence that Egr-1 and NGFR mRNA levels were associated after nerve injury by northern blotting which showed that an increase in Egr-1 levels peaked at 3 hours and preceded the rise in NGFR expression which peaked at 7 days following permanent transection of the rat sciatic nerve (Nikam et al., 1995). This was further reinforced by Gao et al in 2007 who reported that Egr-1 was capable of inducing expression of NGFR in vitro in murine myoblasts and embryonic fibroblasts (Gao et al., 2007).

The above evidence suggests that there is a potential link between Egr-1 and the expression of NGFR in the urothelium. The functions of Egr-1 suggest that it may have a function in disease processes in the bladder such as KIC. However, the expression of Egr-1 in the normal human urothelium and whether it has any relevance to the noted increase in NGFR expression in KIC is yet to be elucidated.

3.2 Aim

The aim of the study was to evaluate and quantify the expression of NGFR and Egr-1 in the normal urothelium and KIC in situ and to establish if there is a link between Egr-1 expression and NGFR in KIC in situ.

3.3 Experimental approach

Tissue obtained by cold cup biopsy or cystectomy from patients with clinically diagnosed KIC was used. A control group of bladder and ureter sections from patients with no history of urothelial atypia was also selected.

Formalin-fixed, paraffin wax-embedded tissues were sectioned (5µm) and dewaxed in xylene and rehydrated through ethanol to water. Antigen retrieval was performed using citric acid. Both NGFR and Egr-1 (see table in appendix for antibody detail) required the use of a tyramide-based catalysed signal amplification kit

(Manufacturer: Dako; Catalogue number: k1500) or the ImmPRESS™ Excel staining kit (Manufacturer: Vector Laboratories; Catalogue number: MP-7602) which were used according to manufacturers' instructions to improve sensitivity of antibody labelling detection. Blocking steps to neutralise endogenous peroxidase and avidin-binding activities were only included if the tyramide-based catalysed signal amplification kit was used (section 2.4).

3.3.1 NGFR and Egr-1 Scoring

NGFR and Egr-1 labelled slides of KIC and control tissues (normal bladder and normal ureter) were scanned using the Zeiss Axioscan. Identical magnification images of all areas of remaining urothelium on the different samples were printed at high quality. These images were then randomised and NGFR and Egr-1 labelling in the urothelium were scored by persons (n = 3) not involved in the immunohistochemical labelling process against a pre-defined scoring criteria.

3.3.1.1 NGFR scoring

- 1- Low NGFR - No or minimal NGFR labelling in the basal urothelial layer only
- 2- Basal NGFR - NGFR labelling present in most/all the basal cells of the urothelial layer
- 3- Basal and intermediate NGFR - NGFR labelling present in all basal cells and expansion into the intermediate urothelium in places
- 4- Intense basal and intermediate – Intense NGFR labelling observed throughout the basal and intermediate urothelium

3.3.1.2 Egr-1 scoring

- 1- No Egr-1 immunoreactivity. No nuclear Egr-1 immunolabelling. A granular cytoplasmic staining may be observed
- 2- Weak Egr-1 positive – weak Egr-1 immunolabelling in a minority of urothelial nuclei. Occasional urothelial nuclei may exhibit relatively intense Egr-1 immunolabelling, and this can present as rare, relatively intense labelled foci in the urothelial layer
- 3- Moderate Egr-1 positive – the majority of urothelial nuclei exhibit moderate Egr-1 immunolabelling
- 4- Strong Egr-1 positive – Essentially all urothelial nuclei exhibit strong Egr-1 immunolabelling

The scoring criteria were available to the person in written format throughout the scoring process. Graph Pad Prism 6 software was used for analysis. The regression analysis between Egr-1 and NGFR labelled specimens was calculated using Graph Pad Prism 6 software.

3.4 Results

3.4.1 NGFR and Egr-1 expression in normal urothelium

NGFR was expressed by basal urothelial cells in both ureteric (n=5) and bladder samples (n=5). In the ureteric samples NGFR was expressed consistently throughout the basal layer of the urothelium (figure 3.1 A-E). The expression of NGFR in the bladder samples was more inconsistent with areas of basal urothelium negative (figure 3.1 F-J). There was never any extension observed into the intermediate and superficial urothelial cells in either the ureteric or bladder samples. In some samples in both ureteric and bladder groups there was some stromal labelling of NGFR.

Egr-1 was displayed as granular cytoplasmic staining with occasionally positive nuclei in ureteric samples (n=3) (figure 3.2 A-C). There was some variation in the expression

of Egr-1 in the normal bladder samples (n=3) which appeared to be more densely labelled with cytoplasmic granules and an increased number of positive nuclei compared to the ureteric samples (figure 3.2 D-F). There was also some stromal labelling in both the normal bladder and ureteric samples.

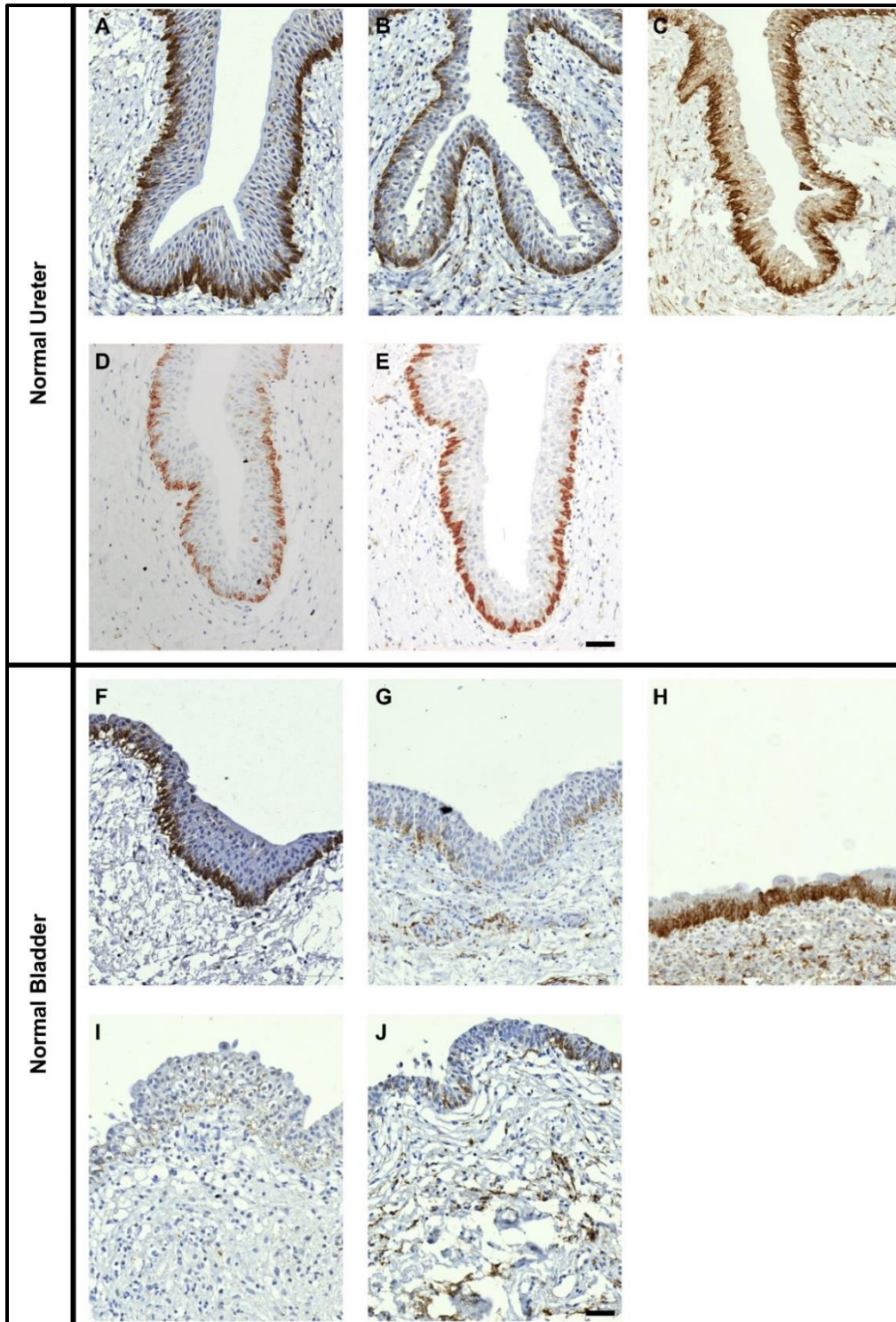


Figure 3-1 NGFR expression in normal bladder and normal ureter sections

Immunohistochemistry of normal ureter and bladder sections labelled for NGFR. NGFR was seen in all basal cells in the ureteric sections (A-E). Labelling in bladder sections (F-J) was also only seen in the basal urothelial cells but displayed a more inconsistent pattern. A – Y1288, B – Y1297, C – Y1304, D – Y1216, E – Y1424, F – Y1075, G – Y1189B, H – Y1303, I – Y998, J – Y994. Scale = 50µm.

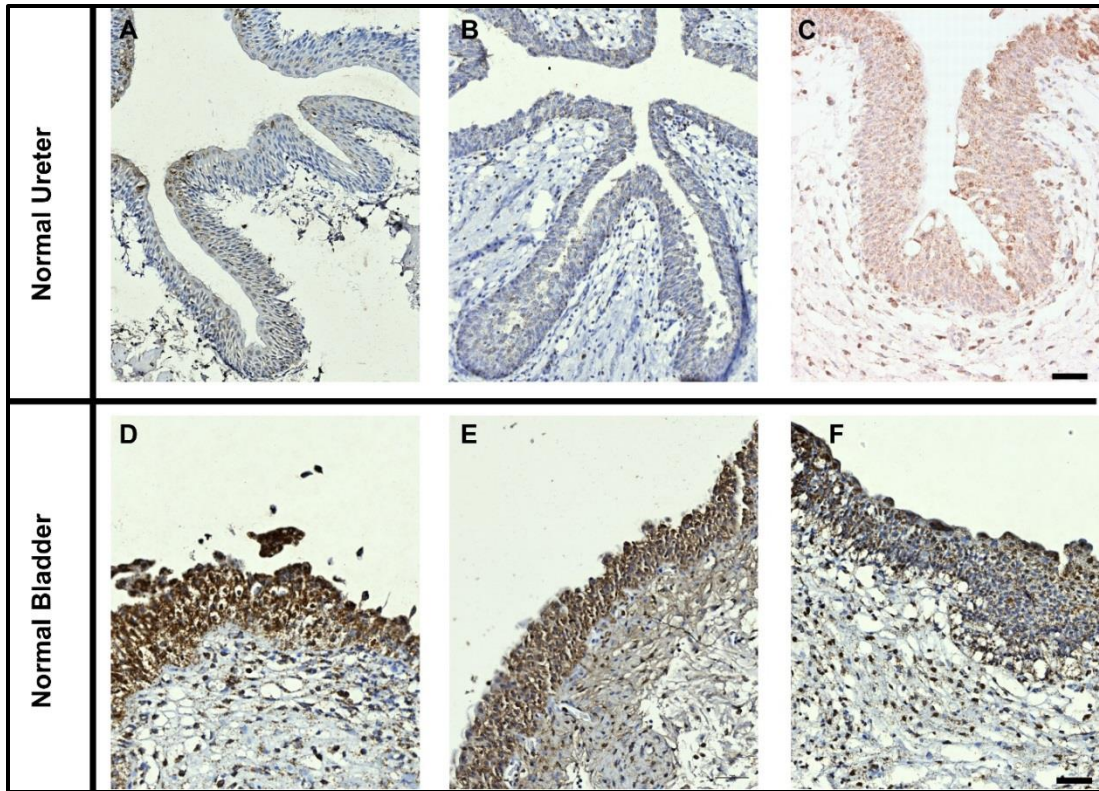


Figure 3-2 Egr-1 expression in normal bladder and normal ureter sections

Immunohistochemistry of normal ureter and bladder sections labelled for Egr-1. Normal ureter sections (A-C) displayed cytoplasmic granules with the occasional densely positive nuclei illustrated in section C. Normal bladder sections (D-F) were more densely labelled with cytoplasmic granules and an increased number of positive nuclei compared to the normal ureter. A – Y1288, B – Y1297, C – Y1216, D – Y1189B, E – Y998, F – Y994. Scale = 50µm.

3.4.2 NGFR and Egr-1 expression in KIC in situ

3.4.2.1 Semi-quantified analysis of NGFR expression

In the KIC samples (n = 24) the urothelium was often damaged and in 10 samples there was complete loss of the urothelium on histological examination (figure 3.3). In the remaining 14 samples the majority of the superficial urothelial cells were lost. Expansion of NGFR expression from the basal into the intermediate urothelial cells was noted in a number of samples. Semi-quantified analysis (section 3.3.1) was used to establish the extent of NGFR up regulation in the samples. KIC samples (n = 14) were compared using a defined scoring criteria (see below) with normal bladder (n = 3) and normal ureteric samples (n = 2).

NGFR scoring criteria:

- 1- Low NGFR - No or minimal NGFR labelling in the basal urothelial layer only
- 2- Basal NGFR - NGFR labelling present in most/all the basal cells of the urothelial layer
- 3- Basal and intermediate NGFR - NGFR labelling present in all basal cells and expansion into the intermediate urothelium in places
- 4- Intense basal and intermediate - NGFR labelling observed strongly throughout the basal and intermediate urothelium

The control samples displayed either low NGFR (1) expression (bladder samples) or basal NGFR (2) expression (ureteric samples). In the KIC samples, 12 displayed either basal and intermediate NGFR (3) or intense basal and intermediate NGFR (4) (figure 3.4). Statistical testing was not performed as the data was class/group data in distinct categories with frequencies too low to support analysis.

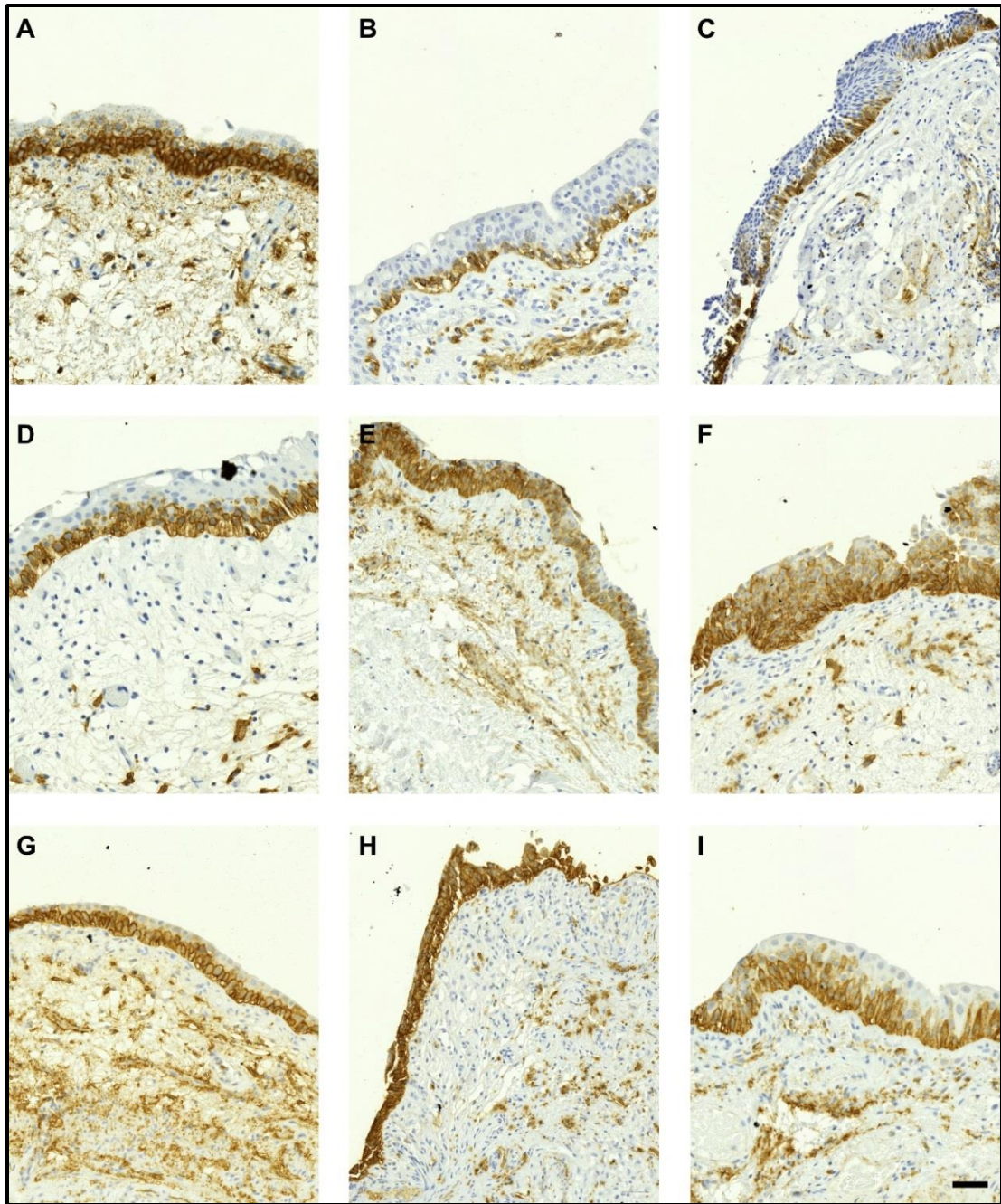


Figure 3-3 NGFR expression in KIC samples

NGFR immunohistochemistry labelling of KIC samples. The majority of samples displayed expansion of NGFR expression from the basal into the suprabasal urothelial layers (A, D, E, F, G, H and I) with some of the samples very intensely labelled for NGFR (E, F and H). Stromal labelling for NGFR is also notable in all the above samples. Scale = 50µm

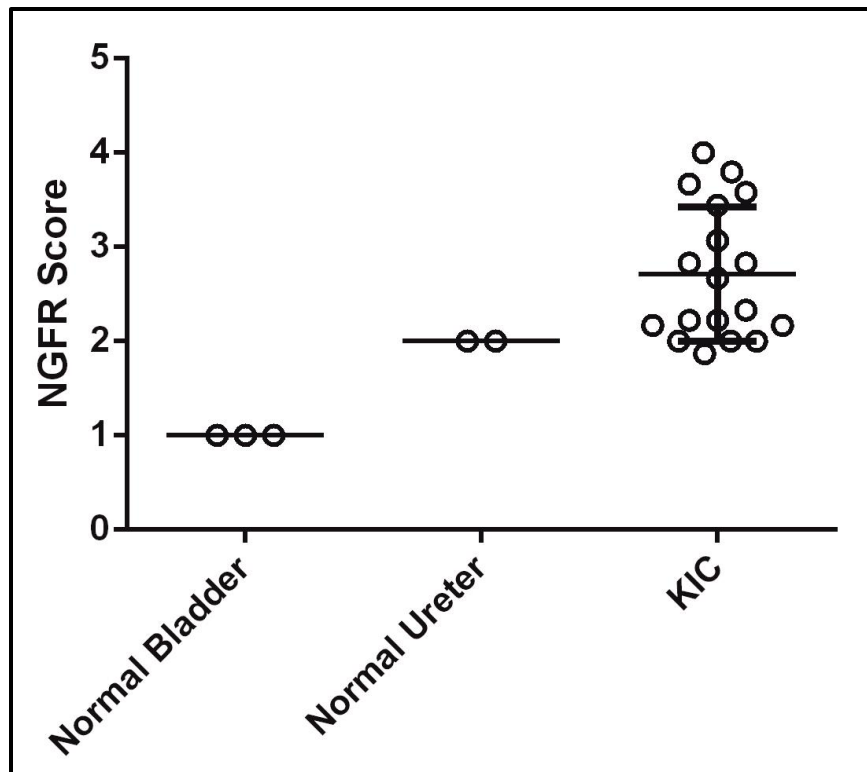


Figure 3-4 Scoring of NGFR expression in normal human urothelium and KIC in situ

Scoring of normal ureteric (Y1288, Y1297), normal bladder (Y994, Y998, Y1189) and KIC samples for NGFR expression. Points on the scatter graph represent the mean score for each sample from all 3 rankers. Using scoring criteria **1- Low NGFR** - No or minimal NGFR labelling in the basal urothelial layer only; **2-Basal NGFR** – NGFR labelling present in most/all the basal cells of the urothelial layer; **3- Basal and intermediate NGFR** – NGFR labelling present in all basal cells and expansion into the intermediate urothelium in places; **4 – Intense basal and intermediate** - NGFR labelling observed strongly throughout the basal and intermediate urothelium. Normal bladder samples scored 1- Low NGFR whereas normal ureteric samples scored 2 – basal NGFR. Variation was seen in the KIC samples. The points in the KIC samples are on average higher than the normal samples. In all scatter plots individual points indicate scoring means, and error bars show +/- one standard deviation.

3.4.2.2 Egr-1 expression and semi-quantified analysis

The same panel of KIC samples were used for analysis of Egr-1 labelling (n = 24). As previously stated there was complete loss of the urothelium in 10 of the samples from the panel. Expression of Egr-1 was variable in the remaining KIC samples which ranged from intense nuclear labelling to minimal cytoplasmic labelling (figure 3.5). Semi-quantified analysis (section 3.3.1) was used to establish the extent of nuclear labelling in the Egr-1 samples (figure 3.6). The KIC samples (n = 14) were compared using the defined scoring criteria (see below) with normal bladder (n = 3) and normal ureteric samples (n = 2).

Egr-1 scoring criteria:

- 1- No Egr-1 immunoreactivity. No nuclear Egr-1 immunolabelling. A granular cytoplasmic staining may be observed
- 2- Weak Egr-1 positive – weak Egr-1 immunolabelling in a minority of urothelial nuclei. Occasional urothelial nuclei may exhibit relatively intense Egr-1 immunolabelling, and this can present as rare, relatively intense labelled foci in the urothelial layer
- 3- Moderate Egr-1 positive – the majority of urothelial nuclei exhibit moderate Egr-1 immunolabelling
- 4- Strong Egr-1 positive – Essentially all urothelial nuclei exhibit strong Egr-1 immunolabelling

The normal bladder control samples displayed weak to moderately intense (mean = 3) Egr-1 labelling. The normal ureter control samples displayed a weaker intensity of labelling with either no Egr-1 reactivity or weak Egr-1 immunoreactivity (mean = 1). The KIC samples displayed a range of Egr-1 immunoreactivity: 7 out of the 14 samples displayed moderate to strong Egr-1 positivity, 4 samples displayed weak Egr-1 positivity and 3 samples displayed no Egr-1 immunoreactivity (figure 3.6). Statistical testing was not performed as the data was class/group data into distinct categories with frequencies too low to support statistical analysis.

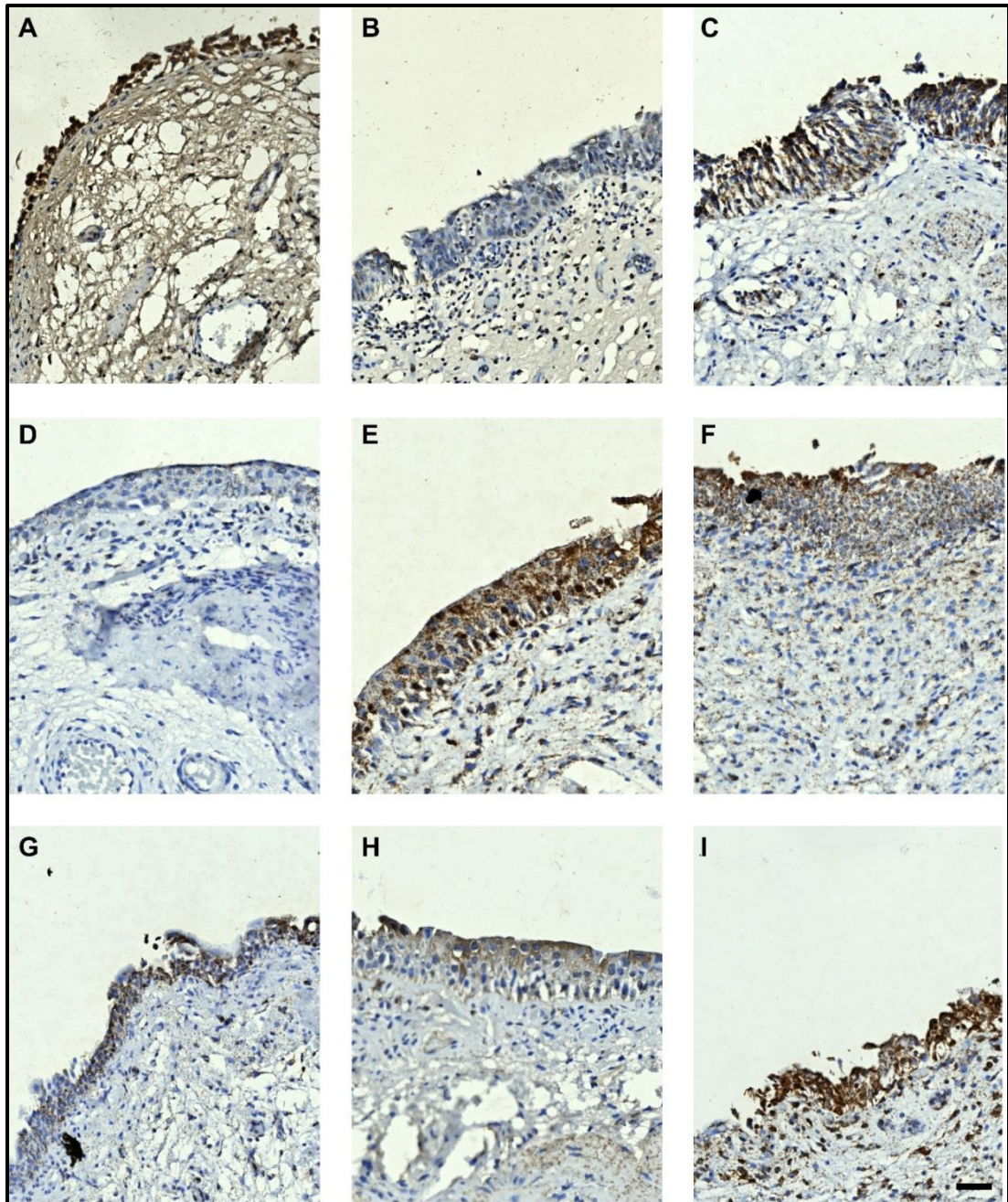


Figure 3-5 Egr-1 expression in KIC samples

Egr-1 immunohistochemistry labelling in KIC samples. Variation was seen between all samples with some samples displaying strong nuclear labelling (A, C, I). Cytoplasmic or minimal labelling was seen in the remaining samples (E, F, G, H) with some showing very little cytoplasmic labelling (B, D). Scale = 50 μ m

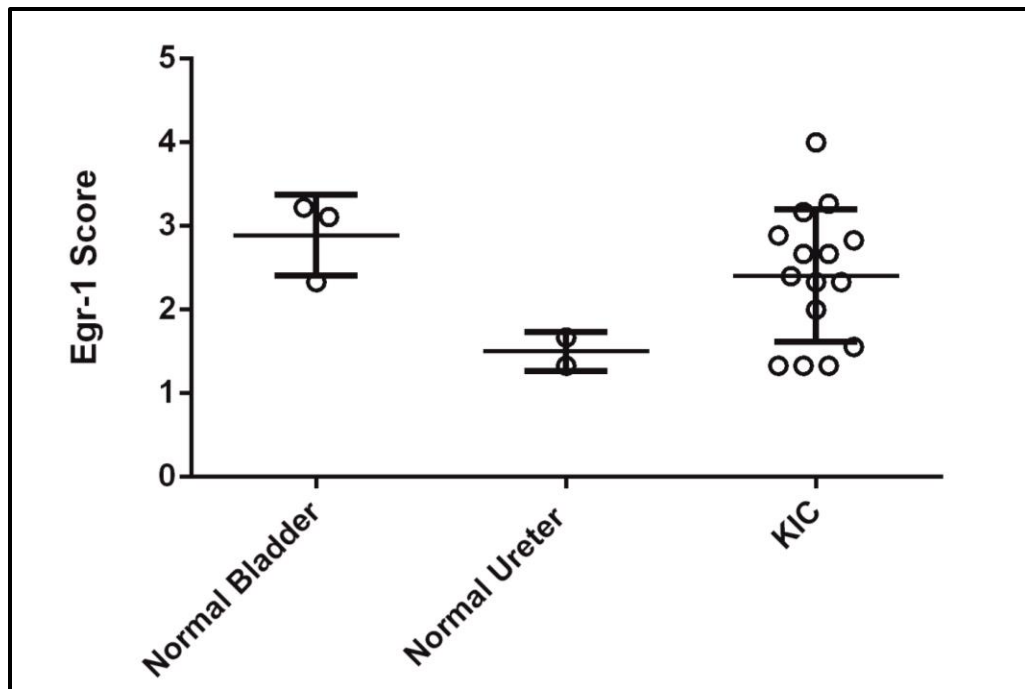


Figure 3-6 Scoring of Egr-1 expression in normal human urothelium and KIC in situ.

Scoring of normal ureteric (Y1288, Y1297), normal bladder (Y994, Y998, Y1189) and KIC samples for Egr-1 expression. Points on the scatter graph represent the mean score for each sample from all 3 rankers. Egr-1 immunolabelling was scored according to predefined scoring criteria: **1 - No Egr-1 immunoreactivity**. No nuclear Egr-1 immunolabelling. A granular cytoplasmic labelling may be observed; **2 - Weak Egr-1 positive** – weak Egr-1 immunolabelling in a minority of urothelial nuclei. Occasional urothelial nuclei exhibited relatively intense Egr-1 immunolabelling, and this can present as rare, relatively intensely staining foci in the urothelial layer; **3 - Moderate Egr-1 positive** – the majority of urothelial nuclei exhibit moderate Egr-1 immunolabelling; **4 - Strong Egr-1 positive** – Essentially all urothelial nuclei exhibit strong Egr-1 immunolabelling normal bladder samples displayed weak to moderate intensity labelling. The ureteric samples displayed a lesser degree of nuclear labelling in comparison to the normal bladder samples. The KIC samples displayed a variety of scores ranging from 1-4. In all scatter plots horizontal lines indicate means, and error bars show +/- one standard deviation.

3.4.2.3 Linear regression analysis of Egr-1 and NGFR samples

A simple linear regression analysis was conducted to establish if there is a relationship between Egr-1 and NGFR in KIC in situ samples (figure 3.7). The analysis resulted in a R^2 value of 4.4×10^{-6} which signifies no correlation of Egr-1 and NGFR in the KIC samples used in the analysis.

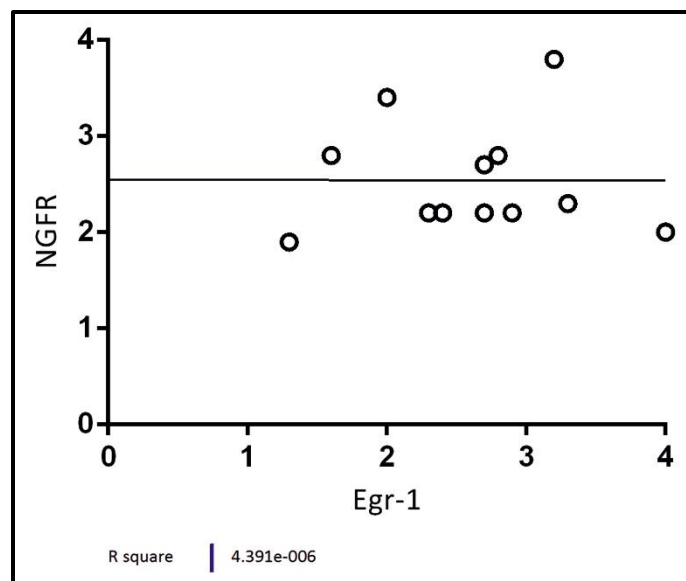


Figure 3-7 Linear regression analysis of NGFR and Egr-1 samples

Linear regression analysis of NGFR and Egr-1 expression in KIC samples in situ showing no relationship between Egr-1 and NGFR ($R^2 = 4.4 \times 10^{-6}$). Therefore in these samples Egr-1 does not directly modulate the expression of NGFR in KIC.

3.5 Results Summary

- NGFR was expressed in basal layer of urothelial cells in both normal ureter and bladder. The expression in the normal bladder was less consistent.
- NGFR expression was never in intermediate or superficial urothelial cells of the normal bladder and ureter specimens.
- NGFR expression was detected in the stroma of some samples, particularly in disease cases.
- Egr-1 was expressed mainly in the cytoplasm of normal ureter with occasional positive nuclei, in normal bladder there was more intense expression with increased number of positive nuclei.
- There was basal expansion of NGFR into the intermediate urothelial cells in the KIC samples compared to normal bladder and ureter controls.
- There was no significant increase in the expression of Egr-1 in the KIC samples compared to normal bladder and ureter controls.
- Simple linear regression calculation did not reveal a link between Egr-1 and NGFR expression.

4 NGFR in KIC – Case study

4.1 Introduction

Ketamine-induced cystitis (KIC) was first reported in 2007 (Shahani et al., 2007). A retrospective review one year later concluded that KIC was a syndrome of cystitis and contracted bladder which could be associated with street-ketamine abuse. The review was unable to establish the precise cause and incidence of KIC (Chu et al., 2008b). The clinical syndrome includes bladder pain, urinary frequency and reduced bladder capacity. This can progress to incontinence and renal damage and may be associated with hepatic dysfunction (Chu et al., 2008a, Shahani et al., 2007).

The main histological findings reported on KIC describe extensive urothelial damage with urothelial ulceration and marked chronic inflammatory changes with infiltrations of lymphocytes and variable number of eosinophils (Chen et al., 2011, Lai et al., 2012, Oxley et al., 2009). Furthermore, Oxley et al remarked that the urothelial atypia was so marked it mimicked carcinoma in situ (CIS) with the typified nuclear enlargement and increased expression of Ki67 and p53 on immunohistochemical analysis (Oxley et al., 2009). In 2013, Baker et al examined a series of twenty one KIC biopsies and cystectomy samples (including re analysis of the seventeen biopsy samples from Oxley et al., 2009) and concluded that the severe bladder pain associated with KIC may be due to a combination of compromised urinary barrier and widespread nerve hyperplasia in the bladder wall (Baker et al., 2013). This study also showed an expansion of NGFR receptor expression in the urothelium of the KIC patients. Chapter 3 of this thesis examined the same series of samples as Baker et al and concluded that there was basal expansion of NGFR from basal into intermediate and even superficial cells where preserved. To date in the literature there is no complete examination of a bladder removed for the management of KIC. Extensive analysis of a bladder would allow for examination of the changes in the urothelium and underlying stroma in different areas (anterior/posterior and superior/inferior) and furthermore the identification of any histopathological anomalies such as von Brunn's nests and the presence of a urachal

remnant. The urachus is a fibrous embryonic remnant of the fetal allantois: a canal that drains the urinary bladder in the fetus. It extends from the posterior aspect of the umbilicus to the apex of the bladder and it is present in one third of adults as a normal variant. The epithelial lining is mixed with areas of transitional urothelium and focal areas mucinous glandular metaplasia (Cappele et al., 2001). Von Brunn's nests are defined as groups of urothelial cells within the lamina propria and submucosa which can be considered a normal variant or can arise as a result of local inflammation and during reactive proliferative change.

4.2 Aim

The aim of this study was to evaluate the clinical presentation, investigation and management path of a patient with severe KIC and to perform regional histological analysis of the KIC bladder after removal during substitution cystoplasty.

4.3 Experimental approach

Patient X was referred to a consultant urological surgeon (SF) at the James Cook University Hospital, Middlesbrough for management of his painful bladder thought to be due to the chronic use of ketamine. In writing this report the patient's case notes, investigations including blood test results, urinalysis and radiological images were collated.

The complete sample obtained following substitution cystoplasty was divided at the time of surgery into anterior and posterior segments. These segments were formalin fixed for 5 days. At the end of this period the anterior section was dissected into 12 pieces and the posterior section was dissected into 16 pieces and the pieces were embedded into paraffin wax. 5µm sections were dewaxed in xylene and rehydrated through ethanol to water before being stained with haematoxylin and eosin (methods section 2.3.3). Immunohistochemical analysis was then performed using

the standard immunoperoxidase technique detailed in section 2.4.1. Signal amplification for NGFR was required using a tyramide-based catalysed signal amplification kit (Dako; Catalogue number: k1500) or ImmPRESS™ Excel staining kit (Vector Laboratories; Catalogue number: MP-7602) which were used according to manufacturers' instructions to improve the sensitivity of antibody labelling detection (methods section 2.4.2).

4.4 Results

Patient X, a 30-year-old male, presented to SF initially in 2008 with an 18-month history of dysuria, haematuria, frequency and urgency. The frequency was very debilitating with a painful urge to void approximately every 30 minutes persisting through the night. The patient gave a history of chronic ketamine abuse starting initially as a recreational weekend user in 2003 and becoming a more frequent user after approximately 2 years. Initially he was only using ketamine at weekends but his usage increased to everyday as he found that the use of ketamine helped to relieve his bladder pain. During his time of chronic abuse he could use several grams per day. He was an otherwise fit and well male with no significant urological or other past medical history. Initial examination did not reveal any abnormality.

Preliminary investigations included blood tests: full blood count (FBC), urea and electrolytes (U+E) and liver function tests (LFT) including gamma-glutamyl transpeptidase (GGT). The FBC and U+E did not reveal any abnormality. All the LFT markers were in the normal range apart from the GGT which was elevated to 132U/L (reference range 1-78U/L). Urinalysis was performed for microscopy, culture and sensitivity which showed 4 per μ l white blood cell and 2 per μ l red blood cells with no significant bacteriuria detected. A further urine sample was also sent for cytological analysis and displayed few scattered squamous epithelial and urothelial cells, plus the occasional inflammatory cell and red blood cell. Radiological investigations included an ultrasound scan (USS), which demonstrated a normal upper urinary tract. A video urodynamic investigation (VUD) was performed which,

on filling (25ml/min), displayed a severe urge to void at only 40ml in the bladder. Screening demonstrated grade 3 vesicouretericreflux (retrograde passage of urine from the bladder to the ureter) on the left and grade 1 on the right.

Initial management included establishing that the patient had stopped abusing ketamine and simple analgesics. He was also commenced on Pentosan Polysulphate a glycosaminoglycan (GAG) analogue designed to reline the bladder. Despite the cessation of ketamine use (patient's verbal statement and fall in GGT) and the use of Pentosan Polysulphate, the symptoms did not improve to a significant extent over a period of several months. At this point he did relapse and begin using ketamine again and this was consistent with a rise in GGT to 250U/L. He also failed to attend several follow up appointments.

On re-presentation approximately 9 months later he had once again ceased his use of ketamine and had a normal GGT of 33U/L. He had also noted at this stage that he had passed grit like material whilst passing urine. A CT KUB (kidney, ureter, bladder) was organised which reported a markedly contracted bladder with calcification in the wall. There was no evidence of ureteric or renal calcification (figure 4.1). The patient also had a cystoscopy and biopsy under general anaesthetic that revealed a shrunken grossly inflamed bladder with capacity of 90ml before pain was elicited. At the base of the bladder there were multiple pieces of calcified debris and some pieces were also noted to be adherent to the mucosa in the dome of the bladder. At this point the patient was considered to have end stage disease and that the bladder was not going to improve with medical therapy; he was therefore offered surgical treatment in the form of either an ileal conduit urinary diversion or a subtotal cystectomy and substitution cystoplasty. The patient elected to have a substitution cystoplasty, a major procedure in which the majority of the bladder is removed and replaced with a new reservoir configured from bowel. The patient would then be reliant on lifelong intermittent self-catheterisation (ISC) for bladder drainage.

During the substitution cystoplasty procedure the bladder was noted to be shrunken and grossly abnormal with the peri-vesicular fat firmly adhered to the outside of the bladder wall. There were obvious chronic and acute inflammatory changes with

extensive bleeding noted from the urothelial surface of the bladder on dissection. The anterior and posterior segments of the bladder were obtained and placed directly into formalin for fixation and routine processing and sectioned as illustrated in figure 4.2 for further analysis. The substitution cystoplasty proceeded without complication and the patient was discharged 10 days after the procedure. At initial outpatient clinic review the patient was found to be doing very well and not experiencing any difficulties with ISC.

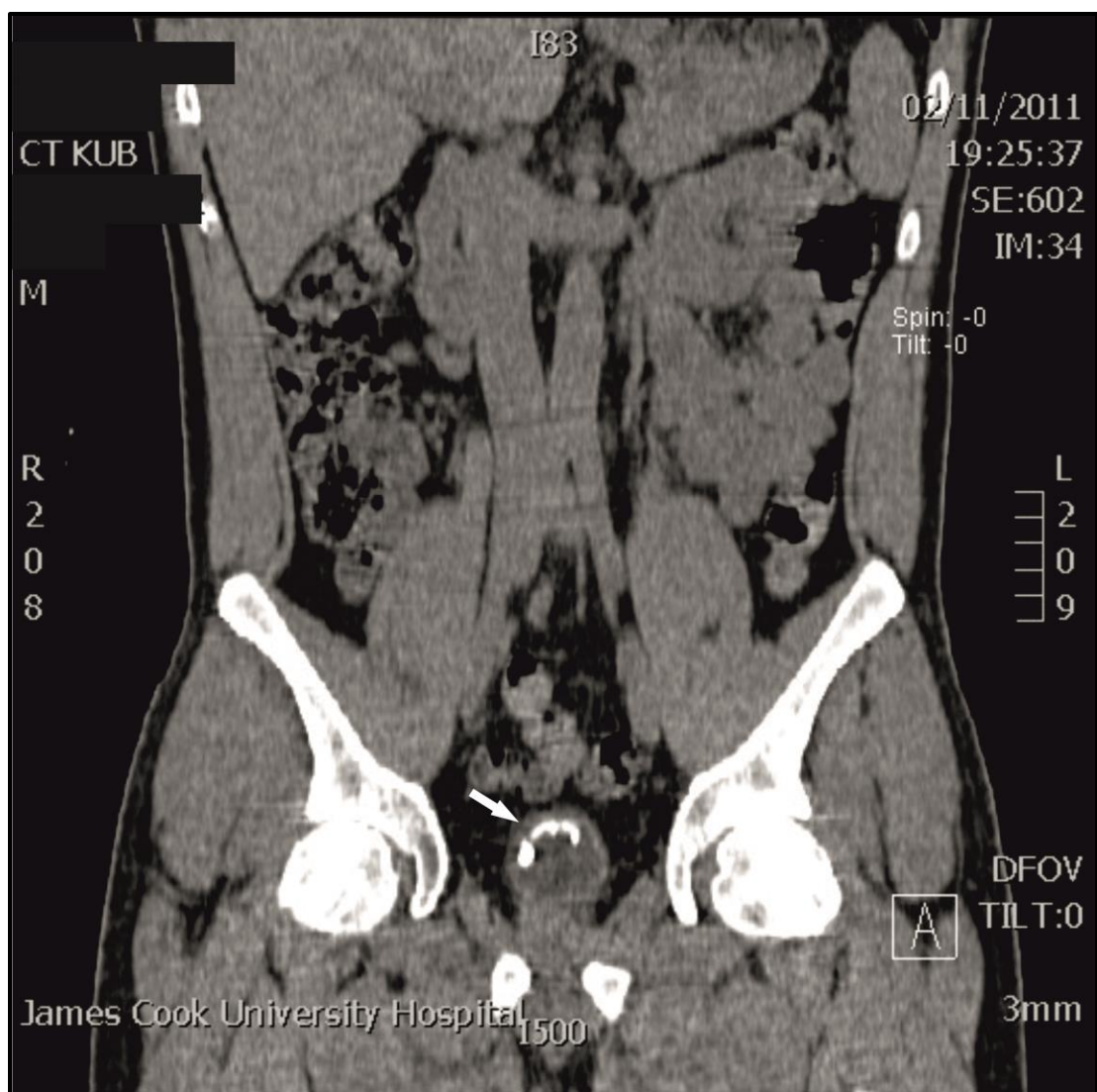


Figure 4-1 CT KUB in end stage KIC

CT KUB from patient X with KIC considered to be end stage disease. CT KUB displayed a small contracted bladder (arrowed) with calcification in the bladder wall. Upper tracts not displayed did not show any evidence of ureteric or renal calcification.

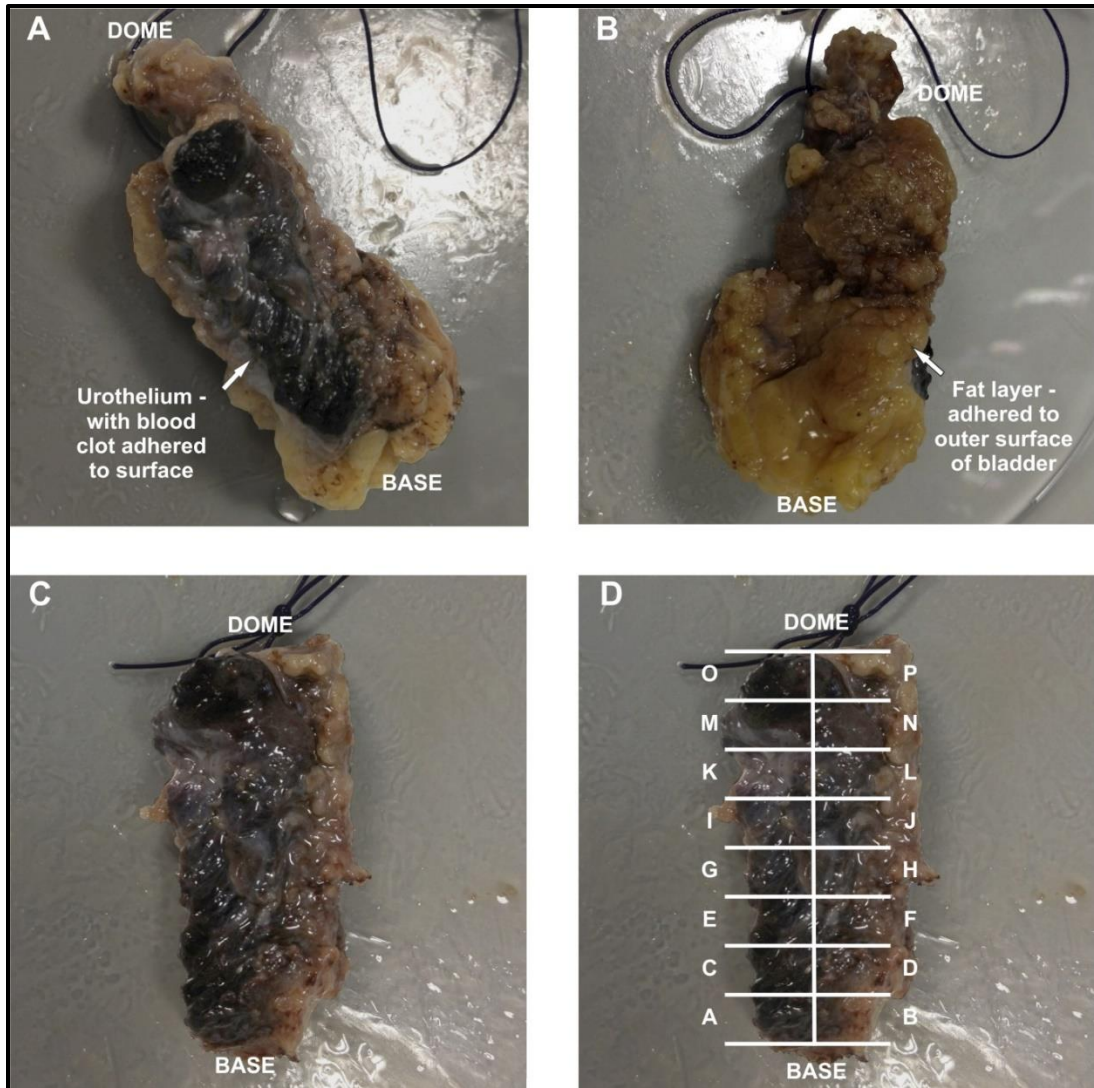


Figure 4-2 Macroscopic images of resected bladder of patient with KIC

Posterior aspect of a bladder taken during substitution cystoplasty for patient with ketamine induced cystitis. **A** - Internal surface of the bladder taken displaying urothelium with adhered clot. Dome and base as marked on the diagram (base incision around 5mm above the ureteric orifices). **B** - External surface of the bladder with pathologically adhered perivesicular fat due to chronic inflammation. Detrusor muscle also noted to be abnormally thickened. **C** - Sample after dissection of the perivesicular fat layer. **D** - Divisions of sample pieces for fixation embedding and histological analysis. A similar specimen was taken from the anterior portion of the bladder; the base incision was taken approximately 5mm above the bladder neck. The sample was divided into 12 sections (A-L), labelled from base to dome as the posterior sample above.

4.4.1 Haematoxylin and Eosin staining

Haematoxylin and eosin staining revealed extensive acute and chronic inflammatory changes (figure 4.3) with widespread loss of the urothelium throughout both the anterior and posterior surfaces of the bladder. There was an increase in small vessels towards the surface of the urothelium in many areas, consistent with chronic inflammatory change (figure 4.3 Anterior G and Posterior A, C and G). Some sections displayed areas of calcification which is considered a mark of chronic inflammatory change. There were several Von Brunn's nests noted (figure 4.3 posterior O), Von Brunn's nests represent areas of urothelium within the lamina propria and submucosa which can be considered a normal variant or can arise as a result of local inflammation and during reactive proliferative change. Acute haemorrhage was evident in some of the sections due to the operative procedure (Figure 4.3 Anterior B and D).

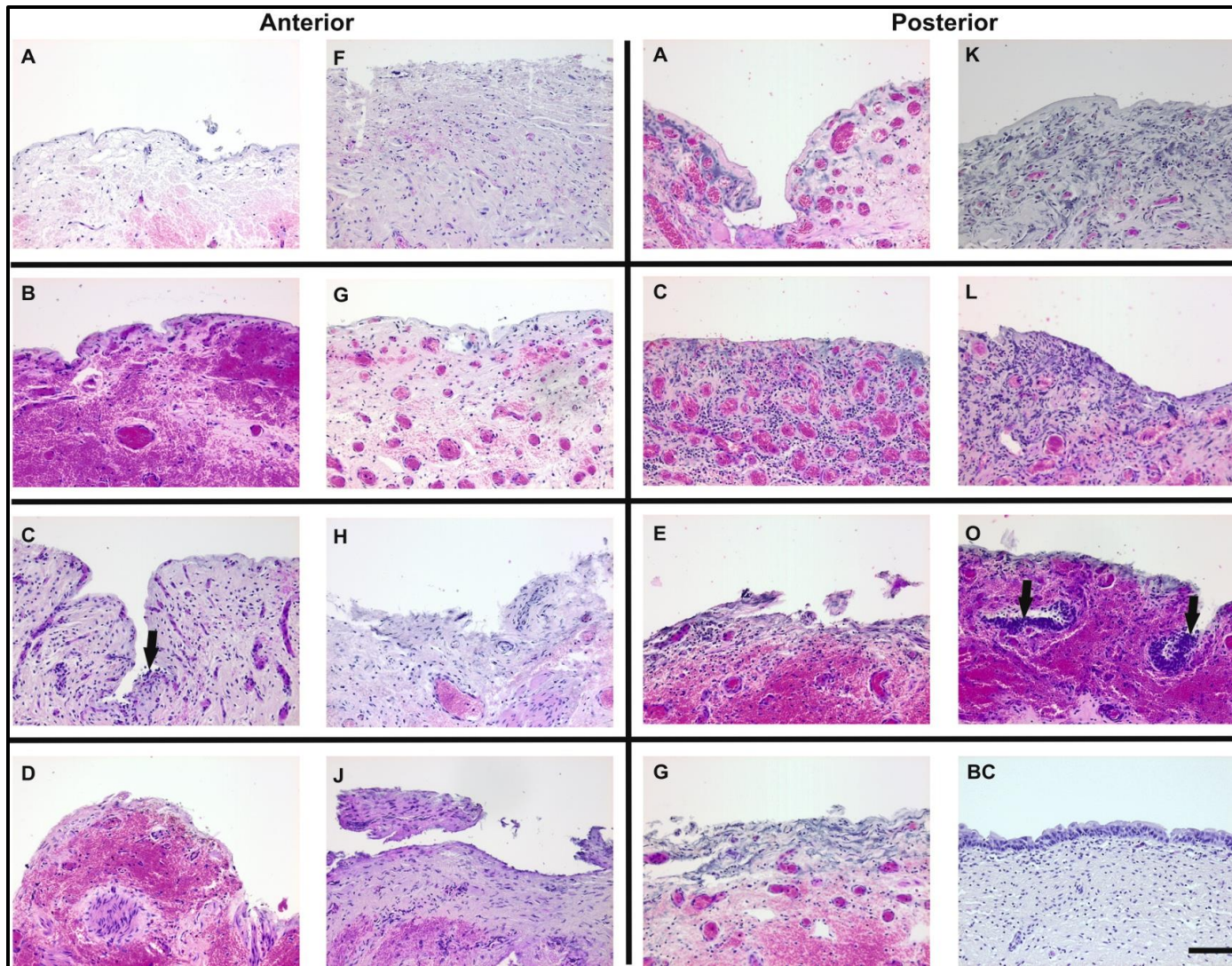


Figure 4-3 H&E staining of the case study KIC bladder

Sections from the anterior and posterior parts of the KIC bladder were stained with haematoxylin and eosin to display overall architecture and pathological features of the bladder. Labelled letters correspond with figure 4.2 – section **A** close to the base of the bladder and section **O** at the dome of the bladder. **BC** is the normal bladder control. Widespread destruction of the urothelium was noted with some acute haemorrhage due to the operative procedure in anterior sections **B** and **D**. Anterior **C** displayed scanty urothelial cells (arrow). The posterior sections (right side) **A**, **C**, **E** and **F** and section **G** in the anterior sections (left side) showed small vessels close to the surface of the bladder corresponding with chronic degenerative changes seen throughout the bladder. The H&E section in posterior **O** displayed two Von Brunn's nests (arrowed) which is consistent with chronic local inflammation and reactive proliferative changes; there was some urothelium evident in these. Scale = 100µm.

4.4.2 NGFR Labelling

Immunohistochemical labelling for NGFR demonstrated a few scanty positive urothelial cells (figure 4.4 Anterior C: arrow) however for the most part the bladder was completely denuded of urothelium. Within the stroma there was intense labelling for NGFR close to the surface which was not evident in the normal bladder control (figure 4.4 Anterior A,C,D,F,H,J Posterior A,C,E,G,L). Several sections displayed well defined peripheral nerve fascicles (figure 4.4 Anterior D: arrow).

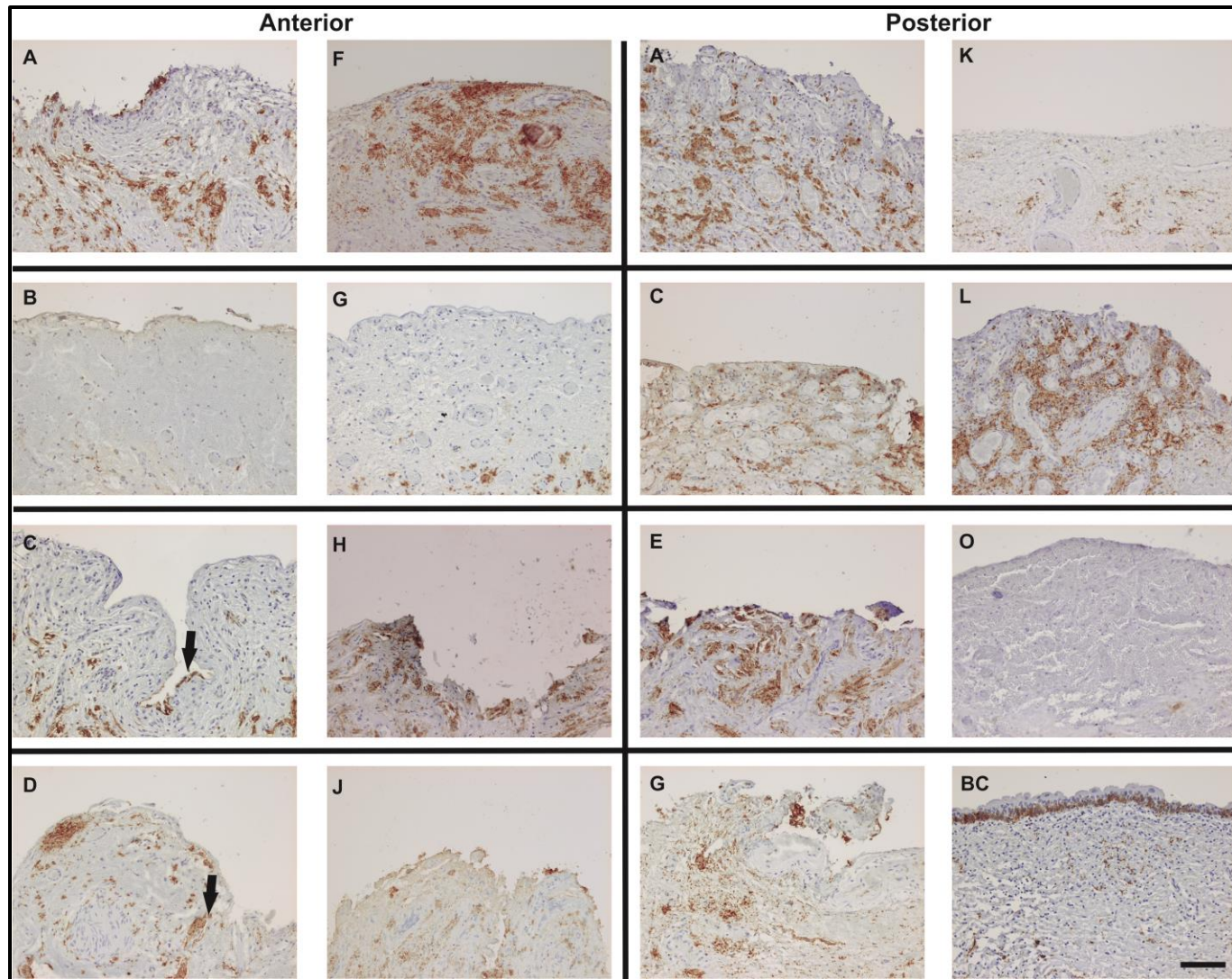


Figure 4-4 NGFR labelling on KIC bladder

Immunohistochemistry for NGFR in the KIC bladder. Letters correspond with figure 4.2: section **A** close to the base of the bladder and section **O** close to the dome of the bladder. Widespread destruction of the urothelium was noted throughout all the sections, some scanty urothelial cells (arrow) in anterior **C** were densely labelled with NGFR. A Peripheral nerve fascicle was evident in anterior **D** (arrow). Normal bladder control displays basal labelling of NGFR in the urothelium and low labelling intensity in the underlying stroma compared to the KIC samples. Scale = 100µm.

4.4.3 Urachus

The bladder (figure 4.2) obtained during the substitution cystoplasty displayed an obvious tortuous tubule with an irregular outline and a transitional cell epithelium (urothelium) in the posterior section at the apex of the bladder section O (Figure 4.2 C; figure 4.5). This is consistent with the known description and position of the urachus. The urachus is a fibrous embryonic remnant of the fetal allantois: a canal that drains the urinary bladder in the fetus. The urachus is present in all infants at birth and gradually regresses in most, a remnant being found in only approximately one third of adults and is considered a normal variant. Defective closure may give rise to pathological variants including complete fistula, cyst or sinus diverticulum. As no communication with the bladder was visualised on radiological imaging (figures 4.1 and 4.6) and there was no evidence of a pathological urachal remnant at the time of the surgery, it was therefore presumed to be a normal variant. The relevance to this study is that the lining of the urachus is of urothelium with areas of focal mucinous glandular metaplasia (Cappele et al., 2001). As there was no communication of the urachus to the bladder identified this allowed direct comparison of urothelium in contact with urine in the bladder and no urine contact in the urachus. This therefore, potentially would provide insight into whether the effects of ketamine are urinary-mediated.

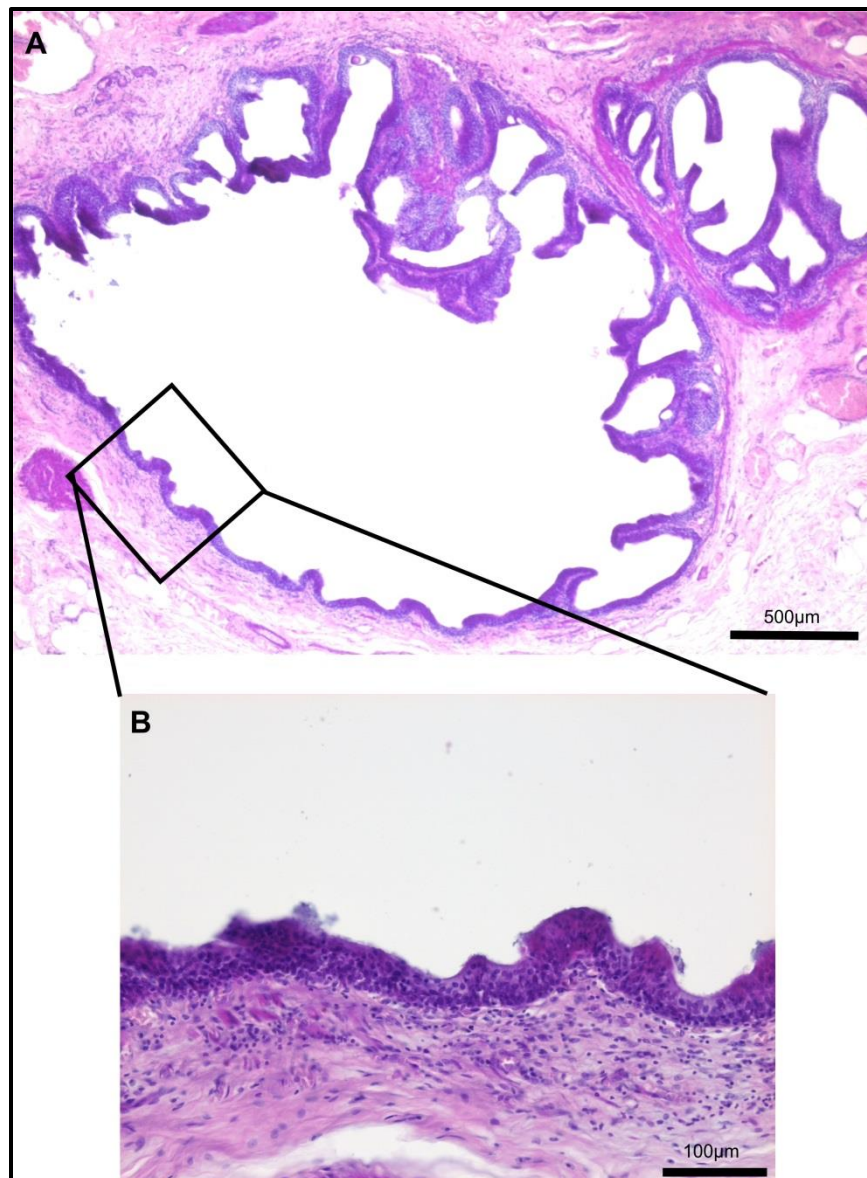


Figure 4-5 H+E staining of the urachus

Examination of H+E section from the dome of the bladder (posterior O from figure 4.2) revealed evidence of a patent urachus. The urachus is an embryological remnant resulting from involution of the allantoic duct and the ventral cloaca. It is lined with transitional epithelium and is present in one third of the adult population. The figure demonstrates a coiled tube like structure **A** with apparent full thickness urothelial lining **B**. Review of the radiological imaging did not suggest patent communication with the bladder cavity.



Figure 4-6 Intravenous urogram (IVU) from patient with KIC

IVU investigation from patient X with KIC. The contrast in the bladder gives a smooth outline with no irregularities at the dome which could signify a patent urachus. Contrast is also seen in the calyces and renal pelvis of the upper tracts (marked *).

4.4.4 Labelling of the Urachus

Further examination of the section containing the urachal remnant revealed several clusters of Von Brunn's nests at the urothelial surface with the basal and intermediate layers of urothelium intact (figure 4.3 Posterior O). Immunohistochemical labelling with NGFR displayed basal labelling of NGFR in the urachal remnant with some absent basal areas consistent with the normal NGFR expression in the bladder as previously described in chapter 3 of this thesis (figure 4.7 A). NGFR labelling within the Von Brunn's nests revealed basal labelling of the urothelial cells throughout with extension into the intermediate and remaining superficial cells in some areas (figure 4.7 B).

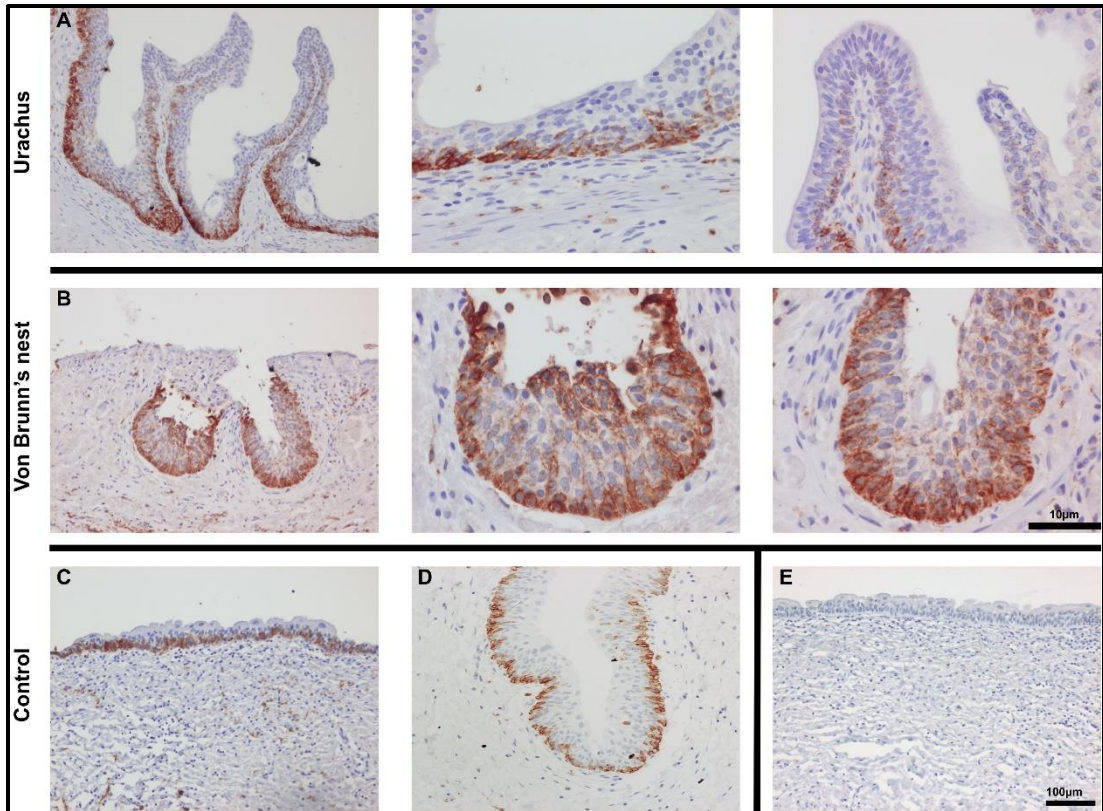


Figure 4-7 NGFR Labelling on Urachal remnant and in Von Brunn's Nests

Immunohistochemical labelling for NGFR on posterior section O at the apex of the bladder containing the urachal remnant (**A**) without communication to the surface of the bladder and several areas of Von Brunn's nests (**B**) at the surface of the urothelium. The urachus displayed basal labelling of NGFR with some negative areas consistent with normal expression in the bladder. The Von Brunn's nests displayed basal labelling of NGFR throughout the areas with some extension into intermediate urothelial cells. **C** and **D** = normal bladder and ureter controls. **E** = negative control.

The same section containing the urachal remnant and Von Brunn's nests was further analysed by immunohistochemistry for the presence of markers associated with urothelial differentiation including CK13 (figure 4.8) CK20 (figure 4.9) and a marker of terminal differentiation UPK3A (figure 4.10).

CK13 (figure 4.8) was expressed in the basal and intermediate cells in both the urachus (figure 4.8A) and Von Brunn's nests (figure 4.8B) similar to the expression in the native urothelium (Figure 4.8 C and D).

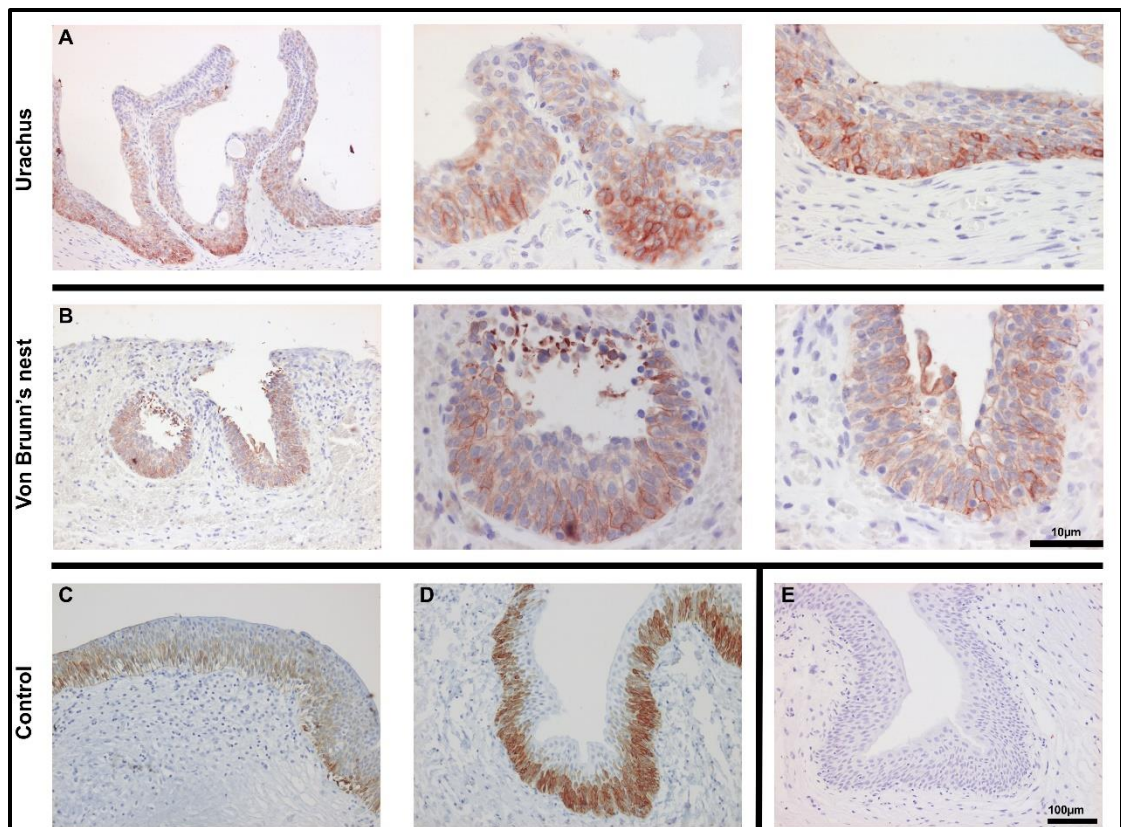


Figure 4-8 CK13 Labelling on Urachal remnant and in Von Brunn's Nests

Immunohistochemical labelling for CK13 on posterior section O at the apex of the bladder containing a urachal remnant (**A**) and several areas of Von Brunn's nests (**B**) at the surface of the urothelium. CK13 labelling was present in the basal and intermediate cells in both the urachus and Von Brunn's nests as seen in native urothelium (**C** and **D**). **E** = negative control.

Expression of CK20 is usually restricted to superficial urothelial cells (figure 4.9C and D). Within the urachus (figure 4.9A) and Von Brunn's nests (figure 4.9B) the expression of CK20 was completely absent.

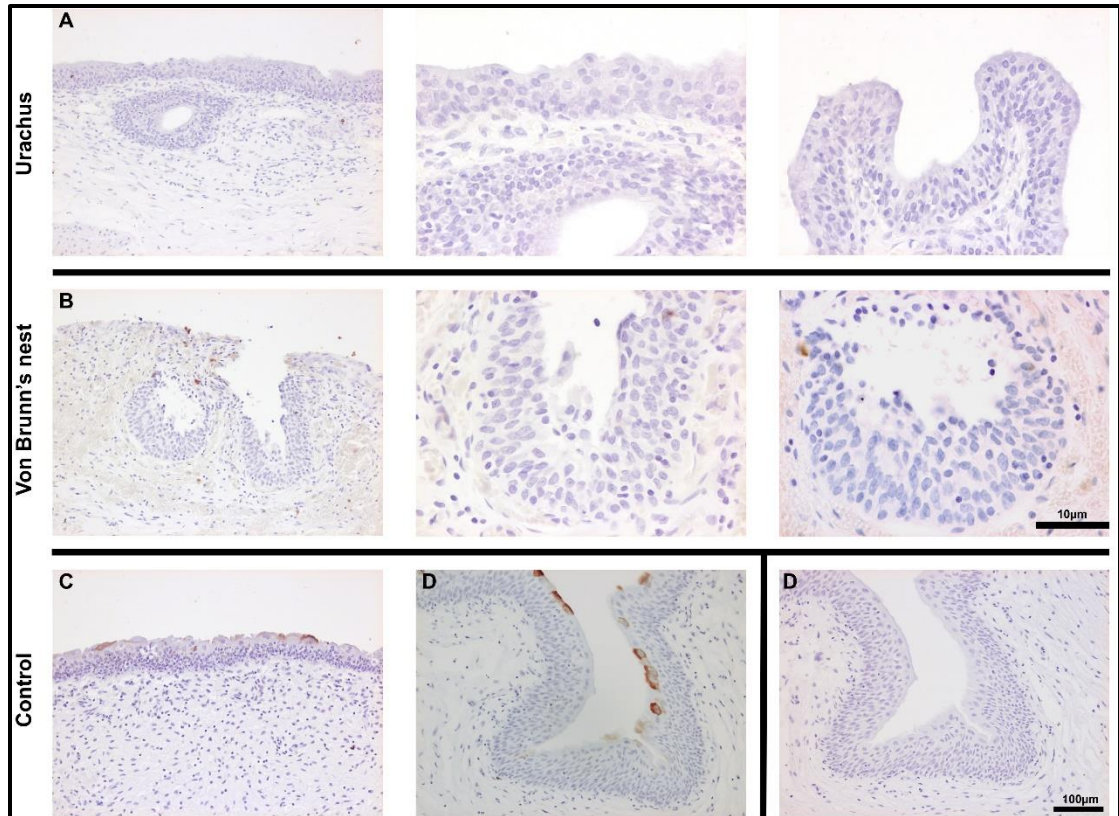


Figure 4-9 CK20 Labelling on Urachal remnant and in Von Brunn's Nests

Immunohistochemical labelling for CK20 on section posterior O at the apex of the bladder containing the urachal remnant (**A**) and several areas of Von Brunn's nests (**B**) at the surface of the urothelium. CK20 labelling is absent in the urachus and Von Brunn nests. **C** and **D** = normal bladder and ureter control respectively displayed labelling of CK20 in intermittent superficial cells. **E** = negative control.

Expression of uroplakin 3A is seen in the superficial apical-membrane in normal urothelium (figure 4.10 C and D). There was no expression of UPK3A in the Von Brunn's nests (figure 4.10B). The urachus had several areas where UPK3A expression was evident in the superficial apical-membrane which identified areas where the urothelial phenotype is present. However, it was not consistently seen throughout the urachus with large superficial areas negative (figure 4.10A). Inspection of the urachus epithelium revealed some columnar type cells not typical of urothelium.

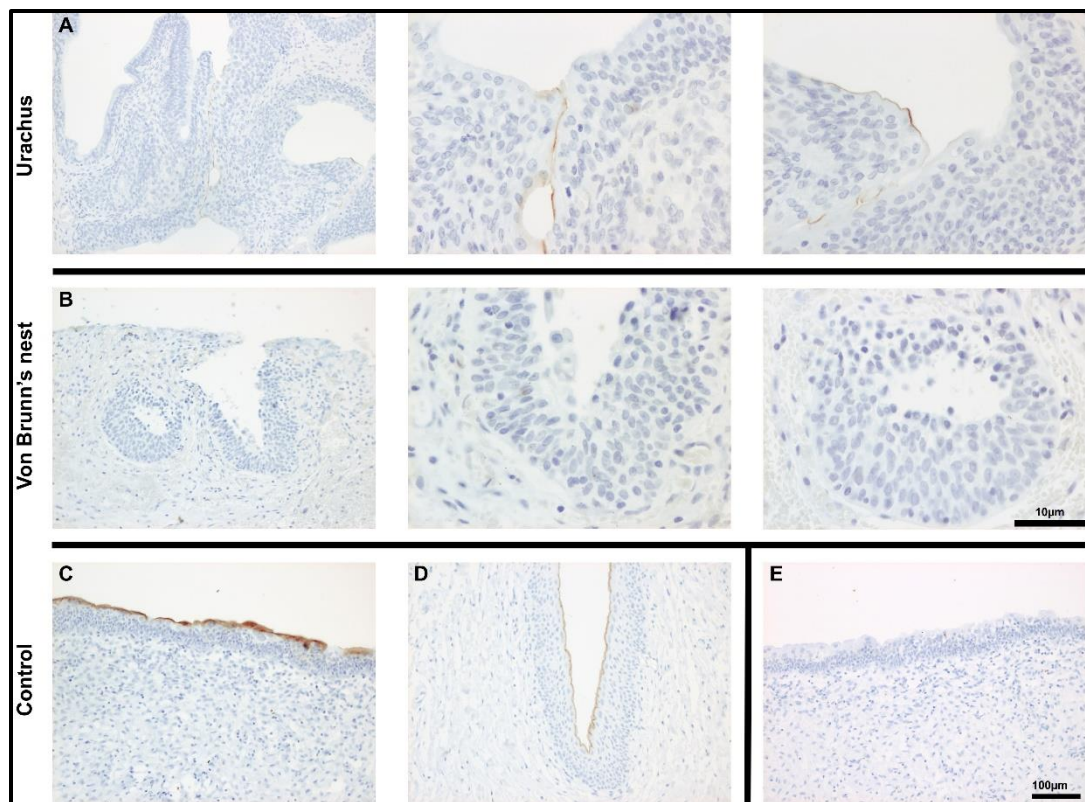


Figure 4-10 UPK3A Labelling on Urachal remnant and Von Brunn's Nests

Immunohistochemical labelling for UPK3A on posterior section O at the apex of the bladder containing the urachal remnant (A) without communication to the surface of the bladder and several areas of Von Brunn's nests (B) at the surface of the urothelium. The urachus displayed several areas of positive superficial apical-membrane labelling for UPK3A however there were large areas that were negative. The Von Brunn's nests were completely negative for UPK3A expression. C and D = normal bladder and ureter controls with superficial apical-membrane labelling. E = negative control.

4.4.5 Nerve distribution

As previously noted in figure 4.4 the KIC bladder had several defined peripheral nerve fascicles. Examination of the section containing the urachus at the apex of the bladder displayed several peripheral nerve fascicles labelled with NGFR which were mainly located in the lamina propria close to the urothelial lumen (figure 4.11). There was minimal expression of neurofilament protein (NFP); the few positive areas were again placed superficially in the lamina propria (figure 4.11). S100 protein was minimally expressed but fine S100⁺ nerve filaments were noted superficially in the lamina propria (figure 4.11)

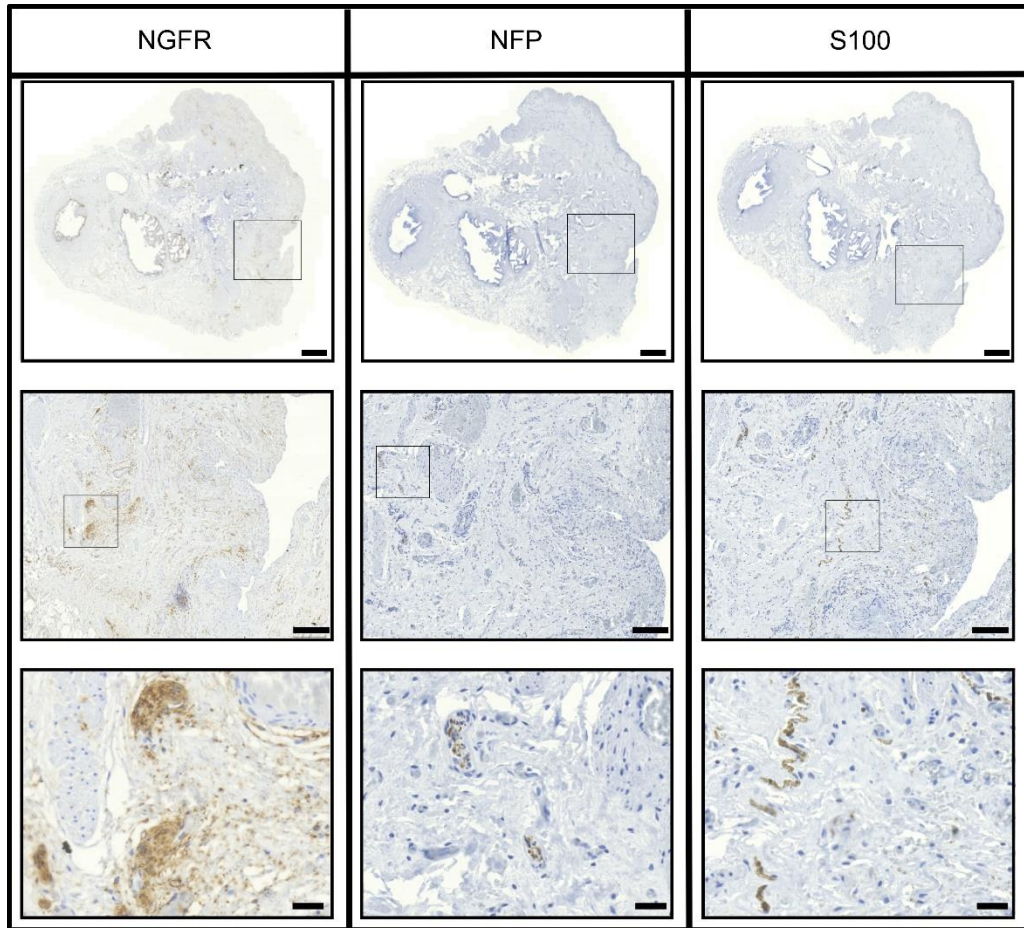


Figure 4-11 Representative peripheral nerve fascicle distribution

Immunohistochemical labelling for NGFR, NFP and S100 on posterior section O at the apex of the bladder containing the urachal remnant. There were several peripheral nerve fascicles labelled positively for NGFR. There was minimal expression of NFP and S100 and for both markers the maximal expression was evident in the superficial lamina propria. Scale bar = 200µm top two rows and 50µm bottom row.

4.4.5.1 Co-localisation of NGFR, NFP and S100

Examination of serial sections of nerve fascicles positive for NGFR revealed few areas of co-localisation for NFP and S100 (figure 4.12).

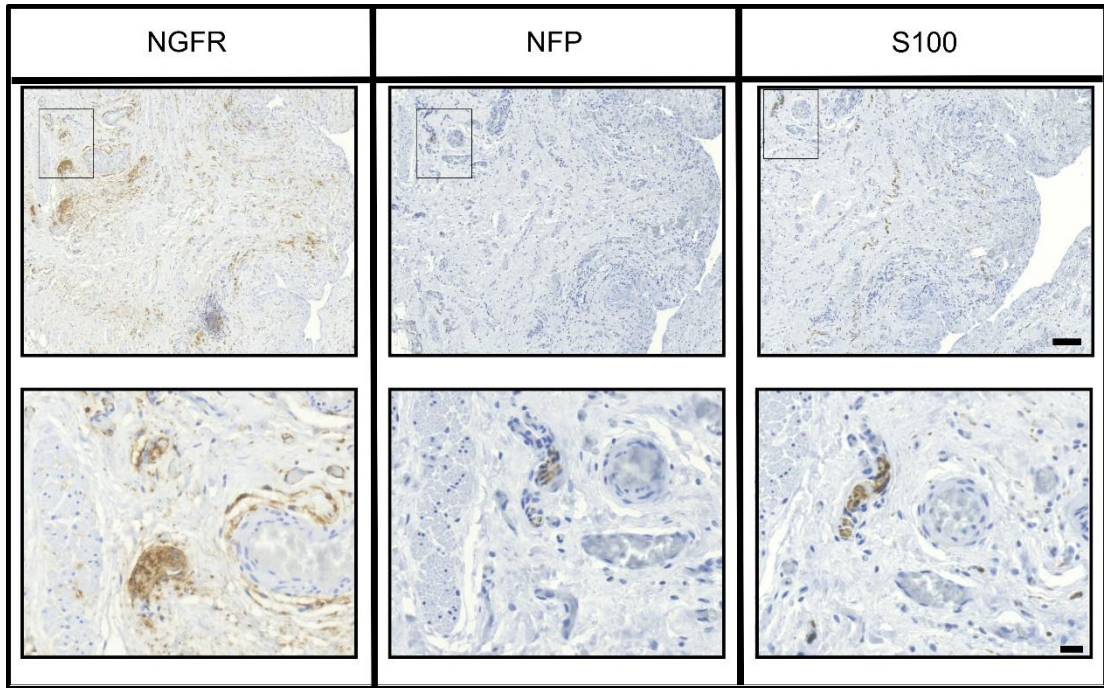


Figure 4-12 Co-localisation of NGFR, NFP and S100

Immunohistochemical labelling for NGFR, NFP and S100 on posterior section O at the apex of the bladder containing the urachal remnant. The section was examined to establish any areas of co-localisation within the three markers. As previously reported in figure 4.10 there was minimal expression of NFP and S100. The box in the NGFR section highlights the previous peripheral nerve fascicle in figure 4.10. The identical area was highlighted in the corresponding NFP and S100 and displayed a small area of co-localisation. Scale bar = top row 100 μ m and bottom row 20 μ m.

4.5 Results Summary

- Histological analysis of a KIC bladder at the end stage of the disease revealed widespread destruction of the urothelium, areas consistent with chronic inflammatory change including an increase in small vessels towards the surface of the urothelium, areas of calcification and the presence of Von Brunn nests.
- NGFR labelling of the same KIC bladder revealed scanty positive urothelial cells, intense stromal labelling close to the surface of the urothelium and several peripheral nerve fascicles.
- A remnant of the urachus was identified and shown to be non-patent with the bladder urothelium. The urachal remnant had basal labelling of NGFR consistent with normal urothelium. The urachal remnant also expressed areas of UPK3A and therefore a differentiated urothelial phenotype.
- Identification of Von Brunn nests in the same sample revealed extension of basal labelling of NGFR into the intermediate and remaining superficial urothelial cells.
- The urachus and Von Brunn nests were negative for the urothelial localisation marker CK20.
- There was evidence of peripheral nerve fascicles densely labelled with NGFR in section posterior O (containing urachal remnant) in the superficial lamina propria. There were some areas of co-localisation of nerves positive for NGFR, NFP and S100.

5 In-vitro expression of NGFR by urothelium

5.1 Introduction

As previously discussed in chapter 1 (section 1.5) the low affinity p75 nerve growth factor receptor (NGFR; p75^{NTR}; CD271) has widespread expression and functions throughout the central and peripheral nervous systems and in variety of other tissues in the body including the urinary tract ((Ruit et al., 1990, Verge et al., 1989, Mukai et al., 2000, Reis-Filho et al., 2006, Vizzard et al., 2000, Wezel et al., 2014). Chapter 3 showed NGFR to be basally expressed in the normal ureter and bladder with an expansion of NGFR into the intermediate and remaining superficial urothelial cells in samples obtained from patients with ketamine-induced cystitis (KIC) (section 3.4; (Baker et al., 2013). Furthermore, it has been shown to be up-regulated in the urothelium of neuropathic bladders and there is some evidence to suggest a regenerative function in the urothelium (Vaidyanathan et al., 1998b, Wezel et al., 2014, Cruz, 2013). Animal models have also identified an up regulation of NGFR in OAB and cyclophosphamide-induced cystitis (Klinger and Vizzard, 2008). The function of NGFR in the urinary tract has yet to be completely elucidated, but the evidence would suggest an important role in inflammatory and other pathological processes within the bladder.

To date, little is known about the in vitro expression of NGFR by human urothelium. In 2014, Wezel et al reported basal expression of NGFR in differentiated cell sheets from cultured porcine urothelial cells (Wezel et al., 2014). Other experimental work has primarily been in murine animal models (Klinger and Vizzard, 2008, Schnegelsberg et al., 2010). Research into in vitro expression of NGFR in human urothelial cells would allow further investigation of the modulation and functions of NGFR.

5.2 Aim

The aim of the study was to establish the expression of NGFR in normal human urothelium in situ (P0) and in vitro at both transcript and protein level.

5.3 Experimental approach

5.3.1 Transcript expression

Three samples of urothelial cells were obtained directly from ureteric specimens to establish an in situ (P0) group (Y1300, Y1301, and Y1053) and a further three independent NHU cell lines were selected as paired proliferating and differentiated groups (Y1160, Y1282, Y1276). RNA was extracted and cDNA synthesised as detailed in sections 2.6.1 and 2.6.2. Specific NGFR primers were designed (see section 2.7.1. and appendix for primer detail) and RT-PCR performed (see section 2.7.2).

5.3.2 Differentiated cell sheets

Three independent NHU cell lines were seeded onto Snapwell™ membranes and differentiated as detailed in section 2.1.2. The transepithelial electrical resistance (TER) readings were monitored up to 7 days. Cell sheets were then lifted with dispase and embedded in paraffin wax (section 2.3.2). Immunohistochemical labelling was performed for NGFR (section 2.4.2)

5.3.2.1 Formation of artificial basement membrane

The extracellular matrix (ECM) components collagen IV and laminin were selected as major constituents of the basement membrane. In addition the stromal component collagen I was selected and phosphate buffered saline (PBS) was used as a control. The stock proteins at 0.1mg/ml concentration were diluted in sterile PBS to give a working concentration of 18.7µg/ml; 0.5ml of the working stock was then added to each 1.3cm² Snapwell™ membrane under aseptic conditions and incubated for 2 hours at 4°C. Excess ECM was then aspirated and urothelial cells pre-treated with ABS were seeded into the pre-treated membranes (see section 2.1.2). Cell sheets were established from one NHU cell line (Y1221) and 3 technical replicates of each treatment group were created. TER readings were monitored until day 7. Cell sheets were then harvested using dispase (section 2.3.2) and immunohistochemical labelling was performed for NGFR detailed in section above. Image analysis with TissueGnostics software was performed on the cell sheets to establish the proportion of NGFR positive cells.

5.3.3 Organ culture

Organ culture was established as detailed in section 2.2 (Y1424). The culture was maintained in RPMI:DMEM (1:1) supplemented with 5% FBS and 2mM L-glutamine. The medium was changed every 48h. Organ cultures were harvested at 7, 10, 14, 17 and 21 days and placed directly into formalin for 48 hours before paraffin wax embedding and Immunohistochemical analysis for NGFR.

5.4 Results

5.4.1 Transcript expression of NGFR

The in situ (P0) samples all displayed NGFR transcript expression (figure 5.1A). There appeared to be greater abundance in Y1300 sample. RT-PCR also detected NGFR expression in all the paired proliferating and differentiated independent NHU cell lines (figure 5.1B). There appeared to be greater abundance of NGFR in the proliferating cells compared to the differentiated cells. This conclusion requires further verification with quantitative analysis as RT-PCR required high cycle number (40 cycles) to demonstrate transcript expression. Brain and pooled cell lines were selected as a positive control for NGFR transcript expression.

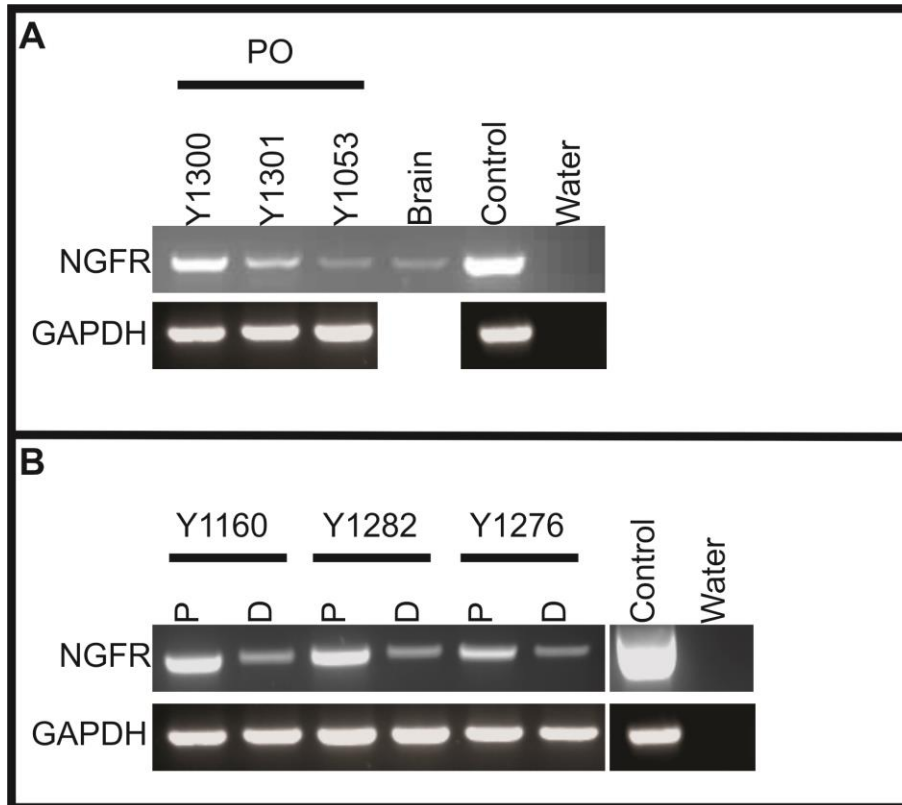


Figure 5-1 NGFR transcript expression in PO, proliferating and differentiated normal human urothelial cells.

A) RT-PCR detected NGFR transcript expression in all in situ (PO) cells (Y1300, Y1301, Y1053)

B) RT-PCR detected NGFR transcript expression from 3 cell lines (Y1160, Y1282, Y1276) in both proliferating (P) and differentiated (D) (ABS + Ca²⁺) cells. There appeared to be greater abundance of NGFR in the proliferating cells but this would require verification with quantitative analysis.

Technical – NGFR RT-PCR at 40 cycles, annealing temperature 60.7°C with brain. NGFR controls in figure **A** brain and pooled cell lines were used as control, in figure **B** genomic DNA was used as control (gap between samples and control is because primer is intron spanning). GAPDH was used as a housekeeping gene to test cDNA integrity in both PO and proliferating/differentiated with genomic DNA control, RT-PCR at 30 cycles, annealing temperature 61.8°C. RT-negative controls did not indicate DNA contamination.

5.4.2 Barrier forming differentiated cell sheets

All cell sheets formed a barrier with a TER $>500\Omega/\text{cm}^2$ by day 7 of the differentiation period. The cell sheets from 3 independent NHU cell lines (Y1221, Y1004, Y1197) revealed variable expression of NGFR (figure 5.2). The NGFR⁺ cells were located basally either individually or more predominantly in clusters with the positive cells extending into the intermediate layers in some areas.

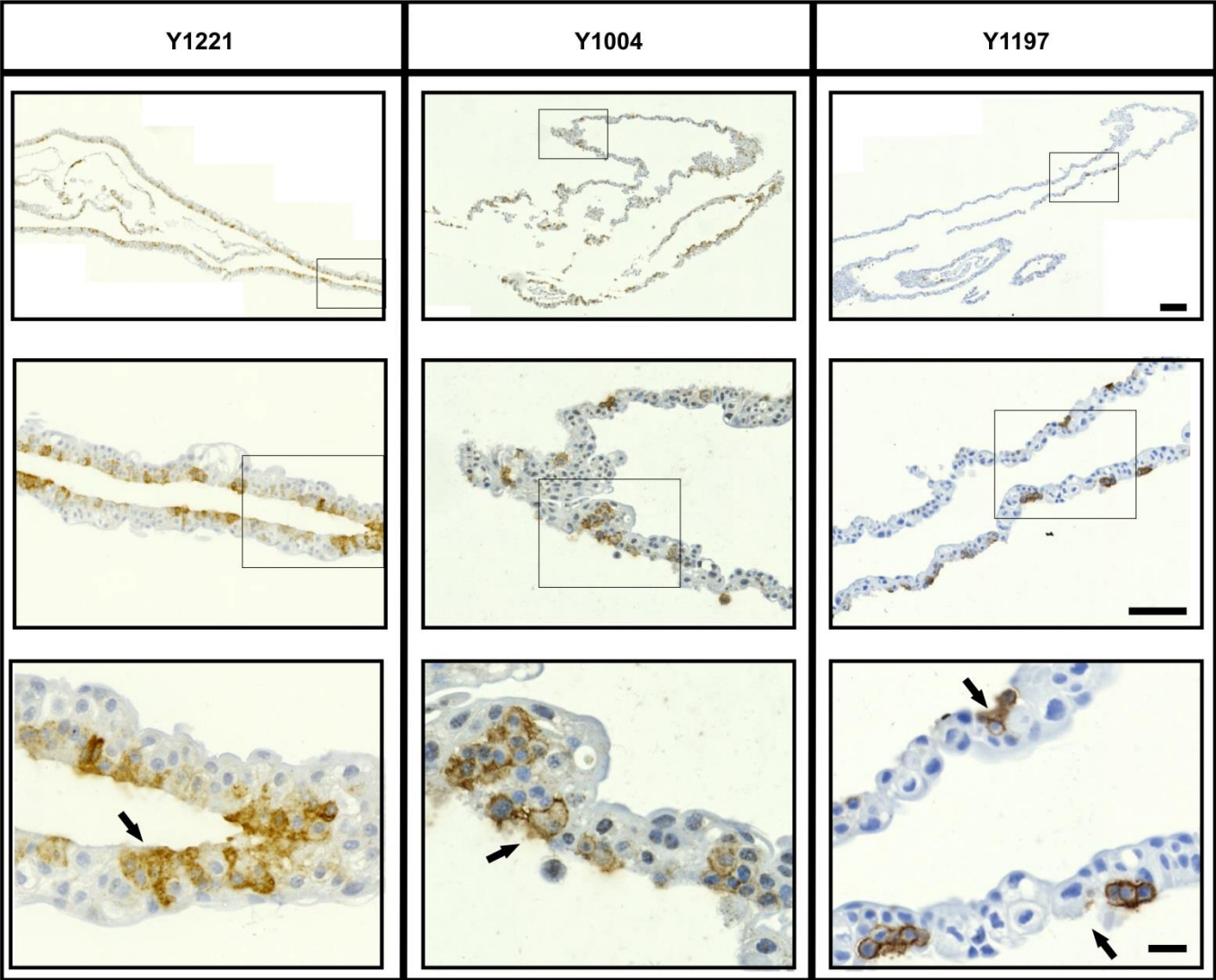


Figure 5-2 NGFR expression on barrier forming differentiated cell sheets

Immunohistochemistry for NGFR on barrier forming differentiated cell sheets (TER > 500 Ω/cm^2) from three independent NHU cell lines. All three cell sheets demonstrated variable expression of NGFR with several areas completely negative for NGFR labelling. The NGFR⁺ cells appeared either individually or more frequently in clusters. The arrows indicate the basal layer of the cell sheet. The NGFR⁺ cells were basally located. Scale bar = top row 200 μm , middle row 100 μm and bottom row 20 μm .

5.4.3 Formation of artificial basement membrane

A functional barrier ($TER > 500 \Omega \cdot \text{cm}^2$) was obtained in all but one of the cell sheets with ECM coatings (Figure 5.3). The single cell sheet (PBS-control) that did not form a functional barrier was not included in further analysis.

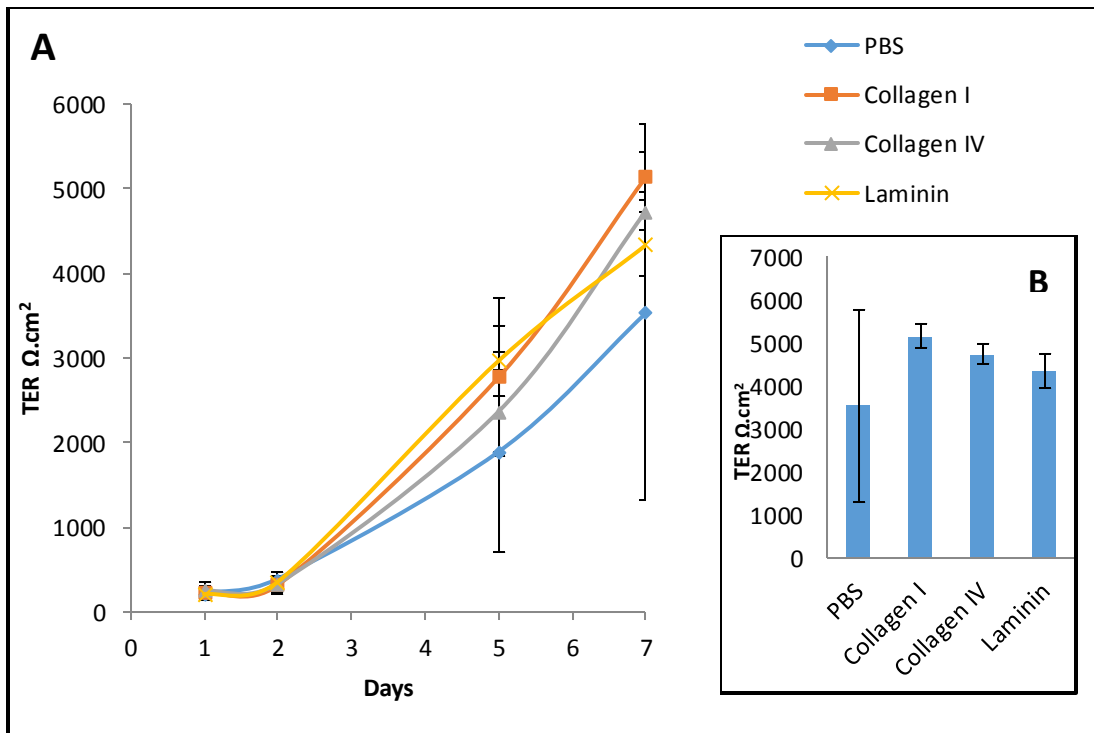
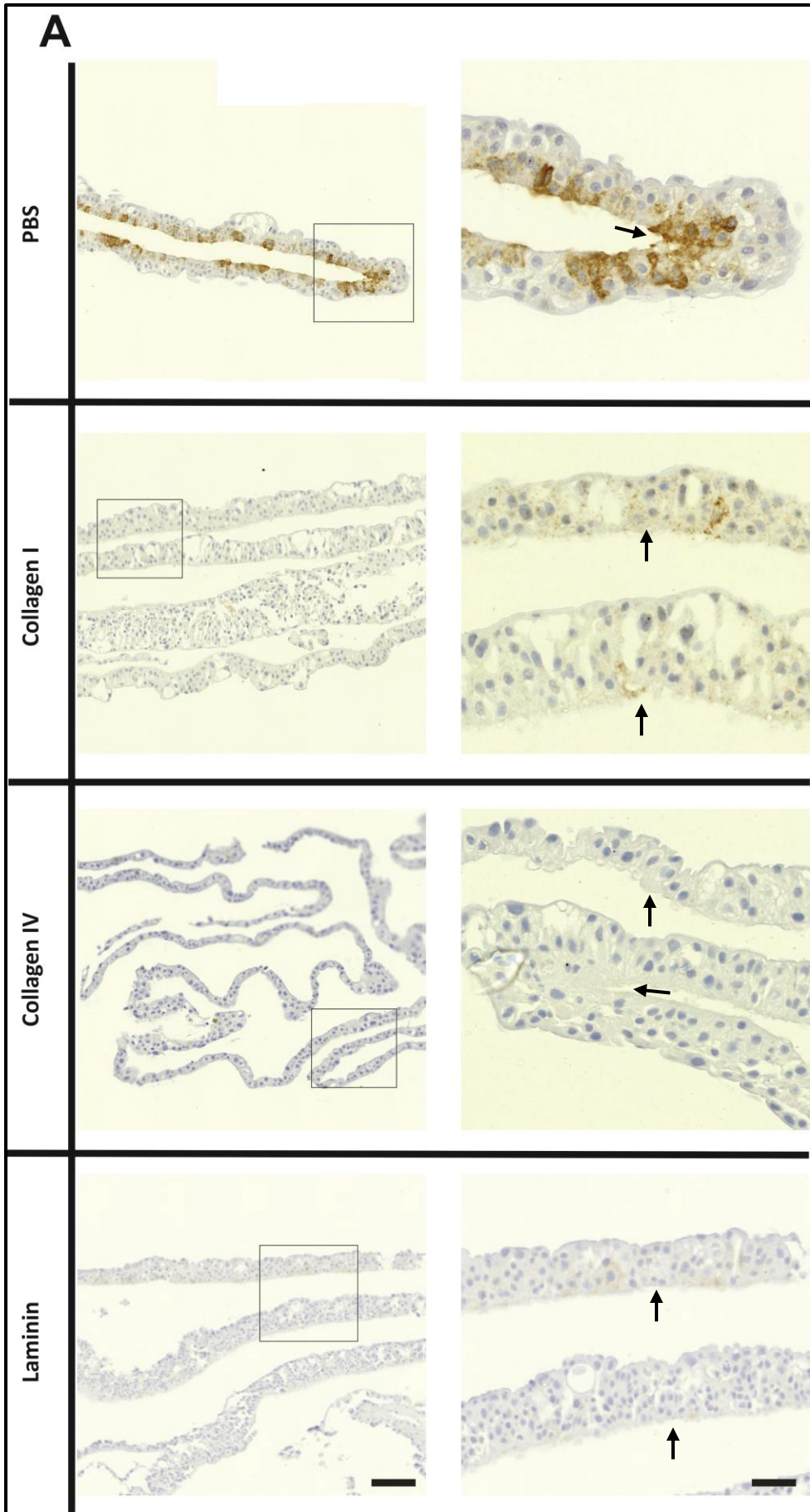


Figure 5-3 Transepithelial electrical resistance (TER) for differentiated cell sheets with artificial extracellular membrane.

A) TER reading for differentiated cell sheets over a period of 7 days. Snapwell™ membranes were coated with artificial extracellular matrix proteins in PBS (control) of collagen I, collagen IV and laminin. The ECM component was applied 1 hour prior to cell seeding. Cell sheets were established from one NHU cell line and 3 technical replicates of were created for each treatment group. All cell sheets formed a barrier ($TER > 500 \Omega \cdot \text{cm}^2$) except one technical replicate in the PBS group (accounting for the large error bar in the PBS group). This cell sheet was removed from further analysis. **B)** TER readings at day 7 time point indicating the formation of a functional barrier ($TER > 500 \Omega \cdot \text{cm}^2$) in all treatment groups. Error bars indicate standard deviation.

Immunohistochemical analysis of the differentiated cell sheets for NGFR displayed a sporadic expression of NGFR⁺ cells which was variable between the replicates in the ECM/control groups. NGFR⁺ cells were on the basal surface of the cell sheet and there were some clusters of positive cells (figure 5.4A). The expression was particularly high in one of the PBS control replicates but remained minimal in the rest of the cell sheets. Expression of NGFR was quantified using TissueGnostic analysis software (figure 5.4B). There was no obvious effect of an ECM artificial basement membrane application on the expression of NGFR⁺ cells.



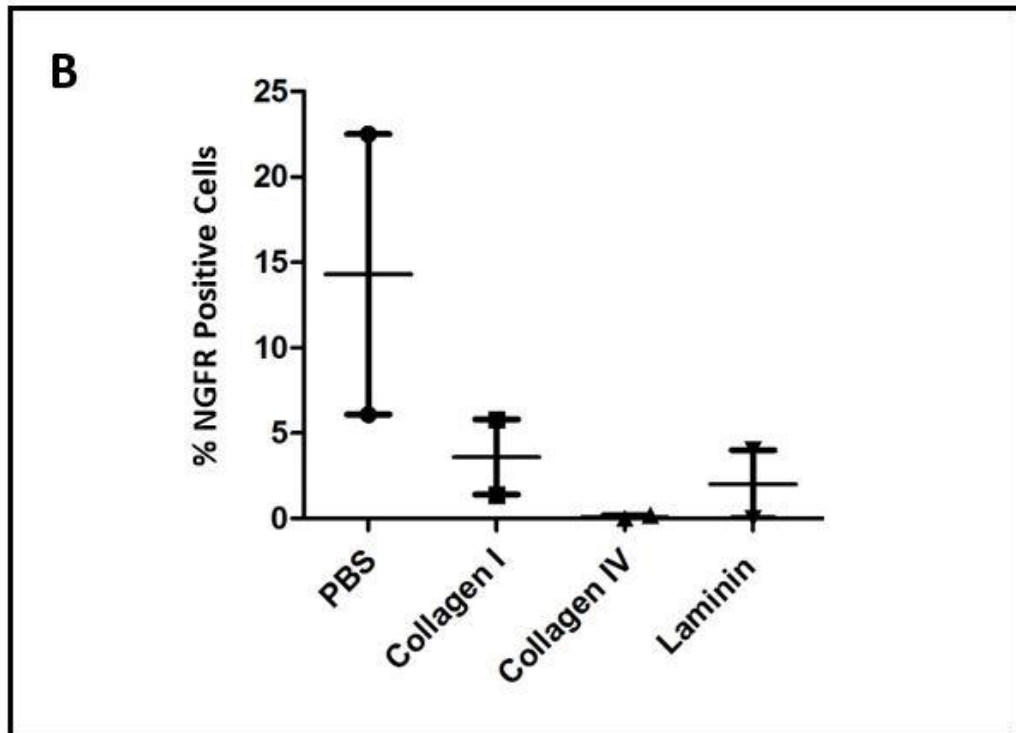


Figure 5-4 NGFR expression in barrier forming differentiated cell sheets with artificial basement membrane

A) Immunohistochemical analysis for NGFR on differentiated cell sheets with artificial basement membrane. Cell sheets were established from one NHU cell line with 3 technical replicates created for each treatment group. All the cell sheets displayed minimal NGFR⁺ cells. The PBS (control) cell sheets had the largest variation in NGFR expression and collagen IV had very few positive cells. The NGFR⁺ cells were located on the basal aspect (arrowed) of the cell sheet with occasional clustering. **B)** Image analysis with TissueGnostic software for total number of cells and percentage of NGFR⁺ cells calculated from DAB membrane intensity (n=2, technical replicates). Variation was seen between all 3 ECM coatings and the PBS control. One PBS control displayed the highest level of labelling with between 20-25% NGFR⁺ cells however the replicate displayed between 5-10% NGFR⁺ cells. The remaining cell sheets displayed between 0-10% with the collagen IV coating having very few NGFR⁺ cells. The horizontal line represents the mean point of all replicates.

5.4.4 Organ culture

Organ cultures from a sample of normal human ureter were established and maintained for a period of 21 days with harvesting time points at 7, 10, 14, 17 and 21 days. A sample of ureter was also taken at initiation of culture to represent the P0/in situ pattern. At all-time points, the basal expression of NGFR was maintained (figure 5.5).

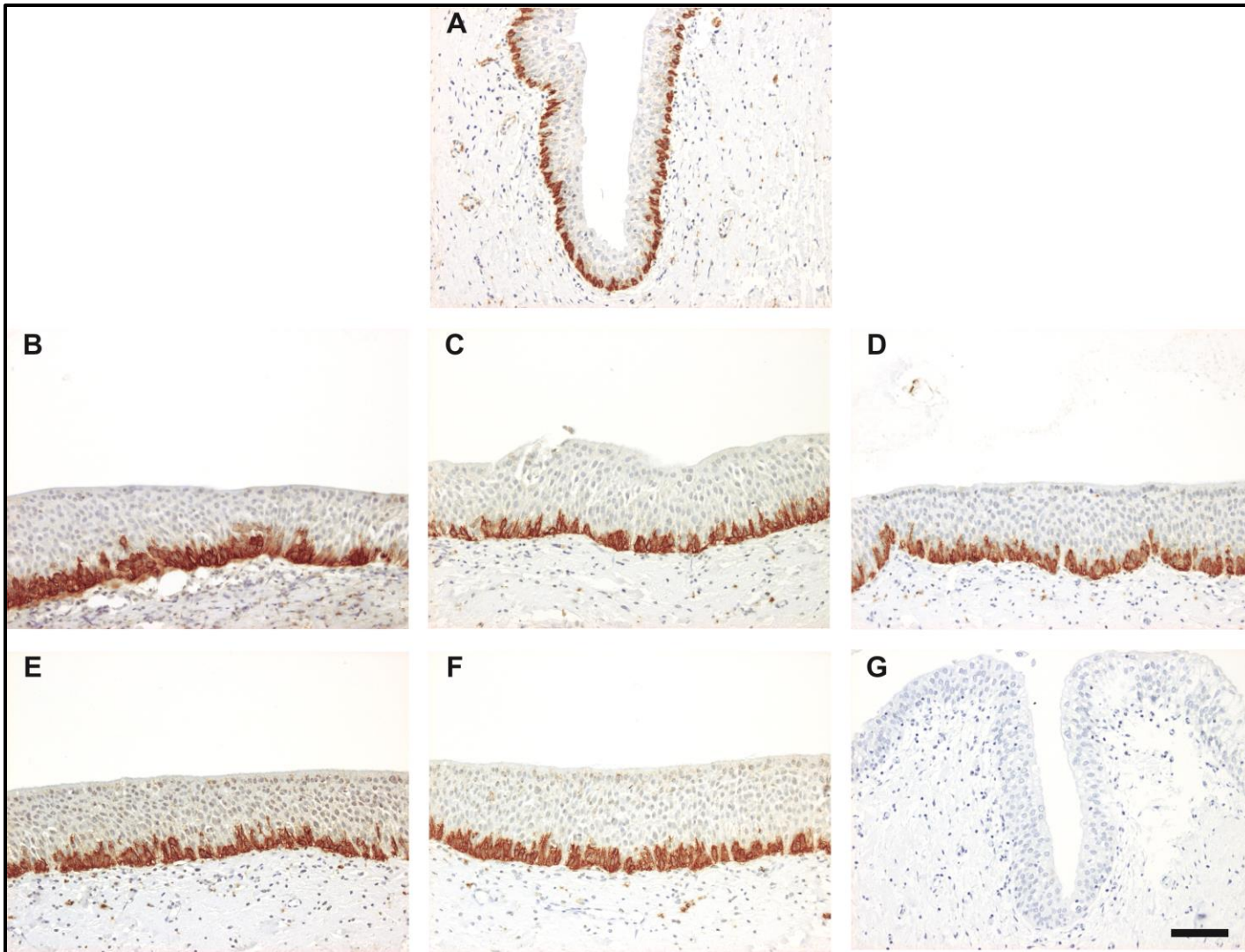


Figure 5-5 NGFR expression in urothelial organ culture

Immunohistochemistry of organ culture sections from normal ureter with NGFR labelling. **A)** section of normal ureter after formaldehyde fixation and embedding prior to organ culture. **B – F** organ culture sections taken at 7, 10, 14, 17 and 21 days respectively. Organ cultures were fixed in formaldehyde and paraffin wax embedded prior to sectioning and labelling. Basal expression of NGFR is seen prominently in all the sections with no distinction between the different time points. **G** – negative control of normal ureter. Scale = 50µm

5.5 Results Summary

- Transcript expression of NGFR was highest in proliferating NHU cells, followed by P0/in situ cells; differentiated cells showed minimal expression.
- Differentiated cell sheets displayed minimal NGFR expression. NGFR⁺ cells were basal in location on the cell sheets and tended to be in clusters.
- The formation of artificial basement membrane using ECM components (collagen I, collagen IV and laminin) had no effect on NGFR expression on differentiated NHU cell cultures
- Organ culture maintained normal NGFR expression in the basal layer of the urothelium.

6 Modulators of NGFR

6.1 Introduction

In vitro studies at the Jack Birch Unit of Molecular Carcinogenesis have shown a direct interaction between the urothelium and ketamine with cell death observed at concentrations >1mM (Wood et al., 2011). It has previously been established that NGFR is up-regulated in the urothelium of KIC samples (chapters 3 and 4; (Baker et al., 2013)). Ketamine is therefore a candidate modulator of NGFR expression in the urothelium. Additional candidate modulators of NGFR were established through a systematic search of the literature (table 6.1).

6.2 Aim

The aim of the study was to identify a panel of candidate modulators of NGFR expression and to examine these, alongside ketamine for evidence of a modulatory effect on NGFR expression in vitro.

Potential Modulator	Background	Modulation of NGFR Evidence
Glucocorticoid Receptor (GR; NR3C1)	<ul style="list-style-type: none"> The GR is a pleiotropic receptor and is found in almost every cell in the body (Lu et al., 2006). Glucocorticoid (GC) hormones, e.g. cortisol, are ligands for GR which have powerful anti-inflammatory and immunosuppressive functions. The anti-inflammatory properties have been exploited with the invention of synthetic glucocorticoids which are used to manage a variety of inflammatory and autoimmune diseases such as asthma, allergy, sepsis and rheumatoid arthritis. Within the urinary system dexamethasone has been used for the treatment of BPS with varying reported degrees of success (RIEDL et al., 1998, Rosamilia et al., 1997). 	<p>In vitro study – cells cultured from sympathoadrenal and nervous system in rats (Yakovlev et al., 1990) - Up regulation of NGFR mRNA after 7 days</p> <p>In vitro study – PC12 cell line (Foreman et al., 2004) - Decrease in NGFR mRNA after 3 days</p>
Cytokines	<ul style="list-style-type: none"> Cytokines are low molecular weight (15-25kDa) secreted proteins, which are considered to regulate the amplitude and duration of the immune-inflammatory responses. IL-1β, IL-6, TNFα, IL-8 were found to be increased in patients with interstitial cystitis (IC)/bladder pain syndrome (BPS) (reviewed in (Wezel et al., 2014) IL6, IL-8, IL-10, IFNα, TNFα have been implicated in several urinary tract infection (UTI) models (Ke et al., 2014) 	<p>NGFR and its ligand nerve growth factor (NGF) are known to play a vital role in the final stages of wound healing and tissue repair. The initial cytokine response seen in wound healing has been implicated in the action of NGF and NGFR (Micera et al., 2007)</p>
Brain derived neurotrophic factor (BDNF)	<ul style="list-style-type: none"> Brain derived neurotrophic factor (BDNF) is a neurotrophin and ligand of NGFR 	<p>BDNF has been shown to be increased after prolonged exposure of ketamine in the cortical and thalamic regions of developing rat brains (Ibla et al., 2009)</p> <p>BDNF serum levels were increased in chronic ketamine users compared to healthy individuals (Ricci et al., 2011). However, Ke et al found that serum levels of BDNF were significantly lower in the chronic ketamine users (Ke et al., 2014). The studies used almost identical methodologies with similar population demographics.</p>
Non-Steroidal anti-inflammatory drugs (NSAIDs)	<ul style="list-style-type: none"> Non-steroidal anti-inflammatory drugs (NSAIDs) are commonly used for the alleviation of pain and reduction of inflammation. Evidence also suggests that NSAIDs may inhibit the initiation and proliferation of some tumours (Sandler et al., 1998, Katz et al., 1991) 	<p>NGFR was an important upstream modulator of the anticancer effects of NSAIDs when used at high doses (Khwaja et al., 2004)</p> <p>NSAIDs activated the p38 MAPK pathway in prostate cancer cells leading to induction of NGFR and apoptosis of the cells (Khwaja et al., 2004, Quann et al., 2007, Wynne and Djakiew, 2010)</p>

Table 6-1 Literature review of candidate modulators of NGFR

6.3 Overall Experimental Approach

The effect of the potential modulators: ketamine, glucocorticoids, cytokines, BDNF and NSAIDS on NGFR expression were assessed sequentially. NGFR transcript expression in cultured NHU cells was examined by RT-PCR and protein expression in differentiated cell sheets was assessed by IHC. The most promising candidates were then further scrutinised using real time qPCR and IHC on treated ureter organ cultures, for summary see table 6.2. Further specific detail on experimental approach for each candidate modulator is given in each modulators results section.

6.4 Results

6.4.1 Ketamine

6.4.1.1 Experimental Approach

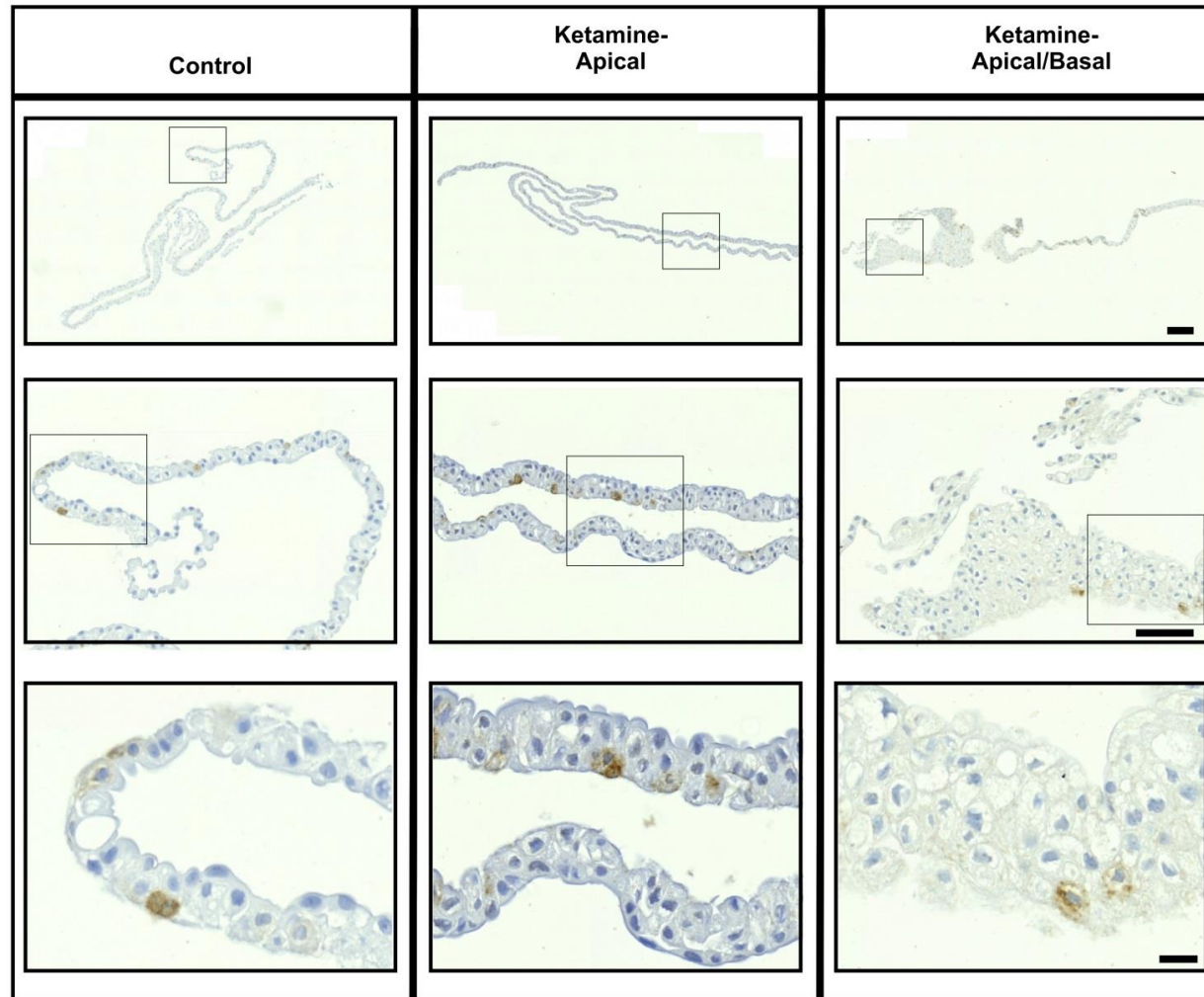
Initial work with ketamine as a potential modulator of NGFR involved the immunohistochemical analysis of differentiated cell sheets (section 2.1.2) which had been treated with ketamine (1mM) in either the apical or apical and basal compartments of the Snapwell™ membrane during the differentiation period. These blocks were provided by Dr S Baker (post-doctoral research associate at the JBU). The cell sheets were established from one independent NHU cell line with 3 technical replicates in each group (control and ketamine). Image analysis using TissueGnostic software was performed. The 1mM concentration of ketamine was selected due to previous in vitro work by Dr S Baker which displayed cell death at higher concentrations.

Expression of NGFR transcript was examined in differentiated NHU cells treated with ketamine (1mM at 24hr and 72hr) and the RT-PCR was performed with the dexamethasone treated cells.

6.4.1.2 Results

The control and ketamine differentiated urothelial cell sheets all had basal NGFR⁺ cells irregularly placed throughout. There was no obvious difference between the control and ketamine treatments and the expression of NGFR in the cell sheets (figure 6.1A). Image analysis with TissueGnostic software to analyse the percentage NGFR⁺ cells revealed variation in NGFR⁺ cells across all treatments and replicates (figure 6.1B). Transcript expression of NGFR following 1mM ketamine treatment did not increase NGFR expression with no bands visualised at either 24hr or 72hr time points (figure 6.3).

A



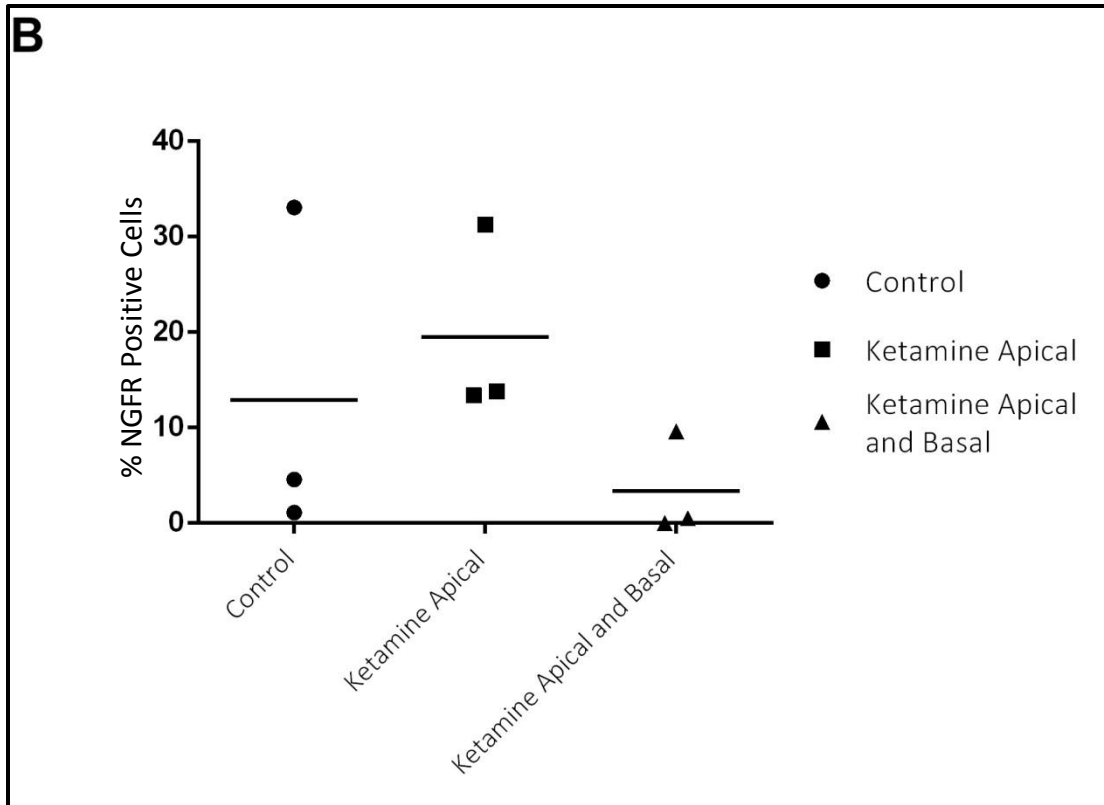


Figure 6-1 Immunohistochemical expression of NGFR in differentiated cell sheets treated with ketamine

A) Differentiated cell sheets treated with ketamine on either the apical or on both the apical and basal surfaces of the Snapwell™ membrane. Cell sheets were all established from one NHU cell line and 3 technical replicates of each treatment group were created. All cell sheets expressed NGFR on the basal surface of the cell sheet. No obvious up regulation of NGFR was seen in any of the treatment groups. Scale – Top row = 200µm, Middle row = 100µm and bottom row = 20µm. **B)** Image analysis comparing the 3 treatment groups (control, ketamine apical, ketamine apical and basal) (n=3). Cell sheets were analysed for percentage of NGFR positive cells based on DAB membrane positive cells. There was variation in the percentage of cells expressing NGFR that was not related to the presence or absence of ketamine. The horizontal line represents the mean point of each treatment group.

6.4.2 Glucocorticoids (dexamethasone)

6.4.2.1 Experimental Approach

Dexamethasone was selected as a synthetic analogue of a glucocorticoid. An AlamarBlue® assay (section 2.1.4) was performed initially to establish any toxic effects of dexamethasone on NHU cells over a log concentration range (0.001µM to 10µM). Differentiated NHU cells from one cell line (Y1004) were treated with dexamethasone over the log concentration for 24 hours and 72 hours. Ketamine (1mM) was included as an internal control alongside a medium-only negative control. The cultures were then prepared for RNA extraction, cDNA synthesis and RT-PCR was completed for NGFR transcript expression (section 2.6).

Differentiated cell sheets were formed (section 2.1.2) from one cell line and treated with dexamethasone in the basal compartment at 100nM and 250nM concentrations with medium (KSFMc) in the apical compartment. An additional treatment arm combined dexamethasone (100nM and 250nM) in the basal compartment and ketamine (1mM) in the apical compartment. The treatments were applied during the differentiation period for 7 days. The concentration of dexamethasone was decided after review of the literature (Walsh et al., 2001, Takahashi and Iizuka, 1991, Rosewicz et al., 1988). Cell sheets were all established from one independent NHU cell line (Y1004) and 4 technical replicates of each treatment group were created. The transepithelial electrical resistance (TER) was monitored. The cell sheets were harvested using dispase at day 7 and immunohistochemical analysis for NGFR and image analysis was performed using TissueGnostic software.

6.4.2.2 Results

An AlamarBlue® assay performed on proliferating NHU cells treated with a log concentration of dexamethasone did not reveal any toxic effects (figure 6.2).

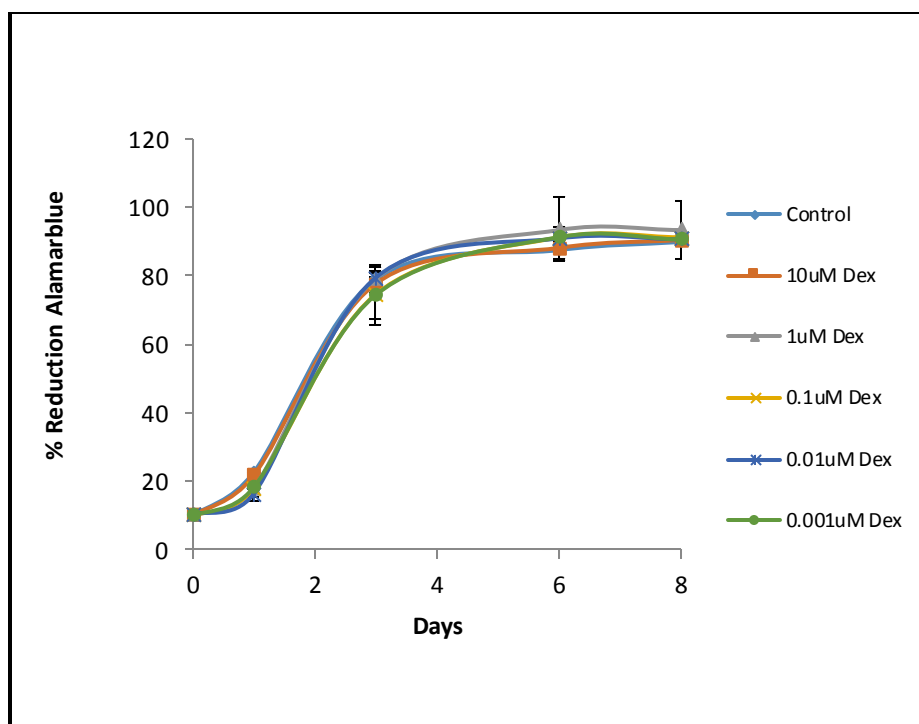


Figure 6-2 AlamarBlue® Assay for proliferating NHU cells treated with dexamethasone

Alamarblue® assay showing log concentration of dexamethasone applied to proliferating NHU cells over an 8 day period. No toxic effects on proliferating NHU cells were identified. Error bars = standard deviation.

Transcript expression of NGFR in differentiated cells treated with dexamethasone was minimal with faint bands only visualised in the 24hr control and 100nM dexamethasone treatment at high cycle RT-PCR (40 cycles). Metallothionein 1G (MT1G) is activated when NHU cells are treated with dexamethasone (Le et al., 2005) and was used to validate the dexamethasone treatments on the NHU cells (figure 6.3).

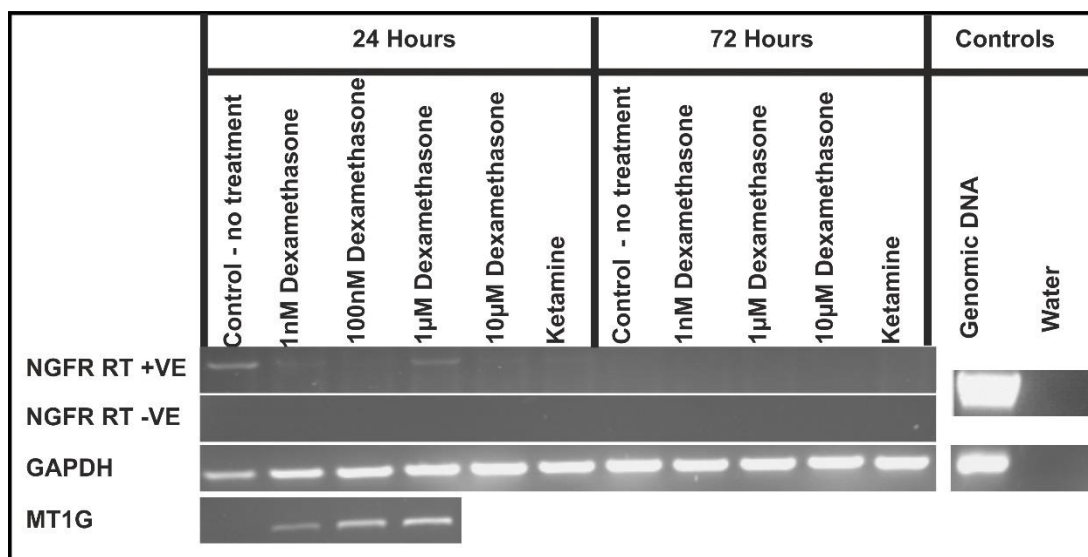


Figure 6-3 Transcript expression of NGFR in differentiated NHU cells treated with ketamine and log concentrations of dexamethasone

RT-PCR for NGFR on differentiated NHU cells treated with dexamethasone at log concentrations (1nM to 10µM) and 1mM ketamine for 24 and 72hours. Minimal expression of NGFR was seen with a faint band at 24 hour in the no treatment control and 1µM dexamethasone only. No expression was seen in the 72 hour time period. Metallothionein 1G (MT 1G) is activated when NHU cells are treated with dexamethasone and was used to establish an effect of dexamethasone treatment on the NHU cells; an increasing induction was noted in NHU cells at the 24-hour time point.

Technical - RT negative controls were included to demonstrate lack of genomic contamination of samples. GAPDH was used as housekeeping gene to test the integrity of the cDNA. Genomic DNA and water were used as positive and negative controls respectively. RT-PCR at 40 cycles, annealing temperature 60.7°C. MT 1G - RT-PCR at 30 cycles, annealing temperature 58°C.

Differentiated cell sheets treated with dexamethasone and dexamethasone/ketamine all formed a barrier with a TER >500Ω.cm² (figure 6.4). All cell sheets displayed basal NGFR⁺ cells which were irregularly dispersed throughout the cell sheet with some clustered areas of NGFR⁺ cells. There was no obvious up regulation of NGFR in the dexamethasone or dexamethasone/ketamine treated cultures and this was confirmed on image analysis using TissueGnostic software (figure 6.5A and 6.5B)

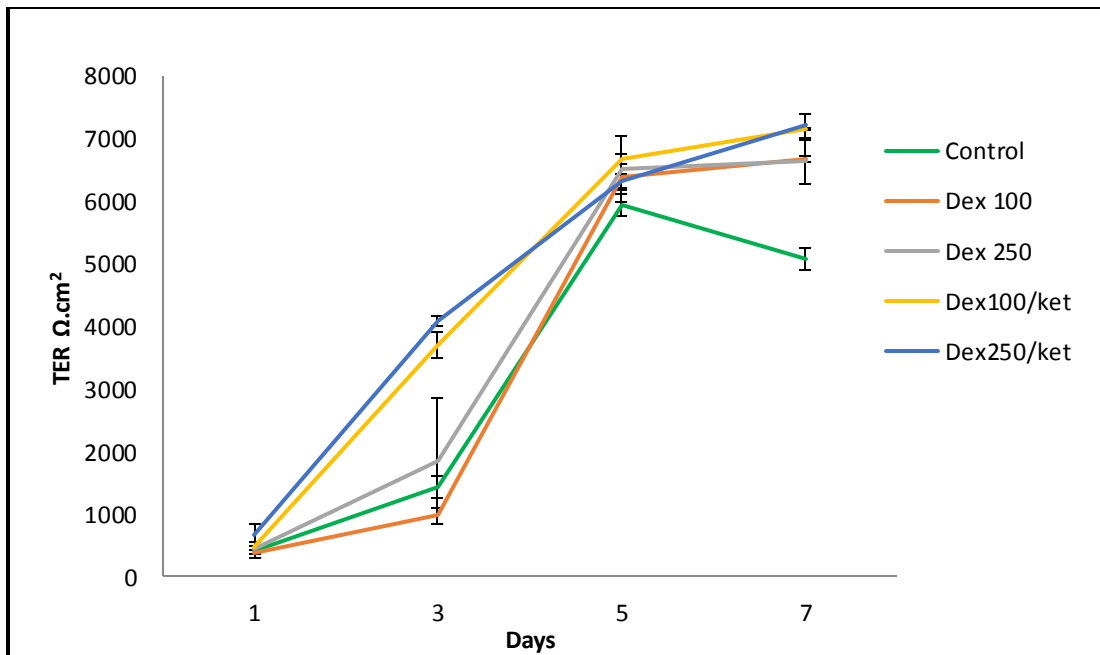
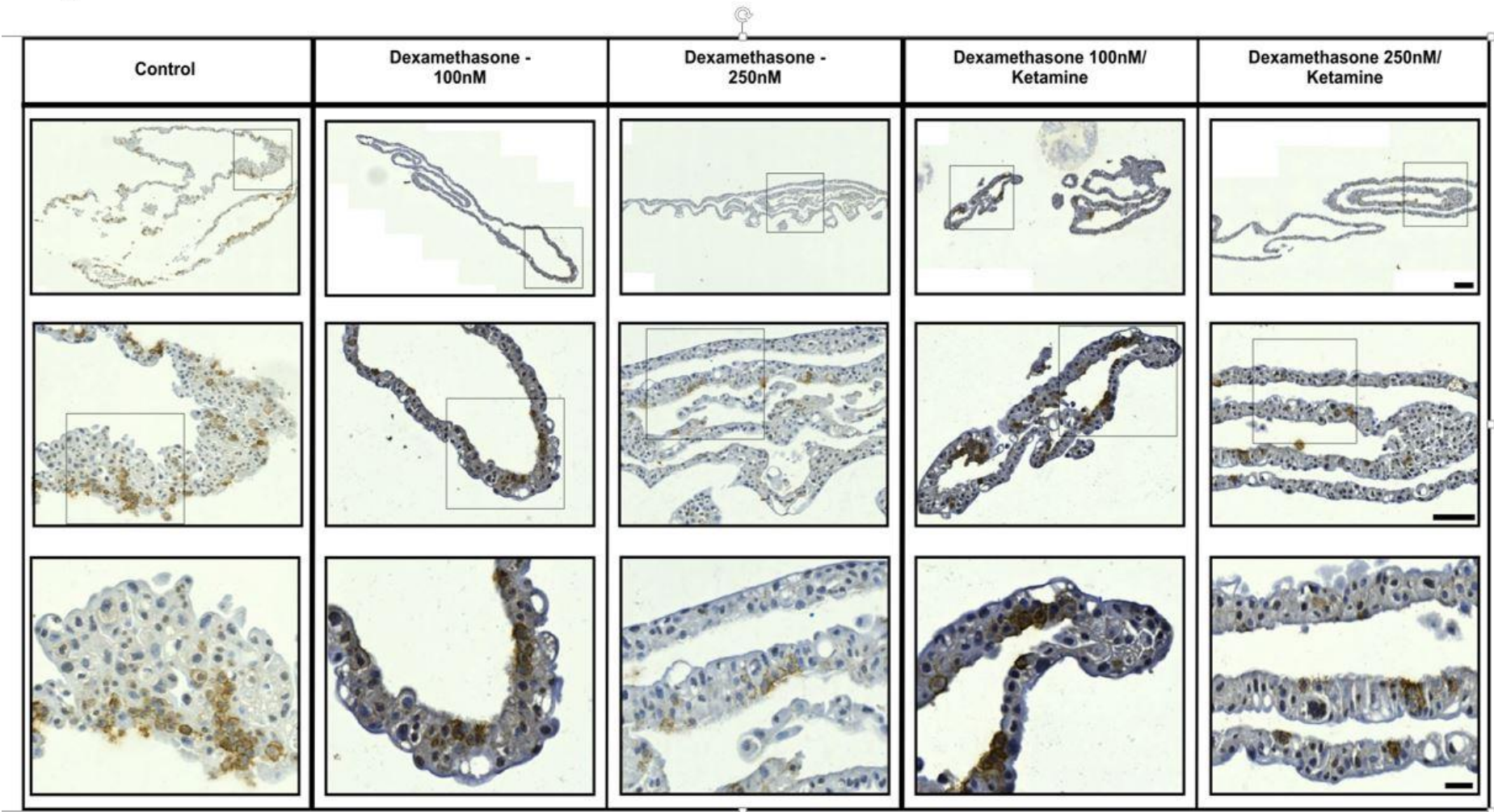


Figure 6-4 TER for differentiated cell sheets treated with dexamethasone and dexamethasone with ketamine.

TER readings for differentiated cells sheets over a period of 7 days. Treated with i) control media in both compartments (KSFMc+ABS+ Ca²⁺); ii) dexamethasone (100nm and 250nm) in the basal compartment and medium (KSFMc+ABS+ Ca²⁺) in the apical compartment of the Snapwell® membrane; iii) dexamethasone in the basal compartment (100nM and 250nM) and ketamine (1mM) in the apical compartment of the Snapwell® membrane. TER readings indicate the formation of a functional barrier (TER > 500Ω.cm²) in all groups. All readings from one cell line with 4 replicates for each treatment. Error bars indicate standard deviation.

A



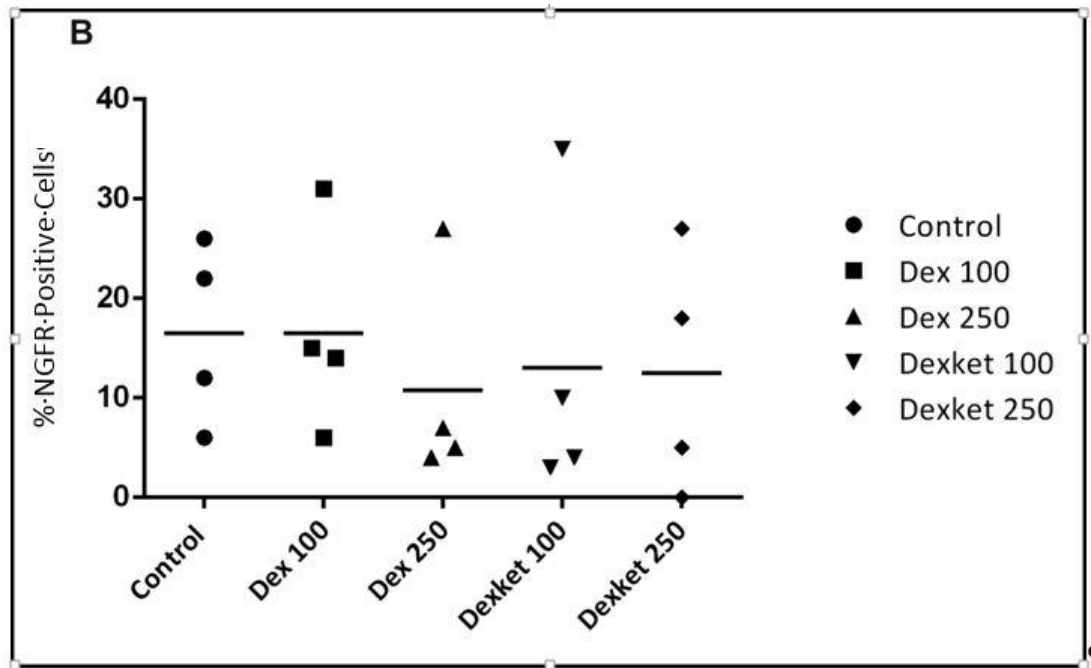


Figure 6-5 Immunohistochemical expression of NGFR in differentiated cell sheets treated with dexamethasone and ketamine

A) Immunohistochemistry for NGFR expression by NHU cell sheets treated with dexamethasone (100nM and 250nM) and dexamethasone (100nM and 250nM)/ketamine (1mM). Cell sheets were all established from one NHU cell line and 4 technical replicates of each treatment group were created. Basal labelling of NGFR was displayed in all cell sheets including control cell sheets with some obvious areas of clustering of NGFR expression. No obvious upregulation was apparent in any of the cell sheets. Scale – Top row = 200 μ m, Middle row = 100 μ m and bottom row = 20 μ m. **B)** Image analysis with TissueGnostic software of the 5 treatment groups (n = 4 technical replicates). Cell sheets were analysed for number of cells and percentage of NGFR positive cells based on DAB positive cells. The scatter plot does not show any correlation between the different treatments. Points are widely spaced for each treatment; the line represents the mean point of all replicates and is between 10-20% NGFR positive cells in all treatment groups. The horizontal line represents the mean point of each treatment group.

6.4.3 Cytokines

6.4.3.1 Experimental Approach

RNA from differentiated NHU cells treated with the cytokines, interferon gamma (IFN γ), interleukin-4 (IL4) and tumour necrosis factor alpha (TNF α) for 48 hours was obtained from previous studies at the JBU performed by Dr N Smith (clinical-research fellow). cDNA synthesis and RT-PCR was performed for NGFR. ICAM 1 expression was used to assess activity of TNF α and IFN γ (section 2.6)

6.4.3.2 Results

Cytokine treatment with IFN γ , IL4 or TNF α did not modulate the transcript expression of NGFR in differentiated NHU cells at 48 hours (RT-PCR at 40 cycles). The expression of NGFR transcript decreased from the proliferating NHUs to the differentiated NHU cells as previously demonstrated. NGFR transcript expression was detected only in the proliferating NHU controls. ICAM 1 displayed bands in IFN γ and TNF α confirming their activity (figure 6.6). As a positive control, ICAM 1 was amplified from cDNA derived from cultures treated with IFN γ and TNF α confirming activity.

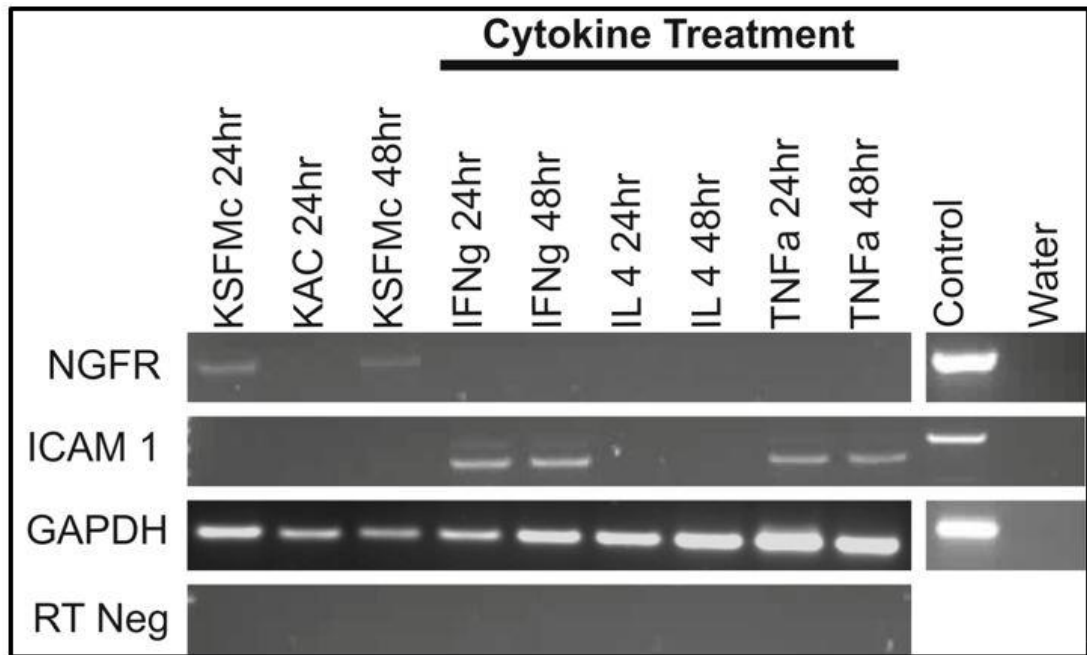


Figure 6-6 Transcript expression of NGFR in NHU cells treated with proinflammatory cytokines

RT-PCR on NHU cells during proliferation (KSFMc 24hr and 48hr) and differentiation (KAC - KSFMc+ABS+Ca²⁺ for 24hr). Cells were treated with cytokines (IFNg, IL4, TNF α) after 6 days of differentiation (KSFMc+ABS+Ca²⁺) for 48 hours. Expression of NGFR was detected in proliferating NHU cells at 24 and 48 hours only. No expression of NGFR was detected in the differentiated NHU cells or the cells treated with the cytokines. ICAM-1 is induced in urothelial cells by IFN γ and TNF α and was used to establish an effect of cytokine treatment.

Technical - RT-PCR at 40 cycles, annealing temperature of 60.7°C. GAPDH was used as housekeeping gene to test the integrity of the cDNA. Genomic DNA and water were used as positive and negative controls respectively. RT negative controls were included to demonstrate lack of genomic contamination of samples. ICAM-1 RT-PCR - 30 cycles, annealing temperature 63°C

6.4.4 BDNF

Proliferating NHU cells (Y1389) were treated with a log concentration of BDNF (0.1ng.ml to 1µg.ml) for 24hr, 3d and 7d. RNA was extracted and cDNA synthesised prior to RT-PCR for NGFR.

6.4.4.1 Results

BDNF treatment of proliferating NHU cells did not modulate NGFR expression over any of the time periods. Low abundance product was amplified in the 0.1ng at 24hr and 0.1ng, 1ng and 1ug at 168hr time points at high cycle RT-PCR (40 cycles). However a repeat RT-PCR at 40 cycles with the same samples did not demonstrate the same pattern confirming a very low expression of NGFR in all the samples (figure 6.7).

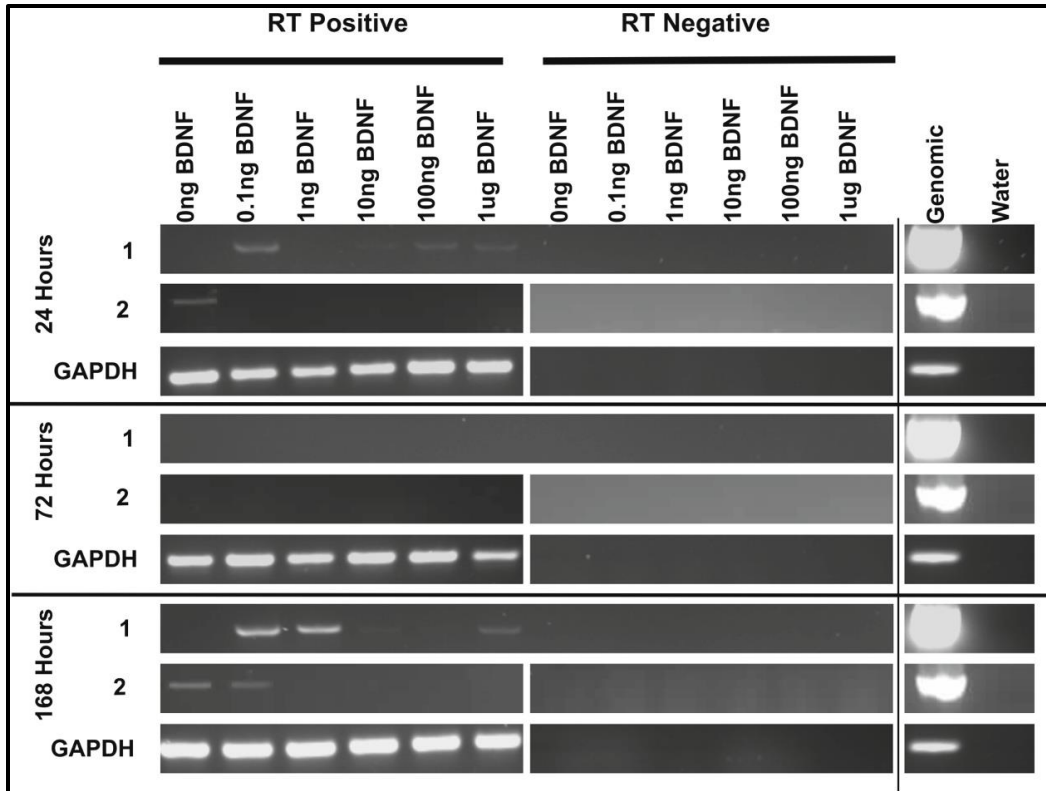


Figure 6-7 Transcript expression of NFGFR in proliferating NHU cells treated with log concentrations of BDNF

RT-PCR for NGFR on proliferating NHU cells treated with log concentration of BDNF (0ng/ml to 1µg/ml) at 24, 72 and 168 hours. Replicates 1 and 2 are technical repeats of the PCR using the same cDNA samples due to high cycle number which potential leads to amplification of minimal amounts of template cDNA. Minimal expression of NGFR is seen in all the samples given the high cycle number with differences notable between the 2 replicates.

Technical - RT-PCR at 40 cycles, annealing temperature 60.7°C. GAPDH was used as housekeeping gene to test the integrity of the cDNA. Genomic DNA and water were used as positive and negative controls respectively. RT – negative controls were included to demonstrate lack of genomic contamination of samples.

6.4.5 NSAID (Ibuprofen)

6.4.5.1 Experimental Approach

Proliferating NHU cells were treated with the NSAID ibuprofen (0.5mM, 1mM, 2mM) over 48hr. The same concentration range was used as (Khwaja et al., 2004). RNA was extracted, cDNA synthesised and RT-PCR performed for NGFR.

6.4.6 Results

Proliferating NHU cells appeared to take an elongated/strand like morphology in culture with increasing concentration of ibuprofen. There was also an increased amount of debris visualised in the culture media of high concentration cultures and reduced cell density (figure 6.8).

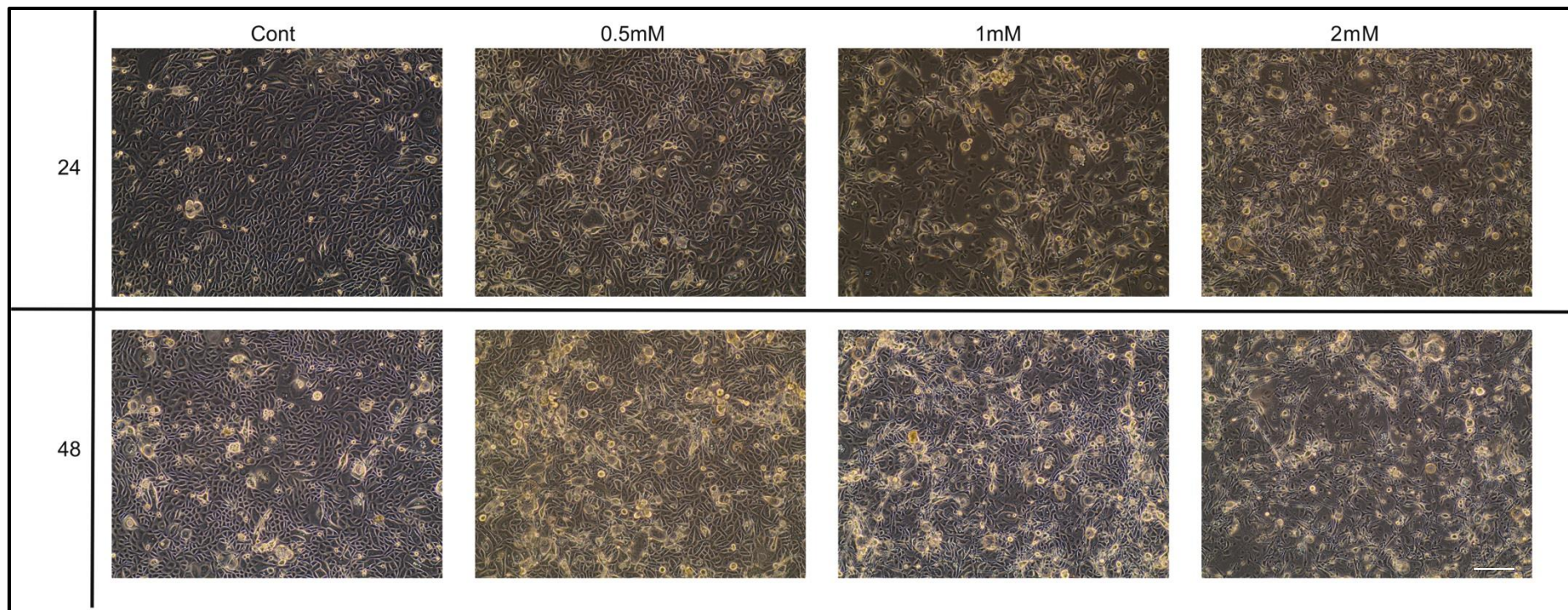


Figure 6-8 Proliferating NHU cell populations in culture with ibuprofen treatment

NHU proliferating cell populations in culture at 24 and 48 hour time periods with ibuprofen treatments (0mM, 0.5mM, 1mM and 2mM). At increasing ibuprofen concentrations there was an increase in amount of debris in the culture medium and cells appeared to become more elongated at the higher concentrations. Scale = 50 μ m

There was an increase in gene expression of NGFR in proliferating NHU cells with up-regulation of NGFR transcript seen at all concentrations of ibuprofen in 2 independent NHU cell lines (Y1497, Y1434). The 2mM ibuprofen concentration appeared to display the greatest abundance of NGFR transcript in both cell lines although ideally this would require verification by qPCR (figure 6.9). RT-PCR was performed at 30 cycles.

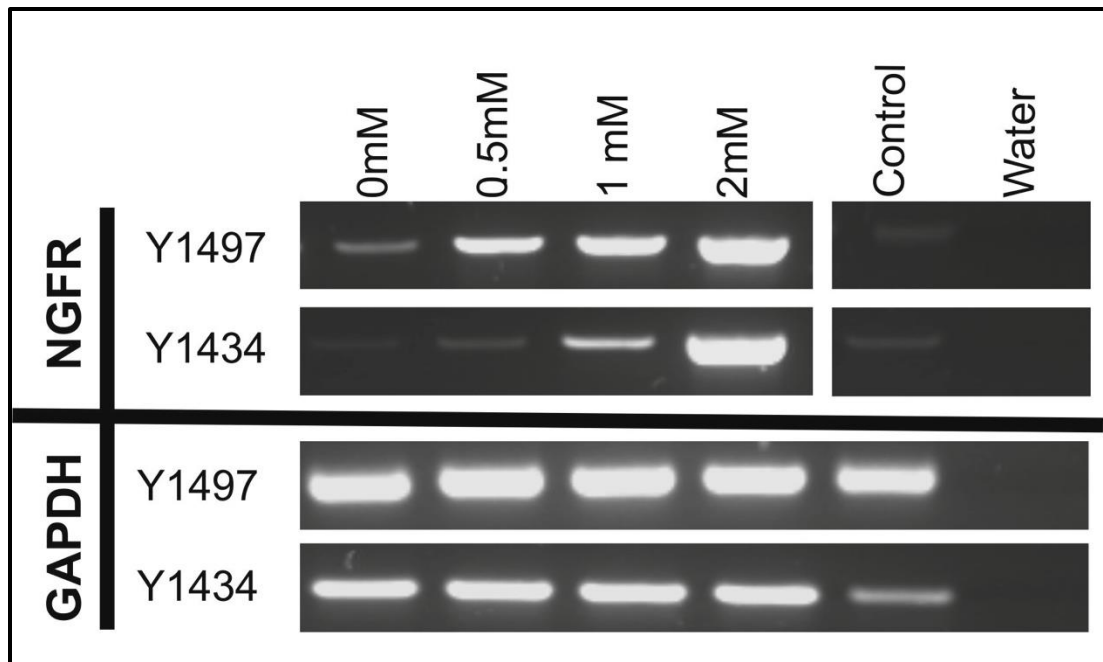


Figure 6-9 Transcript expression of NGFR in proliferating NHU cells treated with ibuprofen

RT-PCR NGFR on proliferating NHU cells treated with ibuprofen (0mM, 0.5mM, 1mM and 2mM) for 48 hours from two independent NHU cell lines (Y1497, Y1434). Induction of NGFR with increasing concentration of ibuprofen was seen in both cell lines.

Technical - RT-PCR at 30 cycles, annealing temperature 60.7°C (control = pooled cell lines). GAPDH used as housekeeping gene at 30 cycles annealing temperature 61.8°C (control = genomic DNA).

6.4.7 Ketamine and ibuprofen

6.4.7.1 Experimental Approach

As presented in table 6.1 it has been suggested that ibuprofen activates the p38MAPK pathway, leading to an induction of NGFR and subsequent apoptosis (Quann et al., 2007, Wynne and Djakiew, 2010). Urothelial cell death was observed in vitro with high (>1mM) concentrations of ketamine (Wood et al., 2011). The following three experiments were conducted to establish whether high dose ketamine treatment up-regulates NGFR as seen following ibuprofen treatment and furthermore if this effect is in common with antibiotic-induced apoptosis in urothelial cells.

In a preliminary experiment proliferating NHU cells were treated with ketamine or ibuprofen for 48 hours to assess if NGFR expression is up-regulated. Cells were treated with higher doses of ketamine (1mM, 3mM and 6mM) than previously used in section 6.3.1. 2mM ibuprofen was selected to proceed with as this was shown to have the greatest effect on NGFR expression in section 6.4.5. RNA extraction, cDNA synthesis and RT-PCR was performed for transcript expression of NGFR.

In the follow on experiment the expression of NGFR in known antibiotic-induced apoptotic pathways was assessed alongside ketamine and ibuprofen treatments. Proliferating NHU cells were treated with 0.5mM, 1mM and 2mM ibuprofen or 1mM, 3mM and 6mM ketamine. Apoptotic controls were included by treating proliferating NHU cells with antibiotics known to cause apoptosis: 0.5µm staurosporine (Sigma) and 0.1mg.ml⁻¹ G418 (Sigma). Quantitative RT-PCR was used to analyse the transcript expression of NGFR.

The effect of ibuprofen and ketamine on NGFR expression in the urothelium was then further investigated using a ureteric organ culture. Organ culture was used as NGFR expression has been shown to be maintained in basal urothelial cells (section 5.4.4) and to facilitate immunolocalisation of NGFR after high dose ketamine treatments. An organ culture (section 2.2) was established and maintained for 14 days with

ibuprofen and ketamine treatments (see table 6.2). Treatments were added after 24 hours and medium was changed every 48 hours. Organ culture constructs were then paraffin wax embedded and sectioned (5µm) for immunohistochemical analysis for NGFR and markers of urothelial phenotype.

Table 6-3 Organ culture treatments and time points

Treatment	Concentration (mM)	Time points (days)
Ibuprofen	0.5	3, 7, 14
	1	3, 7, 14
	2	3
Ketamine	1	3, 7, 14
	3	3

6.4.7.2 Results

In the preliminary experiment, RT-PCR was performed at 30 cycles and there was induction of transcript expression of NGFR at 6mM ketamine concentration but no induction at the 1mM and 3mM concentrations (figure 6.10). 2mM ibuprofen was used as a control to show NGFR up regulation.

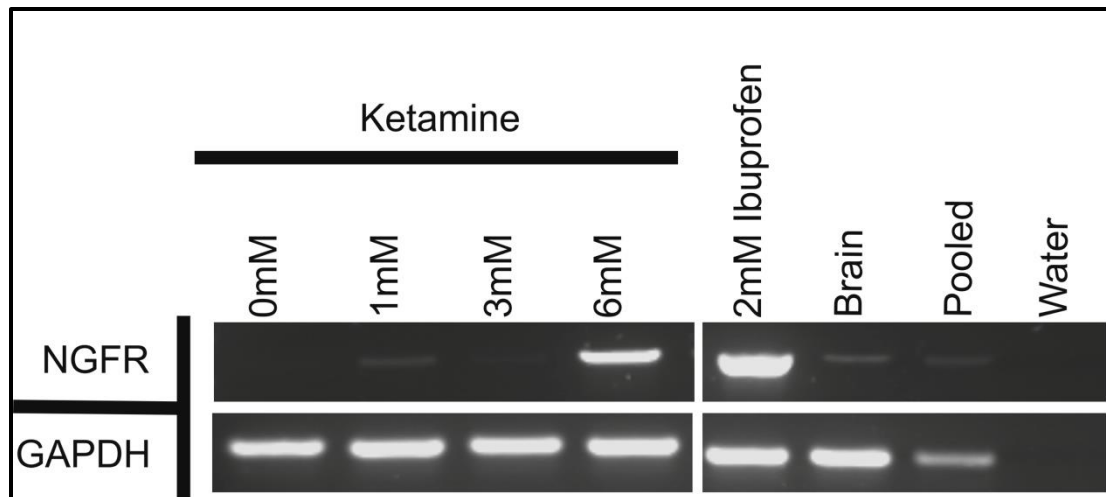


Figure 6-10 Transcript expression of NGFR in proliferating cells treated with ketamine

RT-PCR NGFR on proliferating NHU cells treated with ketamine (0mM, 1mM, 3mM, 6mM) for 48 hours. Induction of NGFR is seen at the 6mM concentration only. 2mM ibuprofen was included as a positive control for NGFR induction. RT-PCR at 30 cycles, annealing temperature 60.7°C (control = pooled and brain cell lines). GAPDH used as housekeeping gene at 30 cycles annealing temperature 61.8°C (control = genomic DNA).

In the second experiment, in culture the proliferating NHU cells treated with ketamine took a more rounded morphology with increasing concentration and detached from the culture dish. This was particularly apparent at the 6mM concentration and at 48 hours very few cells remained adherent (figure 6.11). Subsequently in this experiment it was not possible to perform RNA extraction at the 6mM concentration. The ibuprofen treated cells became elongated as previously described (figures 6.8 and 6.11). Staurosporine appeared very toxic to the urothelial cells with cells becoming rounded and detaching from the culture dish with a similar appearance to 6mM ketamine treated cells. The G418 treatment did not appear to be as toxic as the staurosporine treatment with cells remaining adherent but with a slight change to a more rounded structure compared to controls (figure 6.11)

Quantitative RT-PCR confirmed the induction of NGFR with increasing ibuprofen concentration. The 3mM ketamine increased the expression of NGFR but 1mM did not lead to an induction. G418 and Staurosporine had opposite effects with G418 causing an induction of NGFR almost to the same degree as 2mM ibuprofen and Staurosporine leading to a reduction in NGFR expression (figure 6.12).

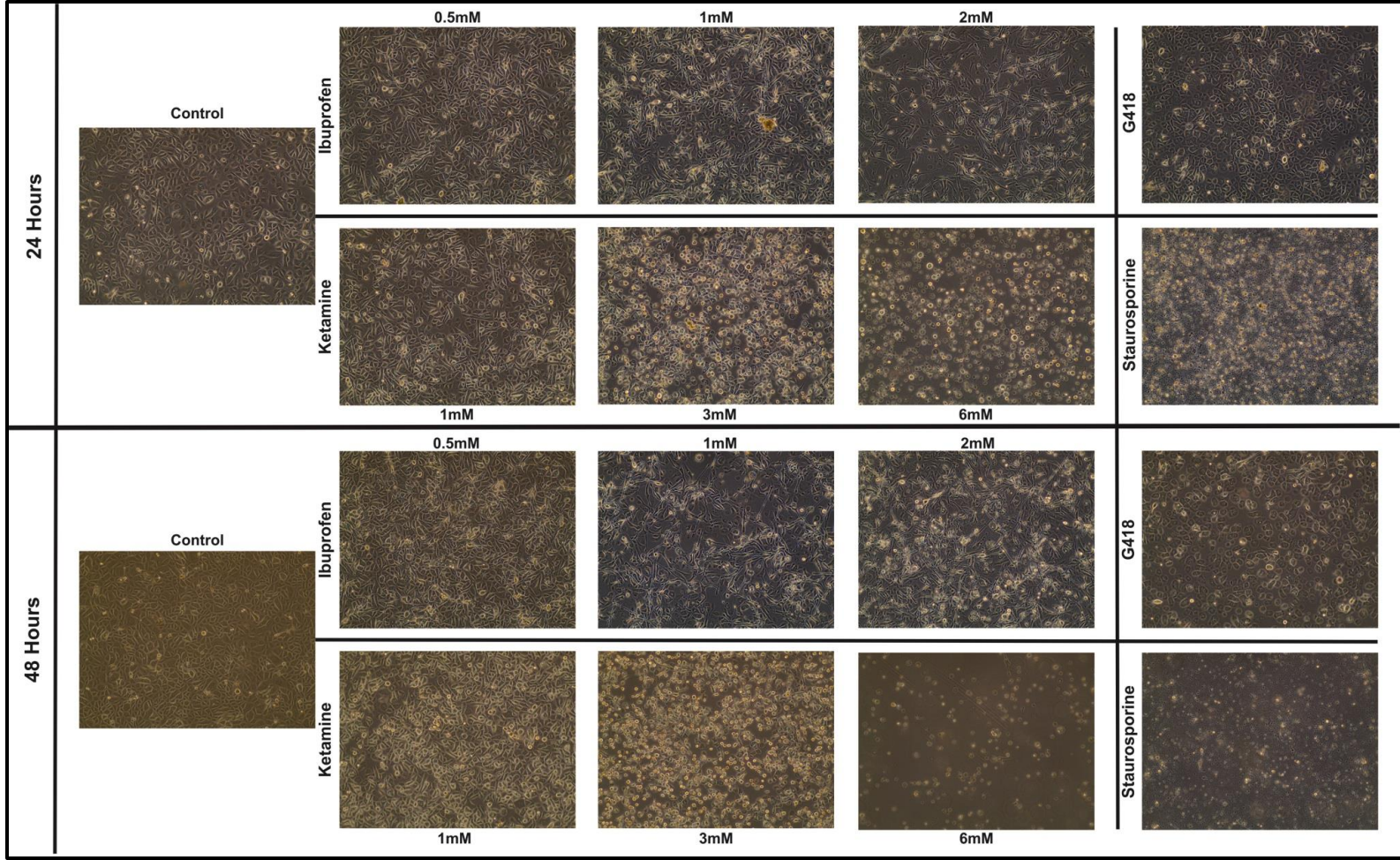


Figure 6-11 Proliferating NHU cell populations in culture with ketamine, ibuprofen, Staurosporine and G418 treatment

NHU proliferating cell populations at 24 and 48 hours with ibuprofen (0.5mM, 1mM and 2mM), ketamine (1mM, 3mM and 6mM), G418 (0.1mg/ml) and Staurosporine (0.5 μ M) treatments. Cells treated with ibuprofen became more elongated and displayed a greater amount of debris with increasing concentration. Increasing concentration of ketamine appeared very toxic to the NHU cells which became rounded in appearance and few cells remained adhered to the culture plate in the 6mM concentration ketamine at 48 hours. Staurosporine and G418 were included as known inducers of apoptosis. Staurosporine appeared very toxic to the NHU cells with many cells lifting from the culture plate at 48 hours. Cells treated with G418 appeared more rounded compared to the control cells. Scale = 50 μ m.

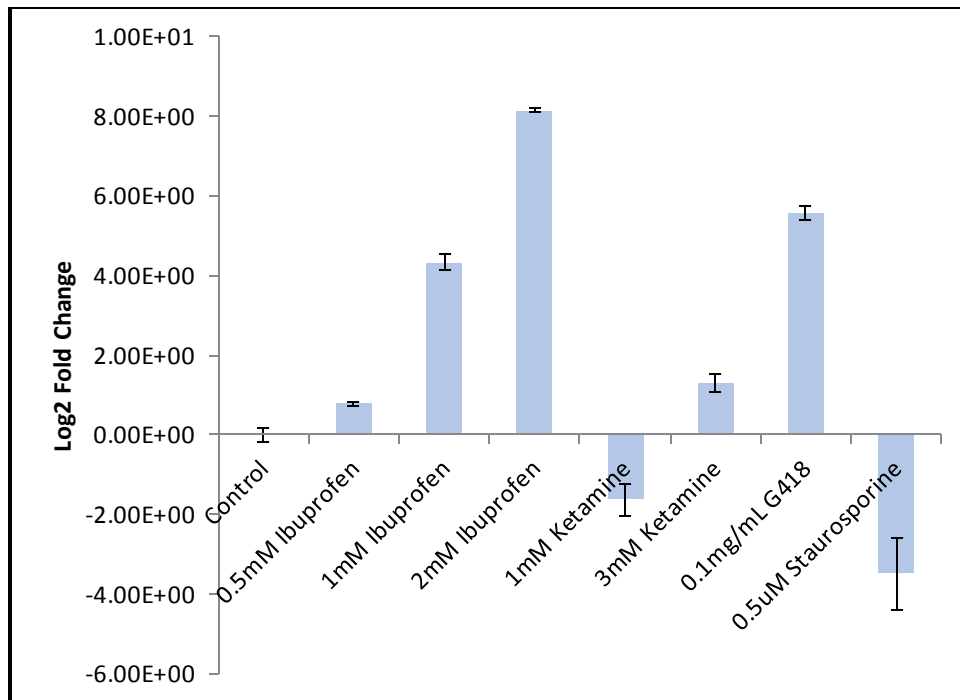


Figure 6-12 Quantitative RT-PCR – Expression of NGFR in proliferating cells treated with ibuprofen, ketamine, G418 and Staurosporine

RT-QPCR analysis of NGFR expression proliferating urothelial cells from one donor (Y1361) treated with ibuprofen (0.5mM, 1mM, 2mM), ketamine (1mM, 3mM), G418 (0.1mg/ml) and Staurosporine (0.5 μ M). A progressive increase in NGFR expression was seen relative to the control in the ibuprofen concentrations. At 1mM ketamine NGFR expression is decreased compared to control whereas at 3mM NGFR expression is increased. G418 increases NGFR expression and Staurosporine decreases expression of NGFR compared to control.

Technical - The data from the cell lines show the amount of mRNA normalised to GAPDH. Each data point is the average of 3 replicates. Error bars indicate standard deviation.

The organ cultures were established and maintained up to 14 days. Immunohistochemical analysis for NGFR at the 3, 7 and 14 day time point displayed normal basal expression of NGFR in the control organ culture (figures 6.13B, 6.14B, and 6.15B) and all urothelial cell layers. At the 3 day time point both the 0.5mM and 1mM ibuprofen concentrations retained all urothelial layers. The 0.5mM ibuprofen had basal urothelial expression of NGFR with some expansion into the intermediate cells; this expansion was much more pronounced in the 1mM ibuprofen concentration in which nearly all intermediate cells were NGFR⁺ (figure 6.13C and D). Of note in the 1mM concentration was the increase in nuclear size compared to the control. At the 2mM ibuprofen concentration the urothelium was markedly thinned with all remaining urothelial cells NGFR⁺. There were also some vacuoles in the remaining urothelium which contained necrotised urothelial cells (figure 6.13E). In both of the ketamine concentrations all urothelial layers remained present with basal labelling of NGFR. However, in the 3mM concentration there were small apoptotic bodies throughout the urothelium (figure 6.13F and G).

At 7 days in both of the ibuprofen concentrations there was a formation of vacuoles at the base of the urothelium and in comparison to the normal integrated cellular structure seen in the control organ cultures separations appear between the cells throughout the urothelium leading to apparent expansion of the urothelium compared to the control (Figure 6.14 C and D). The nuclei also appeared enlarged compared to the control. At 0.5mM concentration the basal expression of NGFR had almost been completely lost but in the 1mM concentration the expression remained expanded into the intermediate urothelial layer. The 1mM ketamine concentration displayed basal only expression of NGFR. Examination of the urothelium revealed separation between some urothelial cells in all of the urothelial cell layers similar to the ibuprofen treated organ cultures (figure 6.14E).

At 14 days, the appearance of the urothelium in the 0.5mM ibuprofen concentration remained very similar to the 7 day time point with vacuoles and separation of the urothelial cells throughout all the layers. The basal layer remained negative for NGFR (figure 6.15C). In the 1mM ibuprofen concentration there was basal expression of NGFR with some expansion into intermediate cells but this was not as pronounced

as at 7 days (figure 6.15D). Of particular note was the irregularity of the urothelial surface with some cells completely detached from the urothelium. The 1mM ketamine concentration also displayed irregularity of the urothelial surface with many cells detaching from the urothelium. The basal expression of NGFR remained at 14 days with some areas of expansion into the intermediate cells (figure 6.15E).

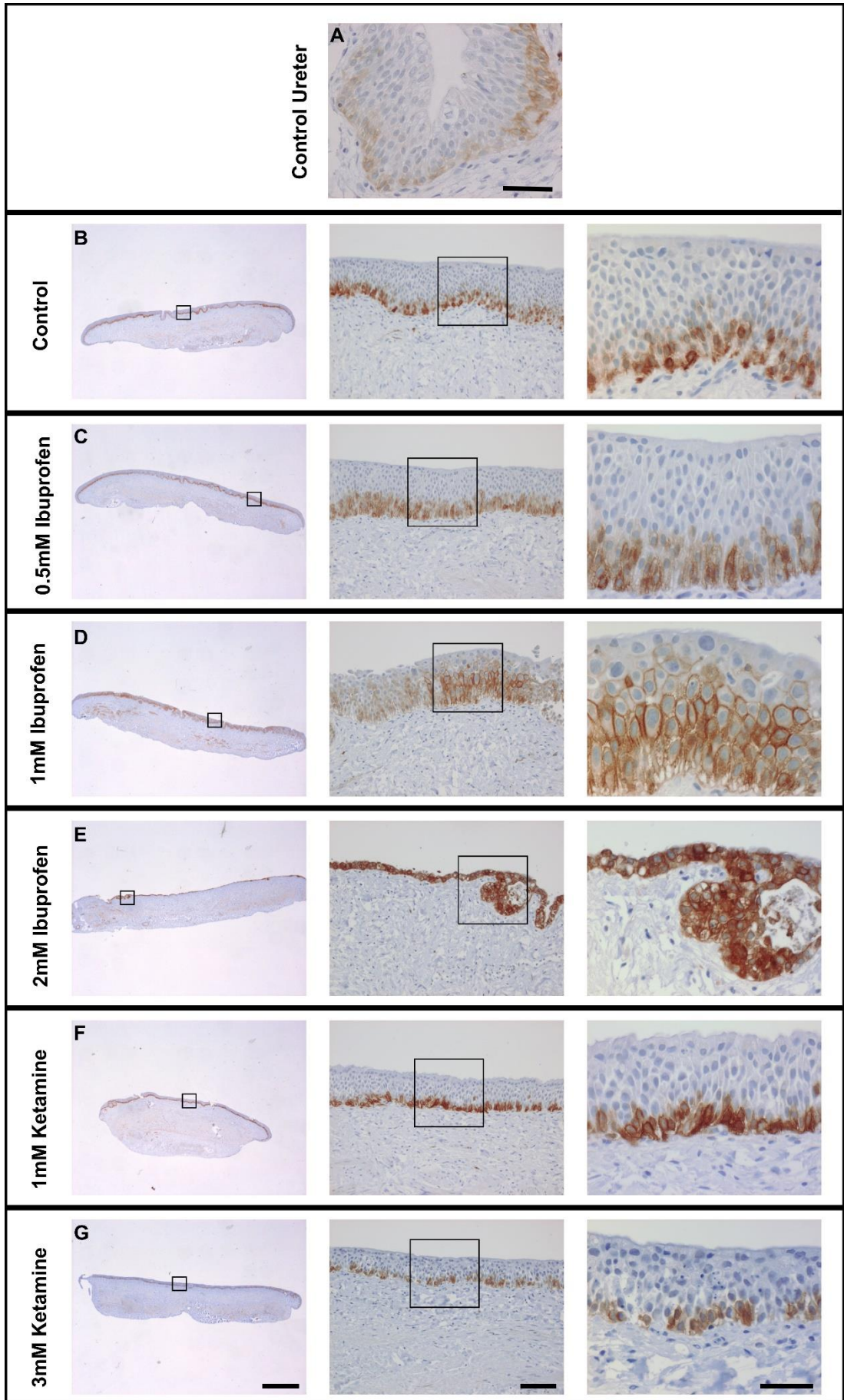


Figure 6-13 Organ Culture with immunohistochemical labelling of NGFR at 3 day time point

A – Control ureter taken at day 0 with basal urothelial labelling. **B** – Control organ culture with basal labelling of NGFR. **C** – 0.05mM ibuprofen with intact urothelium and basal NGFR expression. **D** – 1mM ibuprofen with intact urothelium and basal labelling of NGFR and expansion into intermediate cells. The nuclei appear larger compared to control. **E** – 2mM ibuprofen with loss of urothelium to basal layer. Intense labelling of NGFR is seen in the remaining urothelium. There were also some vacuoles in the urothelium containing dead urothelial cells. **F** – 1mM ketamine with intact urothelium and basal NGFR expression similar to control. **G** – 3mM ketamine with intact urothelium and basal NGFR expression. Note small apoptotic bodies throughout the urothelium. Scale – Left = 200µm, Middle = 100µm, Right and control = 50µm.

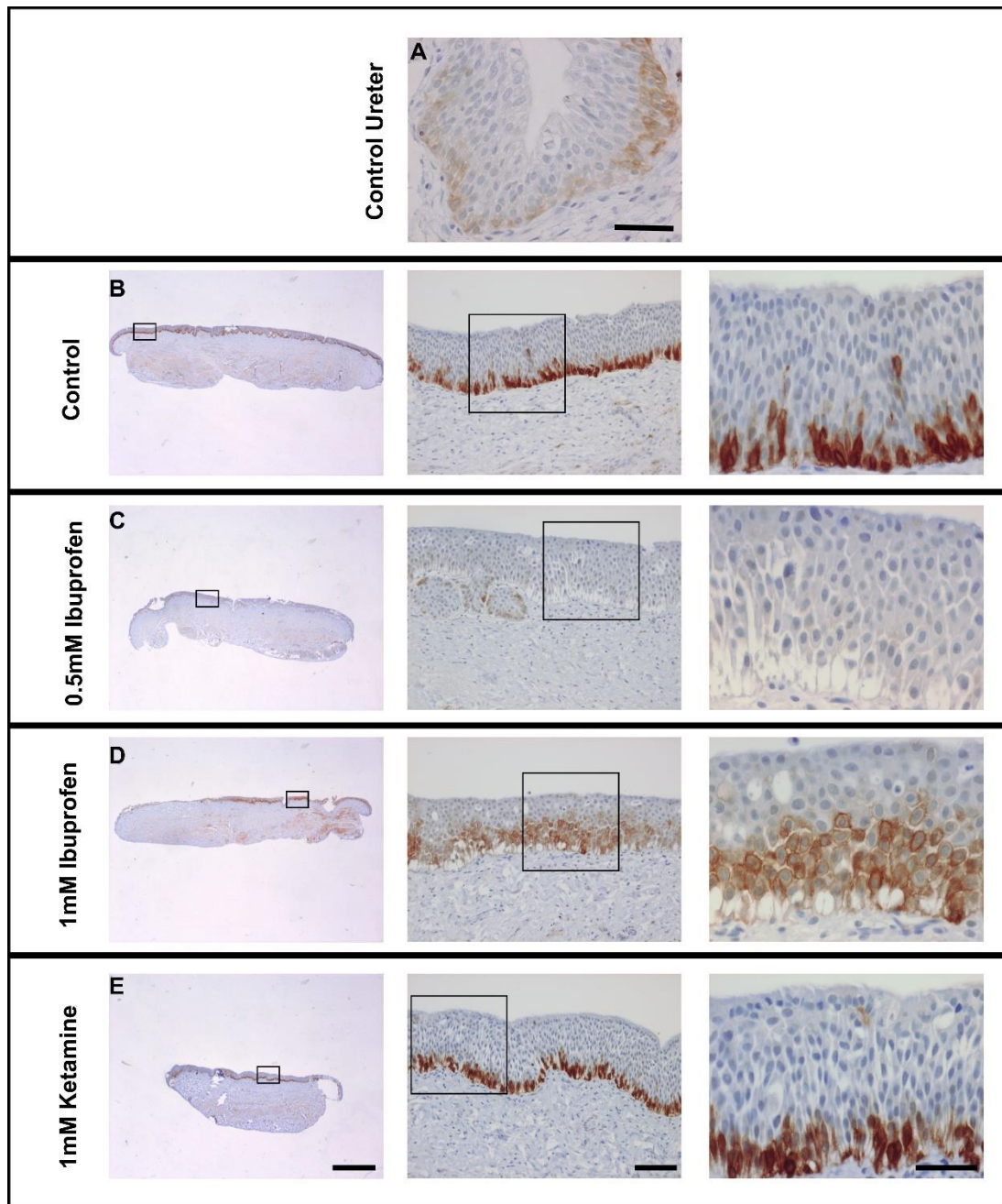


Figure 6-14 Organ Culture with immunohistochemical NGFR labelling at 7 day time point

A & B – control ureter taken at day 0 and control organ culture with basal urothelial labelling of NGFR. **C** – 0.5mM ibuprofen with intact urothelium. Separation and vacuoles at the basement membrane and visible divisions between cells in the intermediate cell layer. Nuclei appear larger compared to the control. NGFR expression is lost. **D**– 1mM ibuprofen with intact urothelium. Separation and vacuoles at the basement membrane are evident as in C. NGFR expansion is noted into the intermediate cell layer. **E**– 1mM ketamine with intact urothelium and basal expression of NGFR. Scale – Left = 200 μ m, Middle = 100 μ m, Right and control = 50 μ m.

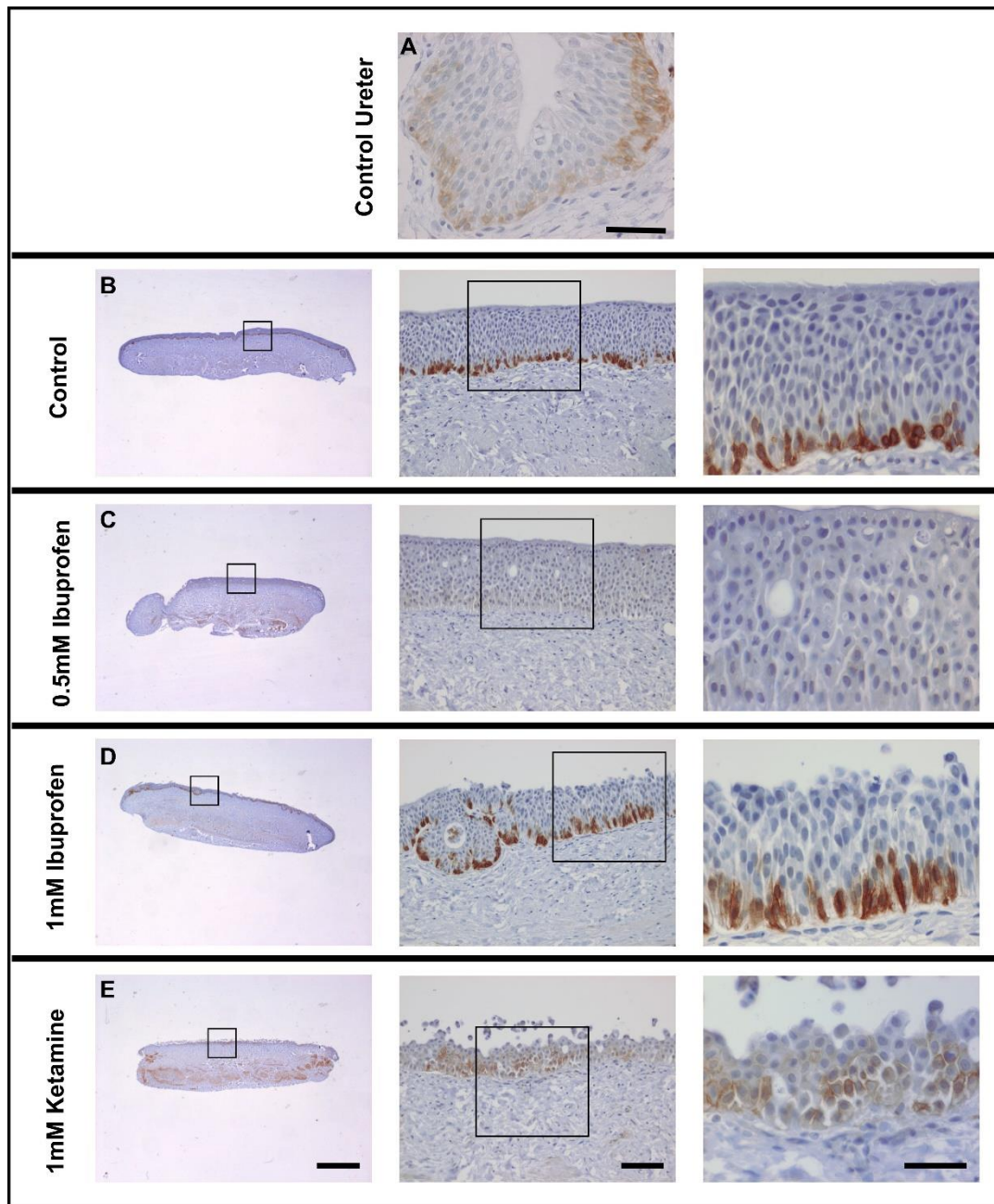


Figure 6-15 Organ Culture with immunohistochemical labelling of NGFR at 14 day time point

A & B – control ureter taken at day 0 and control organ culture with basal urothelial labelling of NGFR. **C** – 0.5mM ibuprofen with intact urothelium, vacuoles and divisions between cells were visualised in the basal and intermediate cell. Basal expression of NGFR was lost. **D** – 1mM ibuprofen superficial urothelial cells appear irregular with some detaching from the surface. In the middle image there was a vacuole containing cell debris. Basal expression of NGFR was seen throughout with some extension into the intermediate cells. **E** – 1mM ketamine superficial and some intermediate cells detaching from an irregular urothelial surface. Basal expression of NGFR with some extension into intermediate cells. Scale – Left = 200µm, Middle = 100µm, Right and control = 50µm.

The organ culture was further analysed by immunohistochemistry for markers of proliferation (Ki67), markers of urothelial differentiation (CK5 and CK13), a marker of terminal differentiation UPK3A and a marker of DNA repair and/or apoptosis (p53). These markers were included to assess the normality of the urothelium in the organ culture system and furthermore to assess any differences noted in the different treatment categories on the overall phenotype and relate to the expression of NGFR.

There was no expression of Ki67 in the in situ (P0) ureter. Nuclear expression of Ki67 was seen throughout the urothelium across all time points in the control organ culture. However across all time points in the ibuprofen and ketamine treatment groups there were only a few Ki67⁺ cells with the majority of the organ cultures negative for Ki67 expression (figure 6.16). The in situ (P0) ureter displayed normal basal and intermediate urothelial cell expression of CK13. In the organ culture the expression remained throughout all samples but was of weaker intensity at the 14 day time point (figure 6.17). This was very similar to CK5 in which normal basal expression was seen at the in situ (P0) ureter and remained in all the cultures but was of weaker intensity at the 14 day time point (figure 6.18). The in situ (P0) ureter was negative for p53 expression and there was limited expression throughout all the organ culture with only a few positive cells in the entire series. The few p53⁺ cells were in the ibuprofen and ketamine-treated cultures with the control organ culture completely negative (figure 6.19). There was no expression of UPK3A throughout the organ culture (figure not shown). Table 6.3 summarises the results of the organ cultures.

Table 6-4

Summary of the expression of the markers for the organ culture at all-time points

Time Point	Treatment	Conc (mM)	Marker					
			NGFR	Ki67	CK5	CK13	UPK3A	P53
3 Days	Control		Basal	Basal/Int/Superficial	Basal	Basal/Intermediate	Negative	Negative
	Ibuprofen	0.5	Basal/Intermediate +	Negative				
		1	Basal/Intermediate ++					
		2	Basal (only remaining)					
	Ketamine	1	Basal					
		3	Basal					
7 Days	Control		Basal		Basal/Int/Superficial	Basal	Basal/Intermediate	Negative
	Ibuprofen	0.5	Negative	Negative				
		1	Basal/Intermediate ++					
	Ketamine	1	Basal					
14 days	Control		Basal		Basal/Int/Superficial	Basal (Weaker)	Basal/Intermediate (Weaker)	Negative
	Ibuprofen	0.5	Negative	Negative				
		1	Basal/Intermediate +					
	Ketamine	1	Basal/Intermediate +					

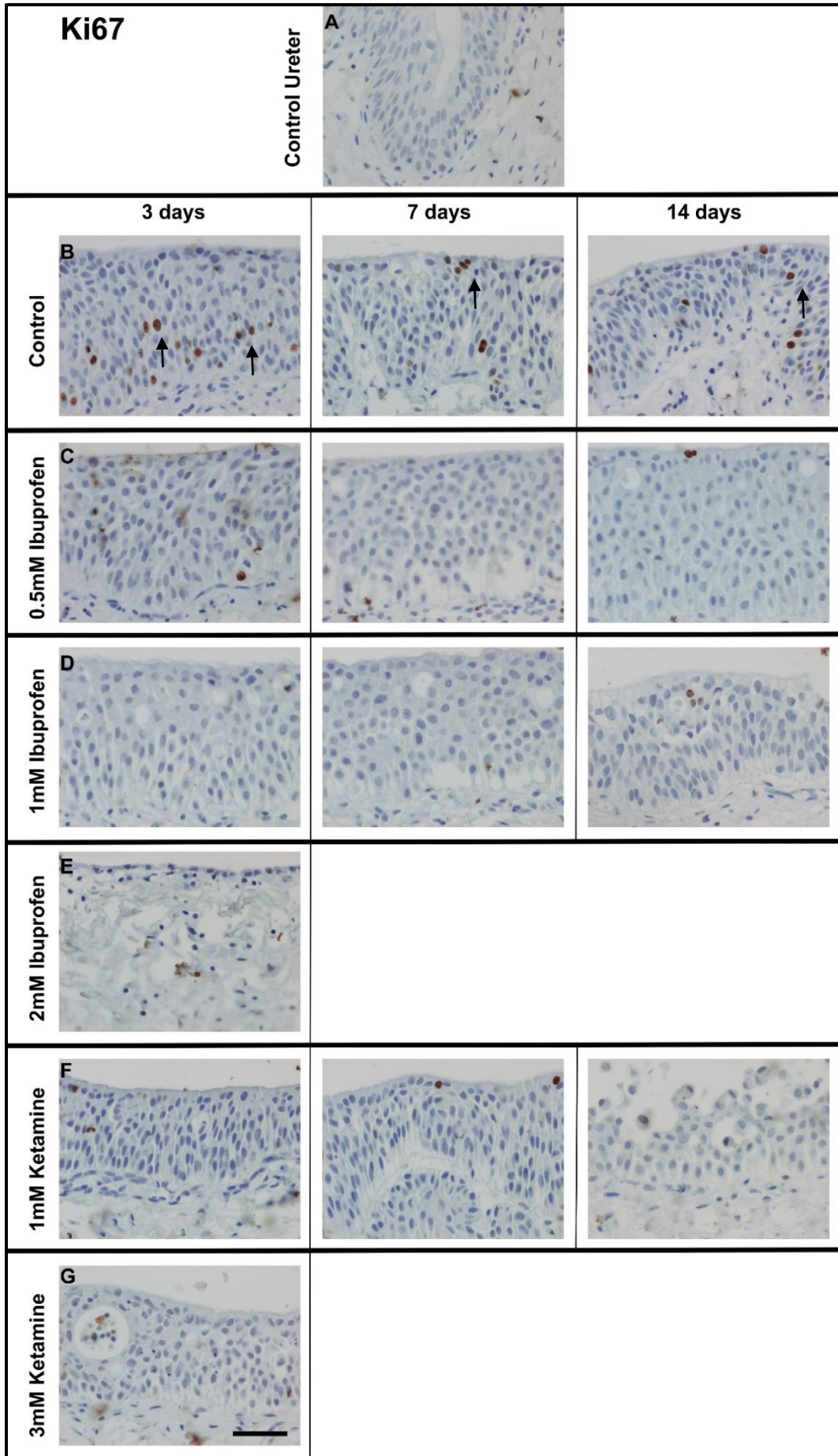


Figure 6-16 Organ Culture with immunohistochemical labelling for Ki67

A – Control ureter taken at day 0 time point with no Ki67⁺ cells. **B**– Control organ culture at 3, 7 and 14 day time points. Ki67⁺ cells at all-time points in urothelial cell layers (arrowed). **C-G** ibuprofen and ketamine treatments at 3, 7 and 14 day time points there was less expression of Ki67 compared to control in B with few Ki67⁺ cells in 0.05mM ibuprofen at 3 & 14 days and 1mM ketamine at 7 days. The cultures were otherwise negative. Scale = 50µm.

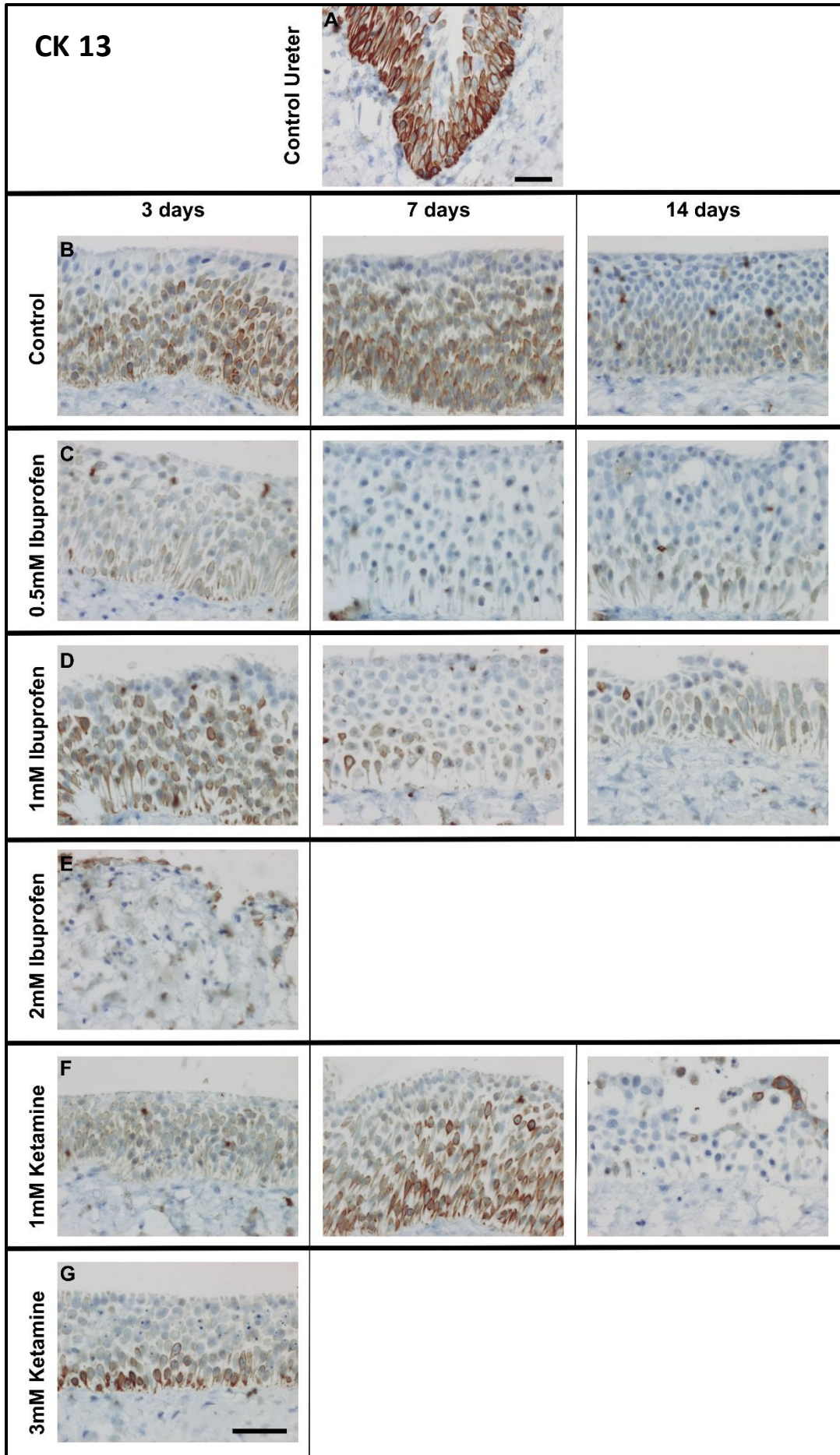


Figure 6-17 Organ Culture with immunohistochemical labelling for CK13

A – Control ureter taken at day 0 time point with basal and intermediate labelling for CK13.
B – Control organ culture at 3, 7 and 14 day time points with basal and intermediate cell labelling for CK13 evident across all time points. Labelling appears less intense at the 14 day time point. CK13 labelling is retained in all treatment groups (**C-G**). Scale = 50µm.

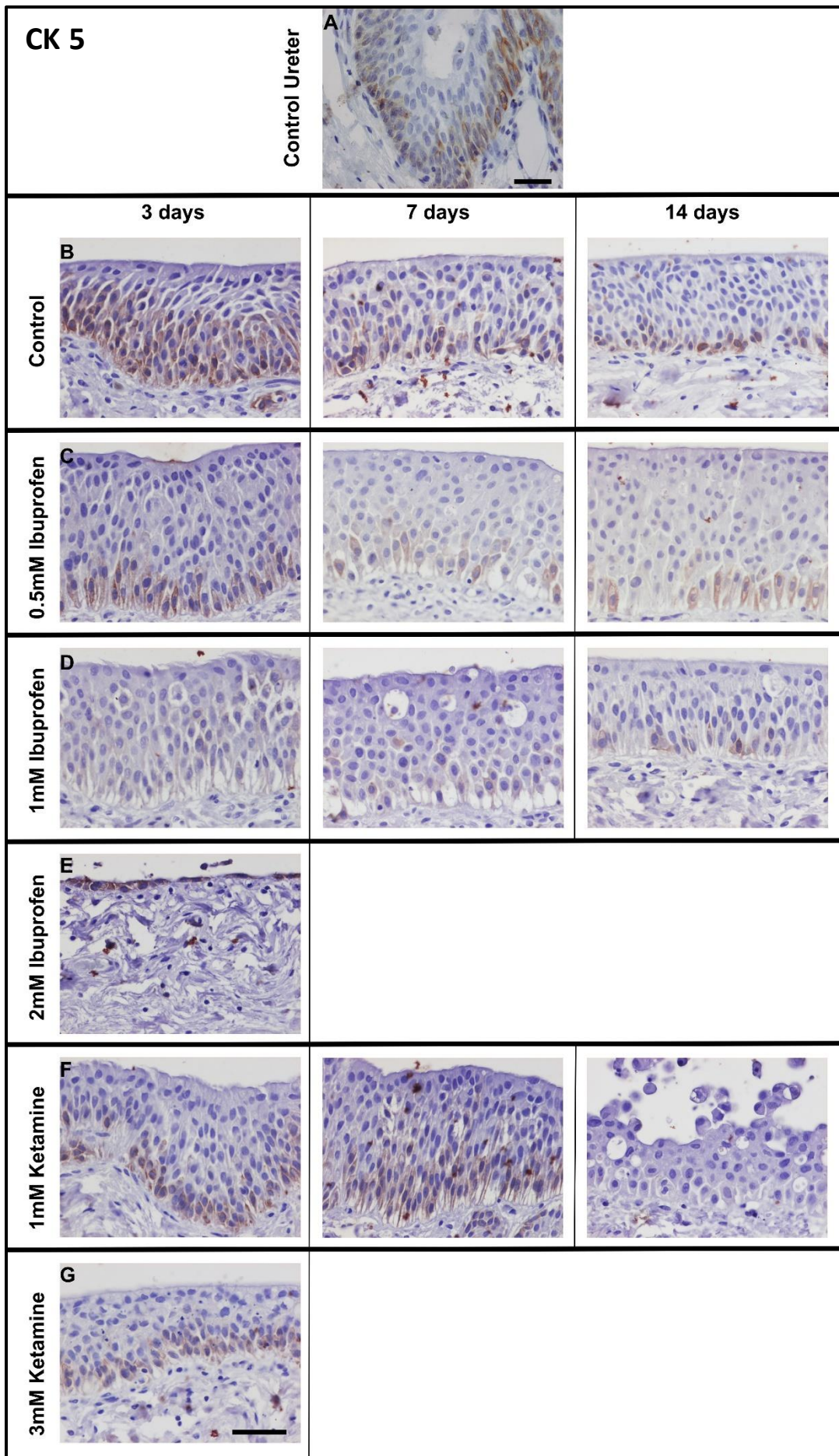


Figure 6-18 Organ Culture with immunohistochemical labelling for CK5

A – Control ureter taken at day 0 time point with basal labelling for CK5. **B** – Control organ culture with CK5 basal labelling retained at all-time points. **C-E** ibuprofen treatments (0.5mM – 2mM) with CK5 labelling in all treatments across the time points. **F** – 1mM ketamine CK5 expression is retained at 3 and 7 day time point with weaker expression at the 14 day time point. **G** – 3mM ketamine retains CK5 expression at 3 day time point. Scale = 50µm.

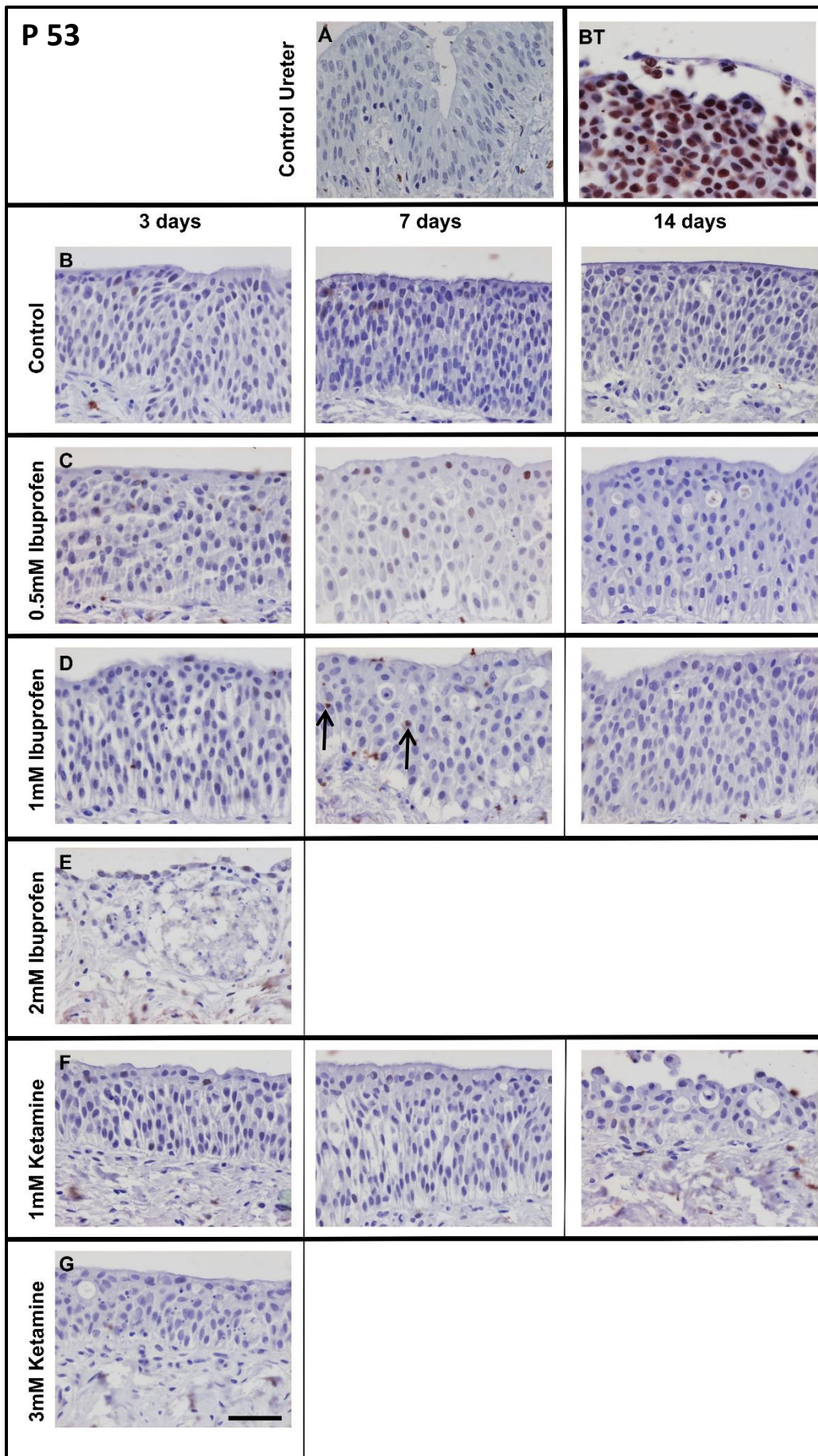


Figure 6-19 Organ culture with immunohistochemical labelling for P53

A – Control ureter taken at day 0 time point with no p53⁺ cells. **BT** – Bladder tumour control with multiple p53⁺ cells. **B** – Organ culture control at 3, 7, 14 day time point with no p53⁺ cells evident. **C-G** ibuprofen and ketamine treatments at 3, 7 and 14 day time points there was no to very minimal p53⁺ cells (arrowed). Scale = 50µm.

6.5 Results Summary

- Glucocorticoids, cytokines and BDNF did not modulate expression of NGFR transcript.
- Ibuprofen treatment led to induction of NGFR transcript expression over 0.5mM, 1mM and 2mM concentration.
- Preliminary investigations showed that treatment of NHU cells with ketamine at concentrations >3mM and G418 led to the induction of NGFR transcript expression
- Organ culture displayed normal basal expression of NGFR and a normal phenotypic expression of CK5 and CK13. There was no expression of UPK3A representing some loss of urothelial differentiation.
- Organ culture with ibuprofen treatments displayed a loss of NGFR expression in the 0.5mM treatment group after the 3 day time point. There was expansion of NGFR into the intermediate cells in the 1mM treatment group. The 2mM treatment lead to extensive urothelial damage after 3 days with all remaining urothelial cells NGFR⁺.
- Organ culture with ketamine treatments displayed basal expression of NGFR at the 1mM concentration with some expansion into the intermediate cells at 14 days. In the 3mM treatment the expression of NGFR remained basal at 3 days.
- Ki67 expression was present in all the urothelial cell layers in the control organ culture but its expression was down regulated in the ketamine and ibuprofen treatment groups.
- In the organ culture there was some evidence of cell death but this did not result in an induction of p53.

7 Discussion

The aim of this project was to examine the expression of NGFR in the normal urothelium and KIC and to examine possible modulators of NGFR expression in the urothelium. The overall results of the study confirm that NGFR protein is expressed in the basal layer of normal human urothelium and in KIC there was expansion from basal into the suprabasal urothelium. An *in vitro* approach demonstrated that transcript expression of NGFR was of greatest abundance in proliferating NHU cells with minimal expression of NGFR transcript in differentiated NHU cells. By developing differentiated urothelial cell sheets it was shown that the normal basal sporadic distribution of NGFR⁺ cells was retained. Ureteric organ culture also maintained the normal basal expression of NGFR. Ibuprofen, high dose (3mM) ketamine and G418 all increased expression of NGFR transcript. Ureteric organ culture confirmed an expansion of NGFR protein in ibuprofen and ketamine treated samples. By contrast, the study excluded glucocorticoids, cytokines and BDNF as direct modulators of urothelial NGFR expression.

7.1 In situ expression of NGFR

The observation that NGFR protein was expressed in the basal layer of the urothelium in both normal ureter and bladder along with the suprabasal expansion of NGFR in KIC supports previous reports in the literature (Baker et al., 2013, Wezel et al., 2014). In this study no evidence was found for a link in the expression of Egr-1 and NGFR. Egr-1 was identified from the literature as a potential transcriptional regulator for NGFR (Chapter 3). Outside of the urinary system, Egr-1 has been associated with cell injury and is also known to be stimulated by a number of inflammatory cytokines and growth factors which may have relevance in KIC (Khachigian, 2006, Ngiam et al., 2007). Nikam et al established a link between Egr-1 and NGFR in Schwann cells after nerve injury in a rat model (Nikam et al., 1995). The reason for the disparity between Egr-1 and NGFR with this study is unclear but two reasons have been identified as

factors which may be of relevance. Firstly, the existing literature around the link with NGFR and the urothelial expression of Egr-1 is limited to rodent studies (Nikam et al., 1995, Gao et al., 2007, Egerod et al., 2009b). Secondly, Egr-1 is an early transcriptional regulator which is generally expressed within a few hours of its induction (reviewed by (Yan et al., 2000)). The existing studies which displayed a link between Egr-1 and NGFR expression occur rapidly after an insult; this is highlighted by Nikam et al which showed activation of Egr-1 in Schwann cells within 3 hours of sciatic nerve transection (Nikam et al., 1995). The findings in this study were established from biopsies from patients with established chronic and often end stage KIC and therefore the link between NGFR and Egr-1 may have occurred at an early stage in the disease process and lost in the approach taken in this study.

The histological review of the bladder taken from a patient during substitution cystoplasty allowed extensive histological analysis of the bladder. The finding of widespread urothelial destruction and areas of chronic inflammation throughout the bladder reinforced the previous findings from urothelial biopsies reported in other studies (Oxley et al., 2009, Chen et al., 2011, Lai et al., 2012). However, these previous studies had not been able to demonstrate the extent of damage to the urothelium and the bladder as a whole. Furthermore, the degree of urothelial damage often makes characterisation of the urothelium difficult from biopsy samples obtained, therefore the analysis of the whole bladder allowed evaluation of any remaining urothelium (Baker et al., 2013). This is highlighted in the report by Oxley et al, which remarked on ulceration and urothelial loss in 7 out of 17 samples and subsequently was unable to perform further immunohistological analysis on some samples (Oxley et al., 2009).

Despite the widespread urothelial loss, the analysis of the entire bladder allowed for the examination of histopathological anomalies such as von Brunn's nests and a urachal remnant. Von Brunn's nests represent areas of urothelium within the lamina propria and submucosa which can be considered a normal variant or can arise as a result of local inflammation and during reactive proliferative change. The urachus is a fibrous embryonic remnant of the fetal allantois: a canal that drains the urinary bladder in the fetus. The allantois becomes progressively obliterated during fetal life

to form the urachus. The urachus is present in all infants at birth and gradually regresses in most, being found in only approximately one third of adults. The urachus is situated in the perivesical space between the transversalis fascia (anteriorly) and the peritoneum (posteriorly). It extends from the posterior aspect of the umbilicus to the apex of the bladder. In adult life it forms the median umbilical ligament and its section is required for mobilisation of the bladder at surgery. The length of the urachus varies from 1cm to 15cm (mean 5cm). In the one third of adults with a retained urachus which is considered a normal variant, the zone of attachment of the urachus at the apex of the bladder may present in 4 different ways:

- At the apex of the papilla
- As a continuity between the bladder mucosa and the internal layer of the urachus
- By termination of the urachus at the outer layer of the bladder mucosa without communication (non-patent)
- Depression of the bladder mucosa indicating termination of the urachus

Defective closure may however give rise to pathological variants including complete fistula, cyst, sinus or diverticulum (Cappele et al., 2001).

Histologically the urachus has three layers: i) internal layer of transitional epithelium with areas of focal mucinous glandular metaplasia, ii) intermediate layer consisting of fibroconnective tissue, iii) an external smooth muscle layer continuous with the detrusor muscle of the bladder. The lumen is often irregular with alternating strictures and dilatations (Cappele et al., 2001).

In the cystectomy specimen studied, the identification of a normal variant of the urachus with no communication with the bladder and several von Brunn's nests in which the urothelium was continuous with luminal surface of the bladder allowed the direct comparison of two states where urothelium was a) in contact with urine and b) the urothelium in the non-patent urachus. Assessment of NGFR expression revealed expansion into the suprabasal urothelium in the von Brunn's nests but normal basal expression in the urachus. These findings may therefore indicate that the change in NGFR expression is due to urinary exposure rather than a systemic

element. The urachus displayed a mixed glandular/transitional phenotype with normal basal/intermediate expression of CK13 and some areas with UPK3A expression representing a normal differentiated urothelial phenotype in these regions. Interestingly, however, expression of CK20 was lost throughout the urachus. Paner et al reviewed urachal remnant expression of CK20 and found loss of expression in regions expressing a urothelial phenotype (0/3) but maintenance of expression in regions with a glandular phenotype (5/6) (Paner et al., 2011). The von Brunn's nests showed loss of differentiation which may reflect the loss of superficial cells of the urothelium but also might reflect an unusual, dedifferentiated phenotype in KIC. In relation to an altered phenotype in KIC, previously, Oxley et al commented that a panel of KIC biopsies revealed urothelial atypia so marked as to mimic carcinoma in situ (CIS), with nuclear enlargement, disorganisation and high immunoreactivity for p53 and Ki67 (Oxley et al., 2009). Oxley et al found expression of CK20 was negative in all KIC samples and it was concluded the changes were therefore more likely due to reactive atypia. In the urothelium the expression of CK20 is a sensitive marker of differentiation and is restricted to the superficial cells. In the case of dysplasia or CIS, CK20 is abnormally expressed throughout all of the urothelial layers (Harnden et al., 1995, Harnden et al., 1996, Harnden et al., 1999a). However, negative expression of CK20 is classed as non-informative for the diagnosis (Harnden et al., 1995, Harnden et al., 1996). This means that it is important to be careful in interpreting the diagnostic significance of CK20 loss in KIC.

7.2 NGFR in vitro expression

The use of an established in vitro cell culture system for culturing urothelial cells in proliferating and differentiated states (Southgate et al., 2002, Cross et al., 2005) provided an excellent basis for an experimental model to examine NGFR expression at transcript and protein levels. From this it was possible to show expression of NGFR transcript in proliferating NHU cells and minimal expression in differentiated NHU cells. Protein expression of NGFR was only apparent in differentiated stratified urothelial cell sheets. The expression of NGFR in the cell sheets was basal and

equivalent to normal bladder and ureter expression, however the expression of NGFR was never as abundant as the normal tissue suggesting the presence of missing factors that are not replicated in the in vitro system. This was supported by the maintenance of basal NGFR expression in the ureteric organ culture model. Nevertheless, the use of the in vitro model provided a good basis for the examination of the modulation of NGFR in a human system as previous models have all been in rodents (Klinger and Vizzard, 2008, Schnegelsberg et al., 2010, Girard et al., 2012)

7.3 Modulation of NGFR expression

Extensive review of the literature revealed several candidate modulators and through experimentation using the in vitro system it was possible to exclude the glucocorticoids, cytokines and BDNF as modulators of NGFR. However, for the first time it has been established that ibuprofen (NSAID) and high dose ketamine (3mM) both modulate the expression of NGFR transcript in proliferating NHU cells and in a ureteric organ culture system. The question arises as to why ibuprofen and ketamine may regulate NGFR. NGFR was identified as an important upstream cellular target in bladder cancer cell lines treated with high dose ibuprofen which led to apoptosis of the cells (Khwaja et al., 2004). However, in situ NGFR-positive urothelial cells have been shown to be primed for proliferation (Wezel et al., 2014). In the literature, it has been established that NGFR has different functions depending on a number of variable factors including cell type, cell differentiation status, neurotrophin binding (pro- or mature form), presence of interacting transmembrane co-receptors and post-translation modification expression (Barker, 2004, Lu et al., 2005, Schecterson and Bothwell, 2010). In particular the expression of the co-receptor Trk A with NGFR has been correlated with survival and proliferation, whereas the expression of NGFR alone is associated with apoptosis (reviewed in (Chao, 2003, Micera et al., 2007, Teng et al., 2010). The examination of the cells in culture in this study revealed evidence of cell death in cells cultured with high concentrations of ketamine (cells displayed evidence of apoptosis) and ibuprofen (change in cell morphology and increased cell debris). The process taking place in the urothelium with NSAID and ketamine

treatment may therefore be a reflection of an NGFR associated apoptotic process. The addition of G418 and staurosporine as pro-apoptotic controls was used to establish if NGFR up regulation was common to all apoptotic processes in NHU cells. G418 is an aminoglycoside antibiotic which blocks polypeptide synthesis by inhibiting the elongation step in both prokaryotic and eukaryotic cells (Eustice and Wilhelm, 1984). Staurosporine is a microbial alkaloid that can induce apoptosis in essentially all cell types and was initially shown to be potent inhibitor of protein kinase C but is now known to inhibit many different protein kinases (reviewed in (Kruman et al., 1998). Intriguingly opposing effects were established, with G418 inducing an increase in NGFR expression and staurosporine inducing a decrease in expression of NGFR; this questions the theory of NGFR up regulation being a generic pathway to apoptosis in urothelial cells.

Further work is required to firstly confirm apoptosis in ibuprofen and ketamine treated urothelial cells. Secondly, to compare the signalling pathways of staurosporine and G418 and establish any similarities in the pathways that G418, NSAID and ketamine signal through. Potential pathways associated with NGFR expression and apoptosis after NSAID treatment include the p38MAPK pathway, which induced NGFR expression and subsequent apoptosis in prostate cancer cells (Quann et al., 2007, Wynne and Djakiew, 2010). The p38MAPK pathway is a general pathway activated in response to stress stimuli such as cytokines, UV radiation, heat shock and leads to apoptosis and autophagy. The p38MAPK pathway is a candidate for activation in ibuprofen and ketamine treated NHU cells and could be relevant in KIC. In the longer term, establishing the relevance of other NGFR associated receptors in the human urothelium such as the TrKs, which to date have only been examined in a rodent model (Murray et al., 2004, Girard et al., 2011), and sortilin may give further information into the function of NGFR in the urothelium.

7.4 Limitations

Limitations from this study arose mainly from the use of an in vitro system. The study demonstrated difficulty with replicating basal expression of NGFR as typically displayed in normal ureteric and bladder specimens, albeit that at both transcript and protein levels there was considerable and unexplained variability in the extent of expression between urothelial tissues from different donors in situ. In vitro, this study was unable to demonstrate the expression of NGFR transcript in proliferating or differentiated NHU cells. At the protein level, cell sheets only demonstrated sporadic NGFR expression. This minimal and variable expression of NGFR at transcript and protein level in the in vitro system made the modulation of NGFR difficult to define and interpret and suggests that the trigger for regulating its expression has not been identified. However, in spite of the limitation of the in vitro system in relation to NGFR in this instance, the use of an in vitro system does allow human-relevant experiments to be performed, which would otherwise be impossible. The use of an in vitro system also alleviates many of the ethical and cross-species implications that would be encountered for example in animal studies.

The use of an in vitro approach in this study allowed for several candidate modulators to be examined and tested systematically, enabling candidate modulators, such as ibuprofen, to then be explored in the organ culture system. The use of organ culture was particularly useful, as the normal basal expression of NGFR was maintained and the results of modulation could be more reliably interpreted. The maintenance of basal expression of NGFR in organ culture may be the result of an interaction between the urothelium and underlying stroma however this theory would require examination in future research studies.

The time periods for potential modulators were also particularly short-term due to the nature of an in vitro model. This means that it is difficult to relate the results of modulation to KIC, which is considered a chronic disease process. However, the direct modulation of NGFR by ibuprofen does give an insight into a specific pathway that may play role in the modulation of NGFR expression in the urothelium, whether

related to KIC disease process or not. Furthermore, the development of an organ culture system should enable a more chronic study of modulation of NGFR in future studies.

Overall, NGFR is a difficult receptor to study due to the complexity of its expression (pro or mature form), its co-receptor expression and the variety of ligands. The use of a human ex vivo approach to study the urothelium in isolation has the advantage of reducing complexity, but has revealed a dependency on other, as yet unidentified, extrinsic factors. This suggests that although an in vitro approach is useful, it can only ever give a partial insight into the regulation and function of NGFR within the bladder

7.5 Conclusions

This study supports a urinary-mediated urothelial damage process in KIC and implicates NGFR upregulation in the pathogenesis. Ketamine and other toxins are able to directly up-regulate expression of NGFR in the urothelium and this study has laid the foundation of an in vitro cell culture and organ culture model for future exploration of the role of NGFR in the repair and damage of urothelium. Central to this, the identification of several NGFR inducers: ketamine, ibuprofen and G418, provide a basis for a future comparative study of downstream pathways and mechanisms which will provide insight into the function of NGFR in KIC and moreover the urothelium and other benign bladder pathologies.

8 References

- ABRAMS, P. 2003. Describing bladder storage function: overactive bladder syndrome and detrusor overactivity. *Urology*, 62, 28-37.
- ABRAMS, P., CARDOZO, L., FALL, M., GRIFFITHS, D., ROSIER, P., ULMSTEN, U., VAN KERREBROECK, P., VICTOR, A. & WEIN, A. 2002. The standardisation of terminology of lower urinary tract function: report from the Standardisation Sub-committee of the International Continence Society. *Neurourology and urodynamics*, 21, 167-178.
- AUTIERI, M. V., KELEMEN, S. E., GAUGHAN, J. P. & EISEN, H. J. 2004. Early growth responsive gene (Egr)-1 expression correlates with cardiac allograft rejection. *Transplantation*, 78, 107-111.
- BAKER, S. C., STAHLSCHMIDT, J., OXLEY, J., HINLEY, J., EARDLEY, I., MARSH, F., GILLATT, D., FULFORD, S. & SOUTHGATE, J. 2013. Nerve hyperplasia: a unique feature of ketamine cystitis. *Acta neuropathologica communications*, 1, 64.
- BARKER, P. A. 2004. p75NTR Is Positively Promiscuous. *Neuron*, 42, 529-533.
- BIRDER, L. & ANDERSSON, K. E. 2013. Urothelial signaling. *Physiol Rev*, 93, 653-80.
- CAPPELE, O., SIBERT, L., DESCARGUES, J., DELMAS, V. & GRISE, P. 2001. A study of the anatomic features of the duct of the urachus. *Surgical and Radiologic Anatomy*, 23, 229-235.
- CHAO, M., CASACCIA-BONNEFIL, P., CARTER, B., CHITTKA, A., KONG, H. & YOON, S. O. 1998. Neurotrophin receptors: mediators of life and death. *Brain research reviews*, 26, 295-301.
- CHAO, M. V. 2003. Neurotrophins and their receptors: a convergence point for many signalling pathways. *Nature Reviews Neuroscience*, 4, 299-309.
- CHEN, Y.-C., CHEN, Y.-L., HUANG, G.-S. & WU, C.-J. 2011. Ketamine-associated vesicopathy. *QJM*, hcr170.
- CHU, F. M. & DMOCHOWSKI, R. 2006. Pathophysiology of Overactive Bladder. *The American Journal of Medicine*, 119, 3-8.
- CHU, P. S. K., MA, W. K., WONG, S. C. W., CHU, R. W. H., CHENG, C. H., WONG, S., TSE, J. M., LAU, F. L., YIU, M. K. & MAN, C. W. 2008a. The destruction of the lower urinary tract by ketamine abuse: a new syndrome? *BJU Int*, 102, 1616-1622.
- CHU, P. S. K., MA, W. K., WONG, S. C. W., CHU, R. W. H., CHENG, C. H., WONG, S., TSE, J. M., LAU, F. L., YIU, M. K. & MAN, C. W. 2008b. The destruction of the lower urinary tract by ketamine abuse: a new syndrome? *BJU international*, 102, 1616-1622.
- COHEN, S. M. 1998. Urinary bladder carcinogenesis. *Toxicologic pathology*, 26, 121-127.

- CROSS, W., EARDLEY, I., LEESE, H. J. & SOUTHGATE, J. 2005. A biomimetic tissue from cultured normal human urothelial cells: analysis of physiological function. *American Journal of Physiology-Renal Physiology*, 289, F459-F468.
- CRUZ, C. D. 2013. Neurotrophins in bladder function: What do we know and where do we go from here? *Neurourology and urodynamics*.
- DALGARNO P. J., S. D. 1996. Illicit use of ketamine in Scotland. *J Psychoact Drugs*, 28, 191-9.
- DENG, F.-M., DING, M., LAVKER, R. M. & SUN, T.-T. 2001. Urothelial function reconsidered: a role in urinary protein secretion. *Proceedings of the National Academy of Sciences*, 98, 154-159.
- DENG, F. M., LIANG, F. X., TU, L., RESING, K. A., HU, P., SUPINO, M., HU, C. C., ZHOU, G., DING, M., KREIBICH, G. & SUN, T. T. 2002. Uroplakin IIIb, a urothelial differentiation marker, dimerizes with uroplakin Ib as an early step of urothelial plaque assembly. *J Cell Biol*, 159, 685-94.
- DMITRIEVA, N. & MCMAHON, S. B. 1996. Sensitisation of visceral afferents by nerve growth factor in the adult rat. *Pain*, 66, 87-97.
- DMITRIEVA, N., SHELTON, D., RICE, A. S. & MCMAHON, S. B. 1997. The role of nerve growth factor in a model of visceral inflammation. *Neuroscience*, 78, 449-59.
- DOMINO, E. F., CHODOFF, P. & CORSSSEN, G. 1965. Pharmacologic effects of CI-581, a new dissociative anesthetic, in man. *Clinical pharmacology and therapeutics*, 6, 279.
- EGEROD, F., BARTELS, A., FRISTRUP, N., BORRE, M., ØRNTOFT, T., OLEKSIEWICZ, M., BRÜNNER, N. & DYRSKJØT, L. 2009a. High frequency of tumor cells with nuclear Egr-1 protein expression in human bladder cancer is associated with disease progression. *BMC cancer*, 9, 385.
- EGEROD, F. L., SVENDSEN, J. E., HINLEY, J., SOUTHGATE, J., BARTELS, A., BRÜNNER, N. & OLEKSIEWICZ, M. B. 2009b. PPAR α and PPAR γ Coactivation Rapidly Induces Egr-1 in the Nuclei of the Dorsal and Ventral Urinary Bladder and Kidney Pelvis Urothelium of Rats. *Toxicologic pathology*, 37, 947-958.
- ERYILDIRIM, B., TARHAN, F., GUL, A. E., ERBAY, E. & KUYUMCUOGLU, U. 2006. Immunohistochemical analysis of low-affinity nerve growth factor receptor in the human urinary bladder. *Urol Int*, 77, 76-80.
- EUSTICE, D. C. & WILHELM, J. M. 1984. Mechanisms of action of aminoglycoside antibiotics in eucaryotic protein synthesis. *Antimicrobial agents and chemotherapy*, 26, 53-60.
- EVANS, R.J. 2011. Proof of concept trial of tanezumab for the treatment of symptoms associated with interstitial cystitis. *J. Urol.*, 185, 1716-1721.

FOREMAN, P., TAGLIALATELA, G., JACKSON, G. & PEREZ-POLO, J. 2004. Dexamethasone blocks nerve growth factor induction of nerve growth factor receptor mRNA in PC12 cells. *Journal of neuroscience research*, 31, 52-57.

GAO, X., DAUGHERTY, R. L. & TOURTELLOTTE, W. G. 2007. Regulation of low affinity neurotrophin receptor (p75^{NTR}) by early growth response (Egr) transcriptional regulators. *Molecular and Cellular Neuroscience*, 36, 501-514.

GIANNANTONI, A. 2006. Botulinum-A toxin injections into the detrusor muscle decrease nerve growth factor bladder tissue levels in patients with neurogenic detrusor overactivity. *J. Urol.*, 175, 2341-2344.

GIANNANTONI, A., CONTE, A., FARFARIELLO, V., PROIETTI, S., VIANELLO, A., NARDICCHI, V., SANTONI, G. & AMANTINI, C. 2013. Onabotulinumtoxin-A intradetrusorial injections modulate bladder expression of NGF, TrkA, p75 and TRPV1 in patients with detrusor overactivity. *Pharmacol Res*, 68, 118-24.

GIRARD, B. M., MALLEY, S. E. & VIZZARD, M. A. 2011. Neurotrophin/receptor expression in urinary bladder of mice with overexpression of NGF in urothelium. *Am. J. Physiol. Renal Physiol.*, 300, F345-F355.

GIRARD, B. M., TOMPKINS, J. D., PARSONS, R. L., MAY, V. & VIZZARD, M. A. 2012. Effects of CYP-induced cystitis on PACAP/VIP and receptor expression in micturition pathways and bladder function in mice with overexpression of NGF in urothelium. *J Mol Neurosci*, 48, 730-43.

HANNO, P., LIN, A., NORDLING, J., NYBERG, L., VAN OPHOVEN, A., UEDA, T. & WEIN, A. 2009. Bladder pain syndrome international consultation on incontinence. *Neurourology and urodynamics*, 29, 191-198.

HARNDEN, P., ALLAM, A., JOYCE, A. D., PATEL, A., SELBY, P. & SOUTHGATE, J. 1995. Cytokeratin 20 expression by non-invasive transitional cell carcinomas: potential for distinguishing recurrent from non-recurrent disease. *Histopathology*, 27, 169-74.

HARNDEN, P., EARDLEY, I., JOYCE, A. D. & SOUTHGATE, J. 1996. Cytokeratin 20 as an objective marker of urothelial dysplasia. *Br J Urol*, 78, 870-5.

HARNDEN, P., MAHMOOD, N. & SOUTHGATE, J. 1999a. Expression of cytokeratin 20 redefines urothelial papillomas of the bladder. *Lancet*, 353, 974-7.

HARNDEN, P., MAHMOOD, N. & SOUTHGATE, J. 1999b. Expression of cytokeratin 20 redefines urothelial papillomas of the bladder. *The Lancet*, 353, 974-977.

HERRING, A. A., AHERN, T., STONE, M. B. & FRAZEE, B. W. 2012. Emerging applications of low-dose ketamine for pain management in the ED. *The American journal of emergency medicine*.

HIROTA, K. & LAMBERT, D. 1996. Ketamine: its mechanism (s) of action and unusual clinical uses. *British journal of anaesthesia*, 77, 441-444.

- HOCKING, G. & COUSINS, M. J. 2003. Ketamine in chronic pain management: an evidence-based review. *Anesthesia & Analgesia*, 97, 1730-1739.
- HOMMA, Y., NOMIYA, A., TAGAYA, M., OYAMA, T., TAKAGAKI, K., NISHIMATSU, H. & IGAWA, Y. 2013. Increased mRNA expression of genes involved in pronociceptive inflammatory reactions in bladder tissue of interstitial cystitis. *J Urol*, 190, 1925-31.
- HU, C. C., LIANG, F. X., ZHOU, G., TU, L., TANG, C. H., ZHOU, J., KREIBICH, G. & SUN, T. T. 2005. Assembly of urothelial plaques: tetraspanin function in membrane protein trafficking. *Mol Biol Cell*, 16, 3937-50.
- HUNNER, G. L. 1915. A rare type of bladder ulcer in women; report of cases. *The Boston Medical and Surgical Journal*, 172, 660-664.
- IBLA, J. C., HAYASHI, H., BAJIC, D. & SORIANO, S. G. 2009. Prolonged exposure to ketamine increases brain derived neurotrophic factor levels in developing rat brains. *Current Drug Safety*, 4, 11.
- KATZ, M. H., ALVAREZ, A. F., KIRSNER, R. S., EAGLSTEIN, W. H. & FALANGA, V. 1991. Human wound fluid from acute wounds stimulates fibroblast and endothelial cell growth. *Journal of the American Academy of Dermatology*, 25, 1054-1058.
- KE, X., DING, Y., XU, K., HE, H., ZHANG, M., WANG, D., DENG, X., ZHANG, X., ZHOU, C. & LIU, Y. 2014. Serum brain-derived neurotrophic factor and nerve growth factor decreased in chronic ketamine abusers. *Drug and alcohol dependence*.
- KHACHIGIAN, L. M. 2006. Early growth response-1 in cardiovascular pathobiology. *Circulation research*, 98, 186-191.
- KHANDELWAL, P., ABRAHAM, S. N. & APODACA, G. 2009. *Cell biology and physiology of the uroepithelium*.
- KHWAJA, F., ALLEN, J., LYNCH, J., ANDREWS, P. & DJAKIEW, D. 2004. Ibuprofen inhibits survival of bladder cancer cells by induced expression of the p75NTR tumor suppressor protein. *Cancer research*, 64, 6207-6213.
- KIM, J. C. 2005. Changes of urinary nerve growth factor and prostaglandins in male patients with overactive bladder symptom. *Int. J. Urol.*, 12, 875-880.
- KIM, J. C., KIM, D. B., SEO, S. I., PARK, Y. H. & HWANG, T. K. 2004. Nerve growth factor and vanilloid receptor expression, and detrusor instability, after relieving bladder outlet obstruction in rats. *BJU Int.*, 94, 915-918.
- KLINGER, M. B. & VIZZARD, M. A. 2008. Role of p75NTR in female rat urinary bladder with cyclophosphamide-induced cystitis. *American Journal of Physiology-Renal Physiology*, 295, F1778-F1789.

- KRUMAN, I., GUO, Q. & MATTSON, M. P. 1998. Calcium and reactive oxygen species mediate staurosporine-induced mitochondrial dysfunction and apoptosis in PC12 cells. *J Neurosci Res*, 51, 293-308.
- KUNJU, L. P., LEE, C. T., MONTIE, J. & SHAH, R. B. 2005. Utility of cytokeratin 20 and Ki-67 as markers of urothelial dysplasia. *Pathology international*, 55, 248-254.
- LAI, Y., WU, S., NI, L., CHEN, Z., LI, X., YANG, S., GUI, Y., GUAN, Z., CAI, Z. & YE, J. 2012. Ketamine-associated urinary tract dysfunction: an underrecognized clinical entity. *Urologia internationalis*, 89, 93-96.
- LE, P. P., FRIEDMAN, J. R., SCHUG, J., BRESTELLI, J. E., PARKER, J. B., BOCHKIS, I. M. & KAESTNER, K. H. 2005. Glucocorticoid receptor-dependent gene regulatory networks. *PLoS genetics*, 1, e16.
- LESTER, L., BRAUDE, D. A., NILES, C. & CRANDALL, C. S. 2010. Low-dose ketamine for analgesia in the ED: a retrospective case series. *The American journal of emergency medicine*, 28, 820-827.
- LIU, B. L., YANG, F., ZHAN, H. L., FENG, Z. Y., ZHANG, Z. G., LI, W. B. & ZHOU, X. F. 2014. Increased severity of inflammation correlates with elevated expression of TRPV1 nerve fibers and nerve growth factor on interstitial cystitis/bladder pain syndrome. *Urol Int*, 92, 202-8.
- LIU, H. T., CHANCELLOR, M. B. & KUO, H. C. 2009. Urinary nerve growth factor levels are elevated in patients with detrusor overactivity and decreased in responders to detrusor botulinum toxin-A injection. *Eur. Urol.*, 56, 700-706.
- LIU, H. T. & KUO, H. C. 2008. Urinary nerve growth factor levels are increased in patients with bladder outlet obstruction with overactive bladder symptoms and reduced after successful medical treatment. *Urology*, 72, 104-108.
- LIU, H. T. & KUO, H. C. 2009. Urinary nerve growth factor levels are elevated in patients with overactive bladder and do not significantly increase with bladder distention. *Neurourol. Urodyn.*, 28, 78-81.
- LOWE, E. M., ANAND, P., TERENCE, G., WILLIAMS-CHESTNUT, R. E., SINICROPI, D. V. & OSBORNE, J. L. 1997. Increased nerve growth factor levels in the urinary bladder of women with idiopathic sensory urgency and interstitial cystitis. *Br J Urol*, 79, 572-7.
- LU, B., PANG, P. T. & WOO, N. H. 2005. The yin and yang of neurotrophin action. *Nature Reviews Neuroscience*, 6, 603-614.
- LU, N. Z., WARDELL, S. E., BURNSTEIN, K. L., DEFRANCO, D., FULLER, P. J., GIGUERE, V., HOCHBERG, R. B., MCKAY, L., RENOIR, J.-M. & WEIGEL, N. L. 2006. International Union of Pharmacology. LXV. The pharmacology and classification of the nuclear receptor superfamily: glucocorticoid, mineralocorticoid, progesterone, and androgen receptors. *Pharmacological reviews*, 58, 782-797.

- MCKENNEY, J. K., DESAI, S., COHEN, C. & AMIN, M. B. 2001. Discriminatory immunohistochemical staining of urothelial carcinoma in situ and non-neoplastic urothelium: an analysis of cytokeratin 20, p53, and CD44 antigens. *The American journal of surgical pathology*, 25, 1074-1078.
- METSIS, M. 2001. Genes for neurotrophic factors and their receptors: structure and regulation. *Cellular and Molecular Life Sciences CMLS*, 58, 1014-1020.
- MICERA, A., LAMBIASE, A., STAMPACHIACCHIERE, B., BONINI, S., BONINI, S. & LEVI-SCHAFFER, F. 2007. Nerve growth factor and tissue repair remodeling: trkA^{< sup>} NGFR^{< /sup>} and p75^{< sup>} NTR^{< /sup>}, two receptors one fate. *Cytokine & growth factor reviews*, 18, 245-256.
- MOORE, K. A., SKLEROV, J., LEVINE, B. & JACOBS, A. J. 2001. Urine concentrations of ketamine and norketamine following illegal consumption. *Journal of analytical toxicology*, 25, 583-588.
- MUKAI, J., HACHIYA, T., SHOJI-HOSHINO, S., KIMURA, M. T., NADANO, D., SUVANTO, P., HANAOKA, T., LI, Y., IRIE, S. & GREENE, L. A. 2000. NADE, a p75NTR-associated cell death executor, is involved in signal transduction mediated by the common neurotrophin receptor p75NTR. *Science Signalling*, 275, 17566.
- MURRAY, E., MALLEY, S. E., QIAO, L.-Y., HU, V. Y. & VIZZARD, M. A. 2004. Cyclophosphamide induced cystitis alters neurotrophin and receptor tyrosine kinase expression in pelvic ganglia and bladder. *The Journal of urology*, 172, 2434-2439.
- NGIAM, N., POST, M. & KAVANAGH, B. P. 2007. *Early growth response factor-1 in acute lung injury*.
- NIKAM, S. S., TENNEKOON, G. I., CHRISTY, B. A., YOSHINO, J. E. & RUTKOWSKI, J. L. 1995. The zinc finger transcription factor Zif268/Egr-1 is essential for Schwann cell expression of the p75 NGF receptor. *Molecular and Cellular Neuroscience*, 6, 337-348.
- NORTON, P. & BRUBAKER, L. 2006. Urinary incontinence in women. *The Lancet*, 367, 57-67.
- OXLEY, J. D., COTTRELL, A. M., ADAMS, S. & GILLATT, D. 2009. Ketamine cystitis as a mimic of carcinoma in situ. *Histopathology*, 55, 705-708.
- PANER, G. P., MCKENNEY, J. K., BARKAN, G. A., YAO, J. L., FRANKEL, W. L., SEBO, T. J., SHEN, S. S. & JIMENEZ, R. E. 2011. Immunohistochemical analysis in a morphologic spectrum of urachal epithelial neoplasms: diagnostic implications and pitfalls. *Am J Surg Pathol*, 35, 787-98.
- QIAO, L. Y. & VIZZARD, M. A. 2002. Cystitis-induced upregulation of tyrosine kinase (TrkA, TrkB) receptor expression and phosphorylation in rat micturition pathways. *Journal of Comparative Neurology*, 454, 200-211.

- QUANN, E. J., KHWAJA, F. & DJAKIEW, D. 2007. The p38 MAPK pathway mediates Aryl propionic acid-induced messenger RNA stability of p75NTR in prostate cancer cells. *Cancer research*, 67, 11402-11410.
- REIS-FILHO, J. S., STEELE, D., DI PALMA, S., JONES, R. L., SAVAGE, K., JAMES, M., MILANEZI, F., SCHMITT, F. C. & ASHWORTH, A. 2006. Distribution and significance of nerve growth factor receptor (NGFR/p75NTR) in normal, benign and malignant breast tissue. *Modern pathology*, 19, 307-319.
- RICCI, V., MARTINOTTI, G., GELFO, F., TONIONI, F., CALTAGIRONE, C., BRIA, P. & ANGELUCCI, F. 2011. Chronic ketamine use increases serum levels of brain-derived neurotrophic factor. *Psychopharmacology*, 215, 143-148.
- RIEDL, C. R., KNOLL, M., PLAS, E. & PFLÜGER, H. 1998. Electromotive drug administration and hydrodistention for the treatment of interstitial cystitis. *Journal of endourology*, 12, 269-272.
- ROSAMILIA, A., DWYER, P. & GIBSON, J. 1997. Electromotive drug administration of lidocaine and dexamethasone followed by cystodistension in women with interstitial cystitis. *International Urogynecology Journal*, 8, 142-145.
- ROSEWICZ, S., MCDONALD, A. R., MADDUX, B., GOLDFINE, I., MIESFELD, R. & LOGSDON, C. 1988. Mechanism of glucocorticoid receptor down-regulation by glucocorticoids. *Journal of Biological Chemistry*, 263, 2581-2584.
- ROSS, A. H., GROB, P., BOTHWELL, M., ELDER, D. E., ERNST, C. S., MARANO, N., GHRIST, B., SLEMP, C. C., HERLYN, M. & ATKINSON, B. 1984. Characterization of nerve growth factor receptor in neural crest tumors using monoclonal antibodies. *Proceedings of the National Academy of Sciences*, 81, 6681-6685.
- RUIT, K., OSBORNE, P. A., SCHMIDT, R. E., JOHNSON, E. & SNIDER, W. D. 1990. Nerve growth factor regulates sympathetic ganglion cell morphology and survival in the adult mouse. *The Journal of Neuroscience*, 10, 2412-2419.
- SANDLER, R. S., GALANKO, J. C., MURRAY, S. C., HELM, J. F. & WOOSLEY, J. T. 1998. Aspirin and nonsteroidal anti-inflammatory agents and risk for colorectal adenomas. *Gastroenterology*, 114, 441-447.
- SCHECTERSON, L. C. & BOTHWELL, M. 2010. Neurotrophin receptors: Old friends with new partners. *Developmental Neurobiology*, 70, 332-338.
- SCHNEGELSBERG, B., SUN, T.-T., CAIN, G., BHATTACHARYA, A., NUNN, P. A., FORD, A. P., VIZZARD, M. A. & COCKAYNE, D. A. 2010. Overexpression of NGF in mouse urothelium leads to neuronal hyperinnervation, pelvic sensitivity, and changes in urinary bladder function. *American Journal of Physiology-Regulatory, Integrative and Comparative Physiology*, 298, R534-R547.
- SHAHANI, R., STREUTKER, C., DICKSON, B. & STEWART, R. J. 2007. Ketamine-associated ulcerative cystitis: a new clinical entity. *Urology*, 69, 810-812.

SIEGEL, R. K. 1978. Phencyclidine and ketamine intoxication: a study of four populations of recreational users. *NIDA Res Monogr*, 119-47.

SKENE, A. J. C. 1887. *Diseases of the bladder and urethra in women*, W. Wood.

SOFRONIEW, M. V., HOWE, C. L. & MOBLEY, W. C. 2001. Nerve growth factor signaling, neuroprotection, and neural repair. *Annual review of neuroscience*, 24, 1217-1281.

SOUTHGATE, J., HUTTON, K., THOMAS, D. & TREJDOSIEWICZ, L. K. 1994. Normal human urothelial cells in vitro: proliferation and induction of stratification. *Laboratory investigation; a journal of technical methods and pathology*, 71, 583.

SOUTHGATE, J., MASTERS, J. R. & TREJDOSIEWICZ, L. K. 2002. Culture of human urothelium. *Culture of epithelial cells*, 2.

STEERS, W., KOLBECK, S., CREEDON, D. & TUTTLE, J. 1991. Nerve growth factor in the urinary bladder of the adult regulates neuronal form and function. *Journal of Clinical Investigation*, 88, 1709.

STEERS, W. D. 2002. Overactive Bladder (OAB): What We Thought We Knew and What We Know Today. *European Urology Supplements*, 1, 3-10.

SUKHATME, V., KARTHA, S., TOBACK, F., TAUB, R., HOOVER, R. & TSAI-MORRIS, C. 1987. A novel early growth response gene rapidly induced by fibroblast, epithelial cell and lymphocyte mitogens. *Oncogene research*, 1, 343.

SUKHATME, V. P., CAO, X., CHANG, L. C., TSAI-MORRIS, C. H., STAMENKOVICH, D., FERREIRA, P., COHEN, D. R., EDWARDS, S. A., SHOWS, T. B. & CURRAN, T. 1988. A zinc finger-encoding gene coregulated with c-fos during growth and differentiation, and after cellular depolarization. *Cell*, 53, 37.

SVENSON, J. E. & ABERNATHY, M. K. 2007. Ketamine for prehospital use: new look at an old drug. *The American journal of emergency medicine*, 25, 977-980.

TAKAHASHI, H. & IIZUKA, H. 1991. Regulation of β 2-adrenergic receptors in keratinocytes: glucocorticoids increase steady-state levels of receptor mRNA in foetal rat keratinizing epidermal cells (FRSK cells). *British journal of dermatology*, 124, 341-347.

TENG, H. K., TENG, K. K., LEE, R., WRIGHT, S., TEVAR, S., ALMEIDA, R. D., KERMANI, P., TORRIN, R., CHEN, Z.-Y., LEE, F. S., KRAEMER, R. T., NYKJAER, A. & HEMPSTEAD, B. L. 2005. ProBDNF Induces Neuronal Apoptosis via Activation of a Receptor Complex of p75NTR and Sortilin. *The Journal of Neuroscience*, 25, 5455-5463.

TENG, J., WANG, Z. Y. & BJORLING, D. E. 2002. Estrogen-induced proliferation of urothelial cells is modulated by nerve growth factor. *Am J Physiol Renal Physiol*, 282, F1075-83.

- TENG, K. K., FELICE, S., KIM, T. & HEMPSTEAD, B. L. 2010. Understanding proneurotrophin actions: Recent advances and challenges. *Developmental neurobiology*, 70, 350-359.
- TOMELLINI, E., LAGADEC, C., POLAKOWSKA, R. & LE BOURHIS, X. 2014. Role of p75 neurotrophin receptor in stem cell biology: more than just a marker. *Cell Mol Life Sci*, 71, 2467-81.
- TORI, S. 1996. Ketamine Abuse 'Special K'. *Middle Atlantic-Great Lakes Organized Crime Law Enforcement Network (MAGLOCLLEN), Pennsylvania*.
- UNODC 2010. World Drug Report 2010. United Nations Office on Drugs and Crime Vienna.
- VAIDYANATHAN, S., KRISHNAN, K., MANSOUR, P., SONI, B. & MCDICKEN, I. 1998a. p75 nerve growth factor receptor in the vesical urothelium of patients with neuropathic bladder: an immunohistochemical study. *Spinal cord*, 36, 541-547.
- VAIDYANATHAN, S., KRISHNAN, K. R., MANSOUR, P., SONI, B. M. & MCDICKEN, I. 1998b. p75 nerve growth factor receptor in the vesical urothelium of patients with neuropathic bladder: an immunohistochemical study. *Spinal Cord*, 36, 541-7.
- VAN DE MERWE, J. P., NORDLING, J., BOUCHELOUCHE, P., BOUCHELOUCHE, K., CERVIGNI, M., DAHA, L. K., ELNEIL, S., FALL, M., HOHLBRUGGER, G. & IRWIN, P. 2008. Diagnostic criteria, classification, and nomenclature for painful bladder syndrome/interstitial cystitis: an ESSIC proposal. *European urology*, 53, 60-67.
- VARLEY, C., HILL, G., PELLEGRIN, S., SHAW, N. J., SELBY, P. J., TREJDOSIEWICZ, L. K. & SOUTHGATE, J. 2005. Autocrine regulation of human urothelial cell proliferation and migration during regenerative responses in vitro. *Exp Cell Res*, 306, 216-29.
- VARLEY, C. L., GARTHWAITE, M. A. E., CROSS, W., HINLEY, J., TREJDOSIEWICZ, L. K. & SOUTHGATE, J. 2006. PPAR γ -regulated tight junction development during human urothelial cytodifferentiation. *Journal of Cellular Physiology*, 208, 407-417.
- VERGE, V., RICHARDSON, P., BENOIT, R. & RIOPELLE, R. 1989. Histochemical characterization of sensory neurons with high-affinity receptors for nerve growth factor. *Journal of neurocytology*, 18, 583-591.
- VIZZARD, M. A. 2000. Changes in urinary bladder neurotrophic factor mRNA and NGF protein following urinary bladder dysfunction. *Experimental neurology*, 161, 273-284.
- VIZZARD, M. A., WU, K. H. & JEWETT, I. T. 2000. Developmental expression of urinary bladder neurotrophic factor mRNA and protein in the neonatal rat. *Brain Res. Dev. Brain Res.*, 119, 217-224.
- WAKABAYASHI, Y., MAEDA, T. & KWOK, Y. N. 1996. Increase of p75 immunoreactivity in rat urinary bladder following inflammation. *Neuroreport*, 7, 1141-4.

- WALSH, S., JORDAN, G., JEFFERISS, C., STEWART, K. & BERESFORD, J. 2001. High concentrations of dexamethasone suppress the proliferation but not the differentiation or further maturation of human osteoblast precursors in vitro: relevance to glucocorticoid-induced osteoporosis. *Rheumatology*, 40, 74-83.
- WEIN, A. J. & ROVNER, E. S. 2002. Definition and epidemiology of overactive bladder. *Urology*, 60, 7-12.
- WEZEL, F., PEARSON, J. & SOUTHGATE, J. 2014. Plasticity of in vitro-generated urothelial cells for functional tissue formation. *Tissue Engineering Part A*, 20, 1358-1368.
- WOOD, D., COTTRELL, A., BAKER, S. C., SOUTHGATE, J., HARRIS, M., FULFORD, S., WOODHOUSE, C. & GILLATT, D. 2011. Recreational ketamine: from pleasure to pain. *BJU Int*, 107, 1881-1884.
- WYNNE, S. & DJAKIEW, D. 2010. NSAID inhibition of prostate cancer cell migration is mediated by Nag-1 induction via the p38 MAPK-p75NTR pathway. *Molecular Cancer Research*, 8, 1656-1664.
- YAKOVLEV, A. G., DE BERNARDI, M. A., FABRAZZO, M., BROOKER, G., COSTA, E. & MOCCHETTI, I. 1990. Regulation of nerve growth factor receptor mRNA content by dexamethasone: in vitro and in vivo studies. *Neuroscience letters*, 116, 216-220.
- YAN, S. F., PINSKY, D. J., MACKMAN, N. & STERN, D. M. 2000. Egr-1: is it always immediate and early? *The Journal of clinical investigation*, 105, 553-554.
- YOUNG, O. D., WOODFORD 2013. *Wheater's Functional Histology: A Text and Colour Atlas*.
- YU, J., LIN, J. H., WU, X. R. & SUN, T. T. 1994. Uroplakins Ia and Ib, two major differentiation products of bladder epithelium, belong to a family of four transmembrane domain (4TM) proteins. *The Journal of cell biology*, 125, 171-182.

9 Appendices

9.1 Abbreviations

ABS	Adult bovine serum
AUM	Asymmetric unit membrane
BDNF	Brain derived neurotrophic factor
BPE	Bovine pituitary extract
BPS	Bladder pain syndrome
BSA	Bovine serum albumin
CK	Cytokeratin
CSA	Catalysed signal amplification
DAB	Diaminobenzidine
DMEM	Dulbecco's Modified Eagle's Medium
DMSO	Dimethylsulphoxide
DNA	Deoxyribonucleic acid
dNTP	Deoxynucleotide triphosphate
D-PBS	Dulbecco's Phosphate buffered saline
ECM	Extracellular matrix
EDTA	Ethylenediaminetetra-acetic acid
Egr-1	Early growth receptor - 1
FBS	Fetal bovine serum
GAPDH	Glyceraldehyde 3-phosphate dehydrogenase
H & E	Haematoxylin and eosin
IC	Interstitial cystitis
IFN	Interferon
IL	Interleukin
KIC	Ketamine-induced cystitis
KSFMc	Keratinocyte Serum-Free Medium with supplements
LUTD	Lower urinary tract dysfunction
LUTS	Lower urinary tract symptoms

NGF	Nerve growth factor
NGFR	Low-affinity nerve growth factor receptor (CD271)
NHU (cells)	Normal human urothelial cells
NSAID	Non-steroidal anti-inflammatory drug
OABS	Overactive bladder syndrome
PBS	Phosphate buffered saline
RNA	Ribonucleic acid
RPMI	Roswell Park Memorial Institute
RT-PCR	Reverse-transcribed polymerase chain reaction
RT-PCR	Reverse-transcribed quantitative polymerase chain reaction
TBS	Tris buffered saline
TER	Transepithelial electrical resistance
TI	Trypsin inhibitor
TNF	Tumour necrosis factor
TrK	Tyrosine Kinase
UPK	Uroplakin
USI	Urodynamic stress incontinence

9.2 List of Surgical samples

Chapter 3			
Sample	Localisation	Age	Gender
Y1288	Ureter	57	M
Y1297	Ureter	27	F
Y1304	Ureter	39	M
Y1216	Ureter	56	M
Y1424	Ureter	34	F
Y1075	Bladder	21	M
Y1189	Ureter	54	F
Y1303	Bladder	12	M
Y998	Bladder	79	M
Y994	Bladder	63	M
Chapter 4			
Sample	Localisation	Age	Gender
Y1450	Bladder	30	M
Chapter 5			
Sample	Localisation	Age	Gender
Y1300	Ureter	62	F
Y1301	Ureter	60	F
Y1053	Ureter	57	M
Y1160	Ureter	25	M
Y1282	Ureter	55	M
Y1276	Ureter	21	F
Y1221	Ureter	63	F
Y1424	Ureter	34	F
Y1004	Ureter	66	F
Y1197	Ureter	73	M
Chapter 6			
Sample	Localisation	Age	Gender
Y1004	Ureter	66	F
Y744	Ureter	56	M
Y1389	Ureter	54	F
Y1497	Ureter	64	F
Y1434	Ureter	41	F
Y1361	Ureter	52	M
Y1517	Ureter	48	M
M = Male/F = Female			

Table 9-1 Table of Surgical specimens in all chapters

Sample		Age	Gender
KIC 1	Y1238	n.d	n.d
KIC 2	Y1239	n.d	n.d
KIC 3	Y1240	n.d	n.d
KIC 4	Y1241	n.d	n.d
KIC 5	Y1248	36	n.d
KIC 6	Y1249	33	n.d
KIC 7	Y1250	28	n.d
KIC 8	Y1251	33	n.d
KIC 9	Y1252	24	n.d
KIC 10	Y1253	41	n.d
KIC 11	Y1254	25	n.d
KIC 12	Y1255	33	n.d
KIC 13	Y1256	21	n.d
KIC 14	Y1257	27	n.d
KIC 15	Y1258	23	n.d
KIC 16	Y1259	21	n.d
KIC 17	Y1260	27	n.d
KIC 18	Y1261	27	n.d
KIC 19	Y1262	20	n.d
KIC 20	Y1263	22	n.d
KIC 21	Y1242	30	M
KIC 22	Y1243	30	M
n.d = no data M = male/ F = female			

Table 9-2 Table of surgical KIC specimens used in chapter 3

9.3 List of antibodies

Primary and secondary antibodies listed for each chapter

Antigen	Antibody	Host	Manufacturer	Cat No	Retrieval	Concentration
Human NGFR (gp 75)	Clone 7F10	Mouse	Novocastra	NCL-NGFR	Citric acid/mw	1 in 100 (Amplification)
Egr-1	Clone 15F7	Rabbit	Cell signalling	4153	Citric acid/mw	1 in 750 (Amplification)
CK13	IC7	Mouse	Abnova	Mab 1864	MW/trypsin	1 in 500
CK20	Ks20.8	Mouse	Symbus Bioscience Ltd	CBL 208	Trypsin	1 in 200
UPK3A	AU1	Mouse	Progen	651 108	Citric acid/mw	1 in 200
Ki67	MM1	Mouse	Novocastra	NCL-L-Ki67	MW	1 in 100
CK5	SP27	Rabbit	Abcam	Ab640 81	MW	1 in 200
p53	DO7	Mouse	Novocastra	NCL-p53-DO7	MW	1 in 100

Table 9-3 Table of Primary antibodies

Secondary antibodies

Mouse – Biotinylated rabbit anti mouse (Dakocytomation – E0354 DAKO A/S Denmark)

Rabbit – Biotinylated goat anti rabbit (Dakocytomation – E0466 DAKO A/S Denmark)

9.4 List of primers

Gene	Forward 5'-3'	Reverse 5'-3'	Size (bp)	NCBI/Ensemble Gene code	Intron Spanning	Control	°C Anneal Extension (min)
NGFR	GGAACAGCTGCA AGCAGAAC	CTGACAGACTCTCC ACGAG	433	ENST00000172229	Yes	Genomic Brain Pooled cell lines	60.7 1.00
ICAM1	CAGCAGACTCCAA TGTGC	CTCTGTTCAGTGTG GCAC	372	NM_000201	No	Genomic	55 0.30
MT-1G	CTTCTCGCTTGGG AACTCTA	AGGGGTCAAGATT GTAGCAAA	309	ENST00000379811	No	Genomic	58 1.15
GAPDH	ACCCAGAAGACT GTGGATGG	TTCTAGACGGCAGG TCAGGT	201	ENST00000229239	No	Genomic	61.8 0.30

Table 9-4

List of primers

9.5 List of suppliers

Abcam

1 Kendall Square, Ste 341
Cambridge, MA 02139-1517
USA

Ambion

Spitfire Close
Ermine Business Park
Huntingdon
Cambridgeshire, PE29 6XY, UK

Agilent Technologies UK Limited

Lakeside Cheadle Royal Business Park,
Stockport
Cheshire, SK8 3GR

Amersham Bioscience UK

Amersham Place
Little Chalfont
Buckinghamshire,
HP7 9NA, UK

Applied Biosystems Lingley House

120 Birchwood Boulevard
Warrington, WA3 7QH, UK

Axygen Supplied by VWR International Ltd

Bayer Bayer Ltd Pharmaceutical Business Group

Strawberry Hill; Newbury
Berkshire, RG13 1JA, UK

Becton Dickinson Biosciences

Between Towns Road
Cowley
Oxford, OX4 3LY, UK

Beckmann Coulter UK Ltd Oakley Court

Kingsmead Business Park
London Road; High Wycombe
Buckinghamshire HP11 1JU

BDH Supplied by Merck

Bioline Ltd 16 The Edge Business Park
Humber Road
London NW2 6EW

Calbiochem supplied by Merck**Cambridge Bioscience Ltd**

24-25 Signet Court
Newmarket Road
Cambridge CB5 8LA

Costar Corning International

Red Wolf House
5 Bolton Street
London, W1J 8BA, UK

Cymbus Biotechnology

Unit J, Eagle Close
Chandlers Ford
Hants, SO53 4NF, UK

Dako UK Ltd Cambridge House

St Thomas Place, Ely
Cambridgeshire CB7 4EX

eBioscience, Ltd.

3 Bishop Square
Hatfield, AL10 9NA, UK

Falcon Supplied by Becton Dickinson**Fisher Scientific**

Bishop Meadow Road
Loughborough
LLE11 5RG Leicestershire, UK

Gibco Supplied by Invitrogen**GraphPad Software**

2236 Avenida de la Playa
La Jolla, CA 92037, USA

Hendley-Essex Ltd

12 Oakwood Hill Industrial Estate
Loughton
Essex, IG10 3TZ

Hybaid 300 Second Avenue

Needham Heights
MA 02494
USA

Invitrogen 3 Fountain Drive

Inchinnin Business Park
114
Paisley, UK

Leica Leica AG

Oskar-Barnack-Straße 11
35606 Solms, Germany
Li-COR Biosciences Ltd. St. John's Innovation Centre
Cowley Road
Cambridge, CB4 0WS, UK

Merck Chemicals Ltd.

Hunter Boulevard
Magna Park
Lutterworth
Leicestershire, LE17 4XN, UK

MP Biomedicals

Europe Parc d'Innovation
BP 50067
67402 Illkirch, France

Novocastra supplied by Leica Biosystems Ltd

Balliol Business Park West
Benton Lane
Newcastle Upon Tyne , NE12 8EW, UK

Nikon

Nikon House
380 Richmond Road
Kingston Upon Thames
Surrey, KT2 5PR, UK

Olympus

Great Western Industrial Park
Dean Way
Southall
Middlesex, UB2 4SB, UK

**Primaria Tissue culture flasks supplied by SLS
Tissue culture plates/flasks supplied
by VWR**

Progen Biotechnik

GmbH Maaßstrasse 30
69123 Heidelberg, Germany
Promega Delta House
Chilworth Research Centre
Southampton, SO16 7NS, UK

Qiagen QIAGEN Ltd

Boundary Court Gatwick Road
Crawley, UK

R & D Systems Europe Ltd

19 Barton Lane
Abingdon Science Park
Abingdon,
OX14 3NB, UK

Serotec Ltd Endeavour House

Langford Business Park
Langford Lane,
Kidlington
Oxford, OX5 1GF

Sigma-Aldrich Co. Ltd

The Old Brickyard
New Road
Dorset SP8 4XT,
UK

Stratagene supplied by Agilent UK

Statspin John Eccles House
Robert Robinson Avenue
Oxford Science Park, Oxford
OX4 4GP, United Kingdom

Thermo Scientific Raymond Lamb distributed by Fischer Scientific

Vector Labs 3 Accent Park
Bakewell Road
Orton Southgate
Peterborough, PE2 6XS, UK

VWR International Hunter Boulevard

Magna Park
Leicestershire
LE17 4XN